RESEARCH REPORT

Battelle
Columbus Laboratories

FINAL REPORT

on

NONCONTACTING DEVICES TO INDICATE DEFLECTION AND VIBRATION OF TURBOPUMP INTERNAL ROTATING PARTS

(Contract NAS 8-26903)

to

NATIONAL AERONAUTICS AND SPACE ADMINISTRATION
GEORGE C. MARSHALL SPACE FLIGHT CENTER

by

D. B. Hamilton, Project Manager
and
Dale Ensminger, D. R. Grieser, A. M. Plummer,
E. J. Saccocio, and J. W. Kissel

March 12, 1973

BATTELLE
Columbus Laboratories
505 King Avenue
Columbus, Ohio 43201

Battelle
Columbus Laboratories
505 King Avenue
Columbus, Ohio 43201
Telephone (614) 299-3151
Telex 24-5454

March 12, 1973

Mr. Forrest Pitsenberger
Technical Manager
National Aeronautics and
Space Administration
George C. Marshall Space
Flight Center
Marshall Space Flight Center
Alabama 35812

Dear Mr. Pitsenberger:

Enclosed are five copies of our Final Report on Contract NAS 8-26903. It has been a great pleasure to work with you and Mr. Ron Young on this program. In my opinion, this has been a particularly successful program. The program success is due, to a great extent, to the fine support provided by yourself and Mr. Young. It would be a pleasure to work with you in the future.

If you have any questions regarding the report or the program, please do not hesitate to contact me.

Sincerely,

D. B. Hamilton
Project Manager

DBH:alb

Enc. (5)

cc: Defense Contract Administration
Services Office (letter only)
Building 1, Section 1
Defense Construction Supply Center
Columbus, Ohio 43215
Attention Mr. Billy Conley, DCRO-GCC
Contracting Officer

TABLE OF CONTENTS

TABLE OF CONTENTS
(Continued)

TABLE OF CONTENTS
(Continued)

TABLE OF CONTENTS
(Continued)

SUMMARY

A three-phase program was conducted to develop devices to measure vibrations and deflections of parts, such as impellers, shafts, turbine wheels, inducers, etc., in operating turbopumps. Three devices were developed to the breadboard stage: ultrasonic Doppler technique, flash X-rays, and light-pipe reflectance.

The ultrasonic Doppler transducer can be applied easily to the outer case of a turbopump and will measure vibration of internal components with a high degree of accuracy so long as a liquid and/or a solid path exists from the transducer to the rotating part. Wave transmission across boundaries between contacting solid members or across solid liquid boundaries is not a basic problem. It is recommended that a follow-on program be conducted to develop the technique from the breadboard stage to a convenient, optimized package suitable for easy application to rotating machinery.

The flash X-ray technique shows promise as a diagnostic technique to view several rotating internal components at once to determine which component might require more accurate measurement by another technique. Although dependent on the specific application, the technique probably is limited to a resolution of about ±0.125 mm (5 mils) in vibration amplitude.

The light-pipe-reflectance technique is easy to apply, will measure a large range of amplitudes, will withstand cryogenic temperatures and temperatures to 540 C, and does not require accurate reflecting surfaces. A hole must be drilled to admit the fiber optic probe; however, the clad probe can be sealed into the stationary members and the flexibility of the probe makes it somewhat easier to get into the desired locations than, say, capacitance or inductance probes.

Each phase of the program is summarized separately below.

Phase I. Feasibility

The study was divided into six technical areas of responsibility:

(1) Ultrasonic techniques

(2) Neutron techniques

(3) X-radiography

(4) Radioisotope and gamma ray devices

(5) Optical devices

(6) Conventional displacement sensors.

Phase I included an extensive literature review to identify candidate techniques, and calculations and experiments to establish feasibility of the various candidates.

Ultrasonic Techniques

The types of techniques evaluated included pulse-echo, resonance, pulse interference, sonic analysis, beam interference or deflection, and Doppler analysis. The Doppler technique, in which an ultrasonic wave is reflected from a vibrating part and the attendant Doppler frequency shift is measured, was selected as the most appropriate for the application on the basis of minimum modification required to the pump. The feasibility of the Doppler method was shown experimentally using laboratory equipment and devices. In addition, the measurements showed that the acoustic transmission properties of the housing of a J-2 turbopump are favorable to the ultrasonic method.

Neutron Techniques

Neutron radiography and directional fast-neutron detection were evaluated. Neutron radiography was found not feasible for the following reasons.

(1) Insufficient flux intensity is available from portable sources for short-time measurements.

(2) The source area of portable sources is too large for thermal sources to permit the measurement sensitivities required.

(3) Fast-neutron sources are, perhaps, sufficiently intense; however, fast neutrons cannot be detected efficiently enough to permit required radiographic resolution.

A directional fast-neutron detector was conceived and evaluated, both experimentally and analytically, and was found feasible for further development. Budgetary constraints, however, precluded development of this approach.

X-Radiography

Flash X-rays, pulsed over a 20 nanosecond interval, were found feasible for real-time measurements. Commercial units are available which produce X-ray energies of 300 kilovolts, 600 kilovolts, and 2 megavolts. Phase I studies demonstrated that X-rays from the lower-power units would not penetrate a J-2 turbopump sufficiently to produce images of internal components.

Optical Techniques

Techniques evaluated included intensity of gap transmission, edge gradient locator, surface triangulation, interferometry, light-pipe reflectance, gap diffraction, Doppler shift, and laser/speckle pattern analysis. Light-pipe-reflectance was selected as the most appropriate for the following reasons.

(1) No requirement for optically flat windows
(2) A clad fiber-optic probe can be used (instead of a clear window in the pump case as would be required for the other techniques)
(3) Accessibility to interior pump section provided by flexibility of fiber-optic bundle
(4) Appropriate sensitivity.

Radioisotope and Gamma Ray Devices

Detection techniques based on simple Mössbauer analysis and vibration of a resonant gamma absorber were evaluated. None were found feasible. Mössbauer analysis was found to be much too sensitive for a use as a turbopump measuring device.

Conventional Displacement Sensors

Magnetic devices based on eddy current and inductance sensors and capacitance devices were evaluated. None were found which appeared to offer a major improvement over those now being used for turbopump vibration measurement. The use of signal transmitters in place of slip rings was judged to be a potential improvement.

Phase II. Development

Three techniques were selected by Battelle-Columbus and NASA for development: ultrasonic Doppler, flash X-ray, and light-pipe reflectance.

Ultrasonic Doppler Technique

A breadboard ultrasonic Doppler system for measuring vibration amplitudes was assembled and evaluation of the system using a J-2 turbopump was conducted during the fourth quarter of the project. Measurements were made of runout of the impeller of the J-2 pump during operation at 1000 rpm.

A new, compact, dual-element ultrasonic transducer was developed during Phase II. This transducer combined the desirable qualities previously determined to be essential in eliminating both electrical and acoustical cross-talk from the system. All Phase III studies of the ultrasonic Doppler method were conducted using this transducer.

Flash X-Rays

A J-2 turbopump on a test stand was used to evaluate the capability of a 2-megavolt flash X-ray apparatus to detect displacement of operating components of the pump. Radiographs were taken of the shaft-bearing-seal assembly and the turbine blade area. Various problems were evaluated and the technique was optimized with respect to X-ray slit size, scattering in the pump, and detector type and sensitivity.

Light-Pipe Reflectance

A commercial unit was purchased and applied to devices rotating up to 35,000 cycles per minute. A protective sleeve was fitted to the fiber optic probe. Measurements were made on the J-2 pump of impeller runout at 1000 rpm.

Phase III. Experimental Verification

Ultrasonic Doppler Technique

Without significant change in calibration, the transducer survived the vibrational environment expected for future pumps. A special calibrator was constructed and measurements were made at 35,000 cycles per minute. Shaft vibration in the J-2 pump was measured during operation at 1000 rpm.

Flash X-Rays

A device rotating at about 18,000 rpm was radiographed and compared with a radiograph taken while stationary. No loss in resolution was detected.

Light-Pipe Reflectance

The fiber-optic probe was exposed simultaneously to 77 K liquid nitrogen and 48.2 MN/m^2 (7000 psi). No change in optical properties was observed after exposure. The probe was exposed to a high vibration environment without deleterious effects. In addition, exposure to a high-velocity fluid stream did not cause probe damage. In Phase II, the technique was shown to be accurate at 35,000 cycles per minute.

CONCLUSIONS AND RECOMMENDATIONS

The program has resulted in four techniques to measure vibration of internal components in liquid-rocket turbopumps. Three of these were developed from the feasibility stage to the breadboard stage. The fourth, the fast-neutron detector, was shown to be feasible but was not developed because of budgetary constraints.

None of the four techniques is likely to be able to measure vibrations for all of the components of interest; therefore, employing a combination of the techniques would be desirable. The ultrasonic Doppler approach shows great promise for routine nondestructive application to turbopumps. To apply it, a liquid or solid path to conduct the ultrasonic waves from the transducers to the part being measured is required. In addition, the pump structure through which the ultrasound is conducted should be shaped to act as a wave guide. This will, in some cases, require very minor modifications to the pump design to permit specific measurements to be made. If such modifications are considered during the design of the pump, they would not be likely to result in extra cost, or even significant inconvenience. Because of the poor acoustic-transmission properties of abradable seals and cooling passages, the ultrasonic technique is not likely to be appropriate for turbine-section measurements. Where liquid-solid paths are available, it is very easy to apply, requiring attachment by clamps or adhesive to the outer case of the turbopump. Sensitivity of the technique is better than 25 microns. A possible bonus with the ultrasonic technique lies in the capability to monitor pump operation with acoustic-signature analysis.

We recommend that further development of the ultrasonic Doppler device be performed to take it from the breadboard stage to a device optimized for manufacture. In addition, we recommend that the use of the technique be considered at this time in the design of the Shuttle turbopumps so minor modifications can be made to admit ultrasonic waves to the components of interest.

The flash X-ray technique was shown to be applicable to the shaft assembly and to the turbine seal of the J-2 pump. For future pumps, the applicability of flash X-rays to specific sections will depend on the particular configuration involved. At this time, the sensitivity of the technique would appear to be in the neighborhood of 0.125 mm (5 mil). For maximum accuracy, it would be convenient to have a known gap, of perhaps 0.375 mm (15 mil), in the pump which appears in the radiograph for calibration purposes. It is possible that the X-ray technique will find the most use as a diagnostic device to identify components which are vibrating excessively so that further measurements can be made by another technique, such as the ultrasonic Doppler method. Flash X-rays are, of course, somewhat less convenient to use, requiring a stationary 2-megavolt apparatus costing about $25,000.

The light-pipe-reflectance device appears to be ideal for cryogenic pump sections, where the possibility exists of drilling holes to admit the fiber-optic probe. In addition, the fiber optic probes will survive 540 C for short periods which suggests that they could be used in the cooler portions of the turbine sections. As with the ultrasonic technique, we recommend consideration of the optical technique during the design phase of shuttle turbopumps.

The light-pipe-reflectance device might be made somewhat more convenient by the development of a dual probe which compensates for surface reflectivity changes. It is our understanding that such a probe is under development by the manufacturer. In addition, various development efforts are being conducted to develop fiber optic probes with higher temperature capabilities.

NONCONTACTING DEVICES TO INDICATE DEFLECTION AND VIBRATION OF TURBOPUMP INTERNAL ROTATING PARTS
(Contract NAS 8-26903)

by

D. B. Hamilton, Project Manager
and
Dale Ensminger, D. R. Grieser, A. M. Plummer,
E. J. Saccocio, and J. W. Kissel

INTRODUCTION

In the past, the development of turbopumps for liquid-rocket engines has required the determination of actual deflections and vibrations of internal parts during operation of prototype units. This has required complicated and costly efforts involving the use of strain gages and slip rings in cryogenic environments, major modification of pump sections to permit mounting of inductance or capacitance sensors, and the use of devices which are mechanically connected to the rotating part.

The purpose of this program was to develop a noncontacting device capable of accurately measuring deflections and vibrations of internal turbopump components without mechanical contact with the rotating part, without the use of slip rings or strain gages, and without the need to make major modifications to the pump prototype.

The measurements considered to be of interest included vibrations of shafts, impellers, inducers, turbine rotors, bearings and seals, and clearances between turbine blades and housings. The range of vibration amplitudes covered by these components is from a few microns up to about 1/2 mm. The measuring techniques developed were required to be appropriate for measuring vibrations in internal pump components rotating up to 35,000 rpm operating in environments of liquid hydrogen or liquid oxygen at pressures up to 48.2 MN/m^2 (7000 psi) under the vibrational conditions anticipated for the Space Shuttle engine.

The program scope required that appropriate measuring techniques be developed to a "breadboard" stage suitable for experimental verification under the required conditions. Devices optimized for particular pump applications were not required.

The program was executed in three phases. In Phase I (Feasibility), a literature survey was conducted to determine candidate techniques, calculations were made to assess feasibility of various approaches, and several feasibility experiments were performed. In Phase II (Development), three techniques were developed to the breadboard stage. In Phase III (Experimental Verification), the three techniques were, as appropriate, subjected to 48.2 MN/m^2 (7000 psi), cryogens, and vibration, and vibration measurements were made on components operating at speeds approximating 35,000 rpm. The work statement for the program is reproduced in Appendix A. The test plan for Phase III is reproduced in Appendix B.

This report is organized into three main sections; each deals with one of the three phases. Each section is organized on the basis of the various technical approaches pursued. At the outset of the program, the work was divided into six areas of technical responsibility and a specialist assigned to each, so the Phase I report section is divided into six technical sections. At the end of Phase I, three approaches were selected for development: ultrasonic Doppler analysis, flash X-radiography, and light-pipe-reflectance analysis. Thus, the report sections which cover Phases II and III are organized according to these three topics.

PHASE I. FEASIBILITY STUDY

Initially, the program was divided into the following general areas of technical responsibility.

(1) Ultrasonic techniques
(2) Neutron techniques
(3) X-radiography
(4) Optical devices
(5) Radioisotope and gamma ray devices
(6) Conventional displacement sensors.

A recognized specialist from Battelle's Columbus Laboratories (BCL) was assigned responsibility for each area. Other specialists were, from time to time, consulted in various related areas. Although the major emphasis was placed on "unusual" techniques which could require minimal modification of the turbopump, effort was also devoted to more "conventional" techniques which could require significant modification, in the event that the other techniques were judged not feasible.

In order to identify candidate systems for development, to identify potential measurement techniques and to determine potential problems in application to turbopumps, a comprehensive literature search was conducted.

A general search was initiated at the beginning of the program to uncover information dealing with vibration or displacement measurement in general, and measurements of turbomachinery in particular. DDC and NASA computer searches (of both classified and unclassified literature) were conducted. The open literature was also searched via abstracts of American, British, French, German, and Soviet sources.

In addition to the general search, each specialist conducted a separate search, seeking more specialized references or keywords than those that were recognized in the general search. In addition to additional DDC and NASA computer searches, the specialized technical libraries at BCL and the personal files of the specialists were included in these efforts. In all, the references and abstracts scanned numbered in the thousands, and the actual papers reviewed (either cursorily or intensively) numbered in the hundreds.

Following the literature search, candidate techniques were screened by a priori judgements based on the specialist's experience, by calculations, and in some cases, by key feasibility experiments.

Each technical area is discussed separately in the following sections.

Ultrasonic Techniques

Ultrasonic waves are capable of penetrating most engineering materials to considerable depths and they do this at low energy levels. In addition, they are capable of being guided through curved paths. They are sensitive to abrupt changes in acoustic impedance and for this reason they have been used to measure thickness of materials, to measure distances to target areas, and to locate defects in materials.

Methods of generating, detecting, and processing ultrasonic data are numerous. Several of these were evaluated as possible means of measuring the deflection of turbopump internal rotating parts. Examination of J-2 pump drawings and others representative of a variety of turbopump designs convinced us that ultrasonic Doppler techniques are the most appropriate and are definitely applicable to turbopumps; however, not all of the desired measurements are likely to be possible using this technique alone. In general, since a solid path is required from an ultrasonic source to the part measured, measurements in the turbine sections will be difficult, if not impossible. In particular, measurements of turbine-blade vibration or clearance, turbine-wheel vibration, or turbine-shaft movement may not be feasible. On the other hand, assessment of impeller or diffuser vibration or other movement in the pump sections definitely appears to be feasible. The attractive feature of the ultrasonic Doppler measurements, of course, is that if the source and receiver are rigidly fixed to the pump case, very little modification of the pump is needed.

A summary of the techniques evaluated is given below.

Methods of Measuring Thickness

Two basic principles are used conventionally to measure thicknesses. These are (1) time of travel of a pulse of energy between two reflecting surfaces, and (2) resonance frequencies of standing waves between two reflecting surfaces.

Methods Based on Pulse Travel Time. These methods are useful for measuring thicknesses or distances between static reflecting surfaces at any depth which does not exceed the penetrable depth of the ultrasonic energy. Electronic gating can be employed to restrict measurements to a specified distance.

Dynamic measurements can be made by recording the travel times between the two reflecting surfaces and the difference between them.

Basis for Rejection. There is much in favor of pulse travel time methods for measuring displacements in the turbopump system. In fact, the Doppler method recommended incorporates some of the favorable aspects of the pulse methods. Three weaknesses of conventional pulse travel-time methods that the recommended method is expected to correct are (1) need for extremely short pulse within the measurement region, (2) sensitivity to spurious echoes occurring between the echoes from the two reflecting surfaces, and (3) poor accuracies of present methods in measuring very small displacements.

Methods Based on Resonance Frequencies of Standing Waves Between Two Reflecting Surfaces. Two methods of measuring thicknesses by resonance are in common use. Both require frequency modulation. The methods used are (1) continuous wave and (2) pulse interference. The continuous wave resonance method is used to measure thicknesses of materials, such as plates, in which one surface is in direct contact with the ultrasonic probe or is separated from it by a liquid path. The pulse interference method of measurement of thicknesses is based on the differences in transmission through a material at resonance and at antiresonance. The pulse may be monochromatic with the frequency swept through a range, or it may be broadband and the received pulse subjected to frequency analysis.

Basis for Rejection. These methods cannot be applied easily to displacement measurement of turbopump components. The continuous wave measurement requires parallel surfaces of fairly large areas and high frequencies of operation. Distances to the vibrating surfaces are excessive compared with the amplitudes of vibration that need to be detected.

Methods of Measuring Vibration Amplitudes

Methods Based on Beam Interference or Deflection. Beam-interference refers to the interference by an obstacle of the propagation of a beam of ultrasonic energy. If a beam of energy is directed between two members which are vibrating relative to each other, the total energy transmitted through the gap is modulated by the relative motion. By sensing the total energy change, it is possible to determine the relative displacement between the vibrating surfaces.

Beam deflection can be used to measure displacements of vibrating bodies by shifts in positions of reflected beams.

Basis for Rejection. Beam interference and beam deflection methods cannot be used in the turbopump to measure deflections. The problem is one of appropriately locating the transducers in the turbopump to obtain the desired beam directions.

Methods Based Upon Doppler Shifts. Doppler shifts are changes in frequency observed by a receiver due to changing the distance traveled by waves between a transmitter of the waves and the receiver. A moving target can produce the changes in frequency even with the transmitter and receiver fixed in position. The change in frequency depends upon the velocity of the target and the direction of its motion.

The Doppler method is recommended for use in measuring the displacements in the rotating parts of the turbopump.

Basis for Recommendation. The Doppler method can be designed to combine the desirable characteristics of pulse methods. For instance, it can be pulsed (using pulse-sampling techniques) and gated, thus eliminating effects from vibrating surfaces that are more remote than those of interest. The received signal can be filtered over a narrow band corresponding to the maximum frequency shifts to be expected due to the target amplitudes of vibration. This filtering eliminates most vibrational noises. A further noise reduction occurs by filtering after the Doppler signal has been extracted.

Pulses for Doppler measurements can be guided to an area of interest through wave guides which may be a normal part of the structure being monitored or, if necessary, additional members conveniently located. The path should not be too complicated. Complicated paths may result in spurious indications.

The major problem with ultrasonic techniques is that of transferring energy from one medium to the next. Transfer from liquid to solid in the absence of cavitation can be accomplished effectively. Transfer from gas to solid or vice versa requires special treatment. The measurements in the turbopump will be restricted to solid and liquid paths.

Published values of the ultrasonic characteristics of cryogenic materials are favorable to the ultrasonic approach to the measurement of the vibration of the rotating parts in the turbopump.

The detector used for measuring displacements by the ultrasonic Doppler method also can be used to detect anomalous sounds (sonic analysis). Sonic analysis is often an inexpensive method of detecting incipient failures of machine parts before they become catastrophic.

Neutron Techniques

Two basic neutron techniques were considered in the feasibility study: neutron radiography and a directional fast-neutron detector. Neutron radiography was found not feasible. The development of a new fast-neutron detector conceived on this program was found feasible. Each is discussed separately below.

Neutron Radiography

Neutron radiography makes use of neutrons instead of X-rays usually used in radiographic techniques. Although neutron sources produce fast neutrons, conventional neutron radiography uses thermal neutrons to take advantage of the higher cross sections displayed by most materials for thermal-neutron capture. At the outset, neutron radiography appeared inherently attractive for the turbopump application, since neutrons can be expected to pass through relatively thick sections of metal.

The way in which neutron radiography might be used to sense vibration amplitudes would be similar to X-radiography. A radiograph might be taken, say, when the vibrating component is in its upper most position. Another might be taken when the component is in its lowest position comparison of the two radiographs might then indicate vibration amplitude, particularly if reference surfaces could be made to appear in the radiographs.

The feasibility study has been conducted on the basis of simple calculations for a simplified pump configuration. The results of this study indicated the following.

(1) Real-time radiographic examination of an operating turbopump is a practical impossibility. The time segments available to form images of components vibrating at the frequencies corresponding to typical operating speeds would require a neutron beam intensity that is not available with any existing type of neutron source.

(2) Pulsed neutron sources--reactor and accelerator--can provide time segments short enough to image components vibrating at typical frequencies, but such sources have other limitations that preclude their application to this problem. A pulsed reactor source could provide an intensity high enough to produce an image within the time of a single pulse, but the pulse rate is very low (typically several pulses per hour) so only extremely stable vibrations could be imaged. The situation with accelerator sources is similar; in this case, however, the source is intensity limited and a large number of pulses would have to be integrated to form an image, thus restricting its application to extremely stable situations.

(3) The application of thermal neutron radiography to this problem is limited by the geometrical nature of the source itself. The finite size and diffuse nature of the source, and the imaging geometry imposed by the shape and size of the turbopump produce a situation in which the geometrical unsharpness is greater than the features of interest. Our analysis indicates that further investigation of thermal neutron radiography is unwarranted.

(4) Several fast neutron sources (californium-252 in particular) provide beam geometries that are equal to or better than those attainable from X-ray sources, and thus have the best potential for this application. From the standpoint of the pump itself, attenuation coefficients are high enough to produce sufficient contrast for imaging. The conventional means of fast neutron imaging are much too insensitive to be used for this application.

(5) Turbopump materials are an important factor, but are secondary in importance to source and imaging factors, particularly in the case of fast neutron radiography. Although certain materials exhibit unusually high attenuation coefficients for thermal neutrons, the incorporation of these materials in turbopump components for the purpose of enhancing contrast does not appear to offer sufficient improvement to offset the inherent disadvantages of thermal neutron radiography in this application.

Details of the analyses leading to this conclusion are summarized below.

Turbopump Model. The turbopump model used in the analysis is shown in Figure 1; the pump was assumed to consist of solid concentric cylinders. The analysis was focused on the annulus between the two components, and in particular comprised the calculation of neutron transmission through the region of the annulus with (1) the cylinders concentric and (2) with the inner cylinder displaced. The contrast difference between these two conditions is indicative of the capability to detect radial vibration of the inner cylinder with respect to the outer (or vice versa). Only two-dimensional aspects were included. In the case considered for thermal neutron transmission the source was assumed to be a line source of 1-inch length, positioned perpendicular to the tangent through the center of the annulus; for the case of fast neutrons, a point source on the same line was assumed.

In the early work using this model, the material was assumed to be titanium. Although this assumption was later found to be incorrect, the conclusions that were drawn from this work would not be altered significantly by the presence of other materials, so the work was not repeated.

Real-Time Imaging. The most desirable method to observe vibrating components is of cource to record the motion of a component in real time; this approach eliminates the possibility of overlooking transients and of introducing ambiguities by sampling processes. The feasibility of applying real-time imaging was examined on the basis of the neutron transmission through the pump model and the signal-to-noise ratio required to produce a discernible image of the gap between the inner and outer cylinders. The signal-to-noise ratio is defined as

$$R = \frac{N_1 - N_2}{\sqrt{N_1}} \quad , \tag{1}$$

where N_1 is the number of neutrons transmitted in the region of the gap, and N_2 those neutrons transmitted through the inner wall of the outer cylinder just adjacent to the gap. The minimum value of R for photographic imaging is 3. The contrast is defined as

$$C = 1 - \frac{N_2}{N_1} \quad . \tag{2}$$

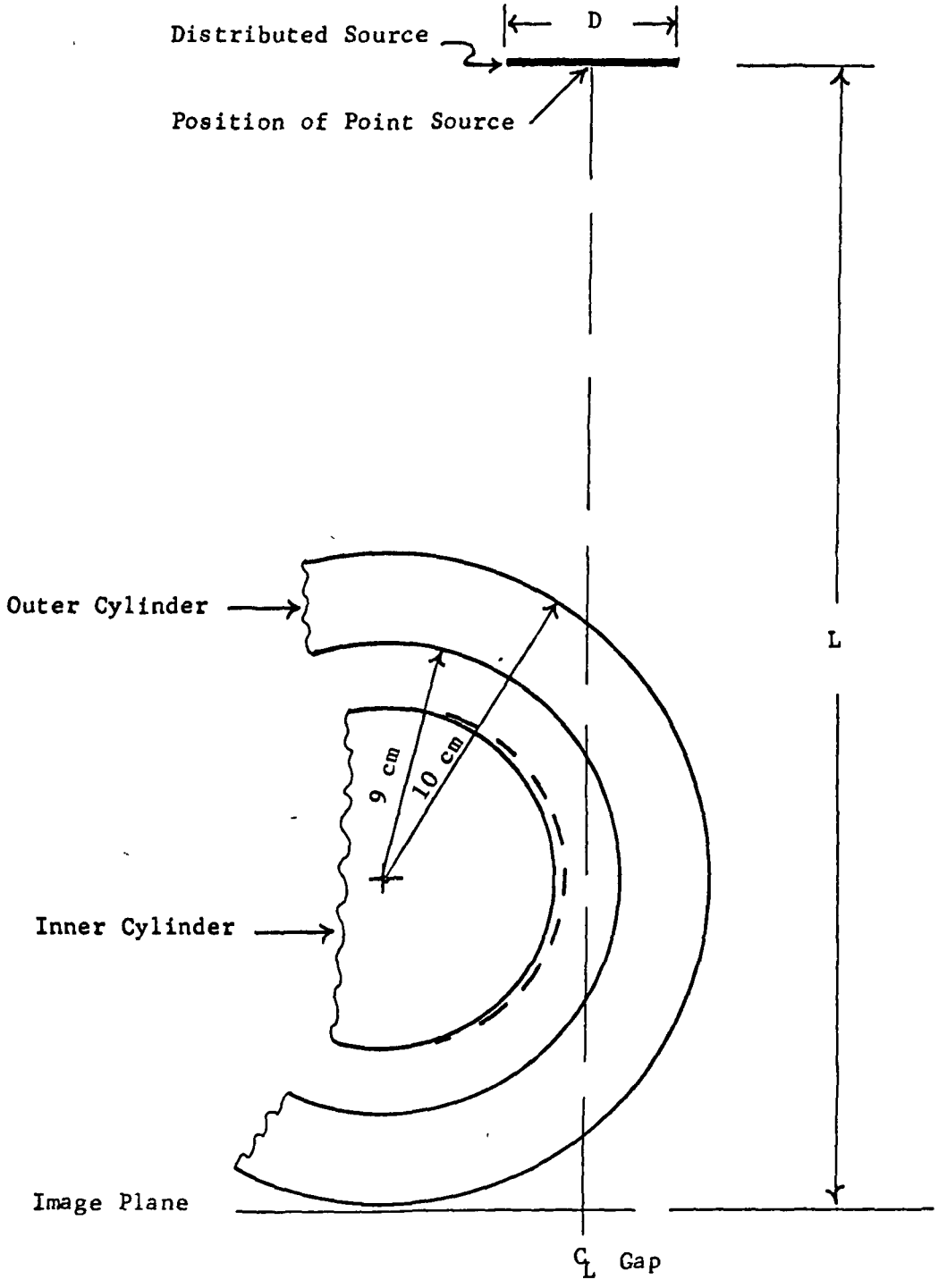

FIGURE 1. PUMP MODEL AND SOURCE LOCATION USED IN ANALYSIS (NOT TO SCALE)

For titanium in the configuration shown in Figure 1, the calculated value of C is 0.384. Combining Equations (1) and (2) and solving for N_1 for the given values of R and C gives

$$N_1 = \frac{R^2}{C^2} = 61.2 \quad . \tag{3}$$

Considering the diameter of a resolution element to be half the gap width and assuming this to be 0.01 inch for the sake of this argument, the required neutron fluence is 1.2×10^5 neutrons/cm^2. For a rotational speed of 36,000 rpm and assuming that the time segment allowable for a single image frame is 1/10 revolution, the frame time is 1.67×10^{-4} seconds and the required transmitted flux is 7.3×10^8 n/cm^2-sec. Furthermore the neutron transmission through the region of the gap is 0.013, so the required flux incident on the pump is 5.4×10^{10} n/cm^2-sec. This flux is considerably higher than the flux available from any collimated thermal neutron source, with the possible exception of a pulsed reactor. Since pulse repetition rates for such reactors are quite low (several pulses per hour) they would be of little value in real-time imaging. For the reasons presented, real-time imaging in this application is considered to be a practical impossibility.

Thermal Neutron Radiography. The alternative to real-time imaging is image formation by time integration of the transmitted neutron beam. One approach to this integrating process is the conventional process of continuous integration that is commonly employed in neutron radiography. The successful application of this approach depends on the ability of the image-forming system to record the time-averaged neutron transmission through a vibrating component with sufficient contrast and resolution to distinguish the difference between this image and one produced under static or stable conditions.

This situation was investigated by the use of the model described above; the neutron transmission profile in the region of the annular gap was calculated for two positions of the inner cylinder. To allow for the effects of the distributed nature of thermal neutron sources, a finite sized source was assumed, and the effects of its distance drom the pump were included. The image plane in all cases was assumed to be tangent to the outer cylinder and perpendicular to a line through the center of the source and the center of the gap.

The results of these calculations are summarized in Figure 2, which shows the relative thermal neutron transmission in the region of the gap for the two positions of the inner cylinder. The normal gap was taken to be 0.5 mm (20 mils), and the displacement of the inner cylinder 0.12 mm (5 mils) inch. The contrast obtained between these two cases is plotted in Figure 4 (with the corresponding fast neutron contrast).

This analysis shows that under the best conditions, thermal neutron radiography does not produce a sufficiently sharp image to show the location of a displaced component (the situation would of course be much less favorable under real conditions where the image would be produced by the time-averaged position of a vibrating component). Figure 4 shows that even though the displacement of the inner cylinder produces a discernable contrast, this contrast is not associated geometrically with the displaced component. The source geometry is responsible for this image unsharpness, and since this is an inherent feature of thermal neutron sources, it is clear that thermal neutron radiography is not suitable for this application.

Fast Neutron Detector

The fact that source geometry and not the neutron absorption properties of the components is responsible for the unsuitability of thermal neutron radiography suggests that the use of fast neutrons might yield the required sharpness, since fast neutron sources of extremely small size are available. Fast neutrons would also have the possible advantage of a somewhat higher transmission through the pump since cross sections are lower at the higher energy. Simply substituting fast neutrons for thermal neutrons, however, does not improve the situation, because the efficiency of conventional detecting and imaging methods is too low for fast neutrons. Further, the ratio of scattering to capture cross sections is high enough for most materials to substantially reduce contrast. A new detector concept, described subsequently, was to overcome these difficulties with fast neutrons.

To assess the suitability of using fast neutrons to detect component displacements, the calculations described above were repeated for a point source of neutrons and with appropriate changes in neutron absorption coefficients. The results of these calculations are shown in Figures 3 and 4.

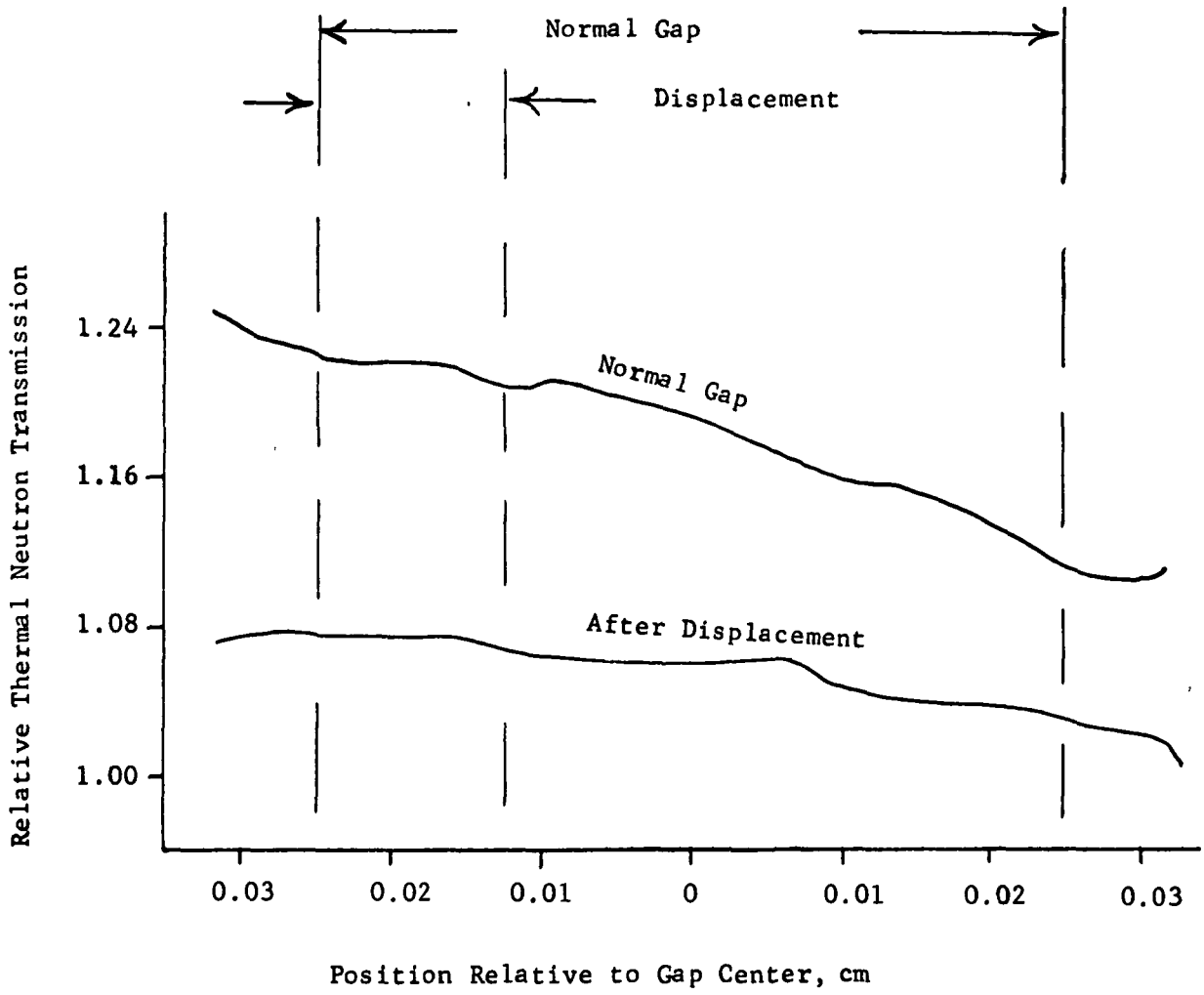

FIGURE 2. THERMAL NEUTRON TRANSMISSION PROFILE

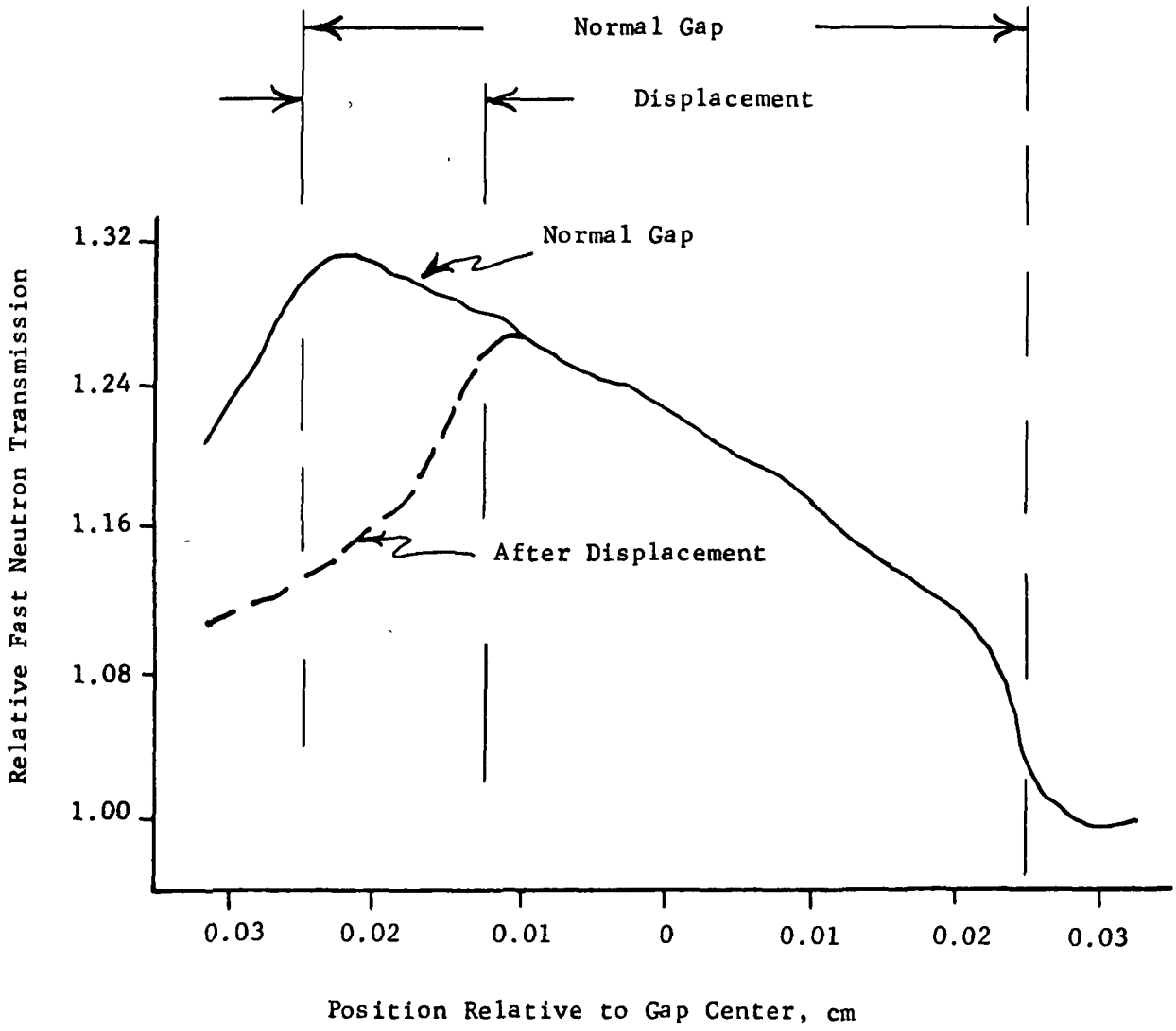

FIGURE 3. FAST NEUTRON TRANSMISSION PROFILE

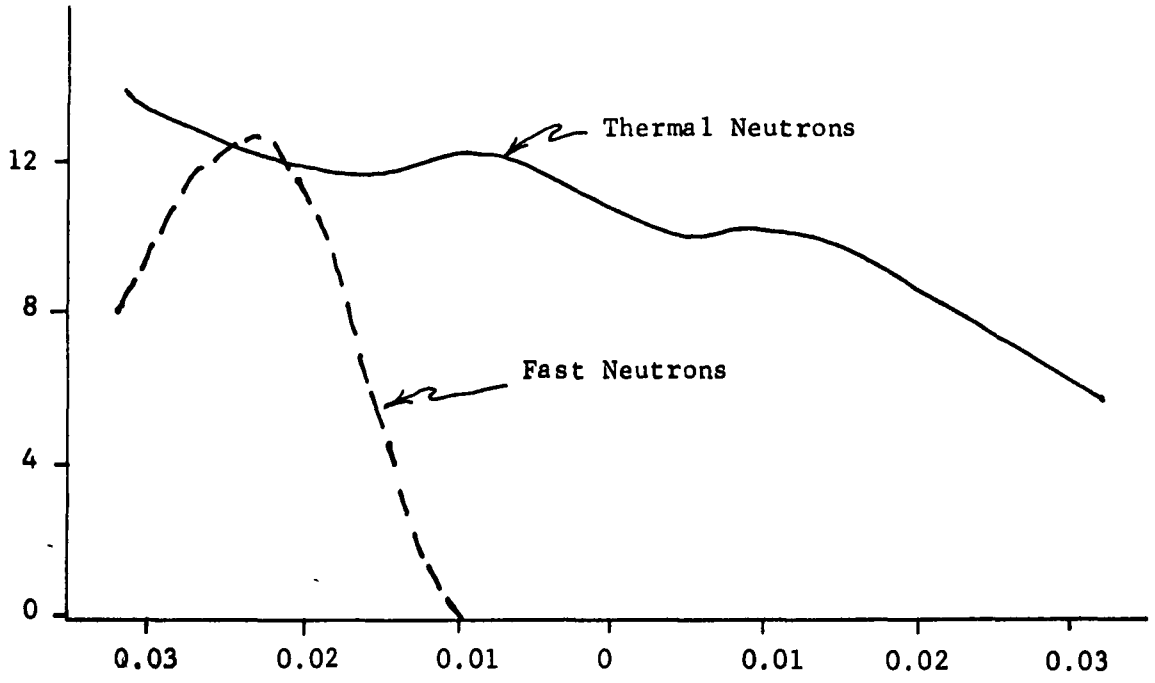

FIGURE 4. THERMAL AND FAST NEUTRON CONTRAST IN REGION OF GAP FOR 0.12 mm DISPLACEMENT OF INNER CYLINDER

The calculations clearly show that fast neutrons would yield significantly more information than thermal neutrons and it appears that they would yield sufficient information to image displacements somewhat smaller than the 0.12 mm (5 mil) displacement used in the calculations.

Detector Concept. The detector consists simply of a long thin tube of an organic scintillator material; the length provides the thickness necessary to achieve a high collection efficiency, the diameter determines the resolution, and the use of an organic material supplies the required sensitivity to fast neutrons. Calculations were made to estimate sensitivity, and a device was constructed and evaluated experimentally.

Figure 5 is a sketch of the fast-neutron detector itself. A glass capillary tube is filled with liquid organic scintillator. Fast neutrons captured by the liquid scintillator ultimately produce light photons which are detected by a photomultiplier tube. Electrical pulses from the photomultiplier are taken through conventional amplifiers and scalers for shaping and storage.

Vibration of turbopump components is measured by locating the neutron source and the detector along the tangent to, say, a radially vibrating shaft or impeller. As the shaft or impeller vibrates in and out of the beam, more or less neutrons are absorbed and the change in intensity is noted at the detector. The use of a long, narrow tube of liquid scintillator is to provide directionality. When the axis of the tube is aligned with the direction of the beam, the intensity is maximum.

Two possible ways exist to make vibration measurements. The electrical signal from the photomultiplier could be gated over a short time interval corresponding to a particular shaft or impeller position, and neutron counts for this position integrated over a number of revolutions. Comparison of two positions 180 degrees apart would yield vibration displacement magnitudes. Such a measurement could be made with a relatively low intensity source. Conversely, the time interval could be enlarged, or the source intensity increased, to make a real-time measurement.

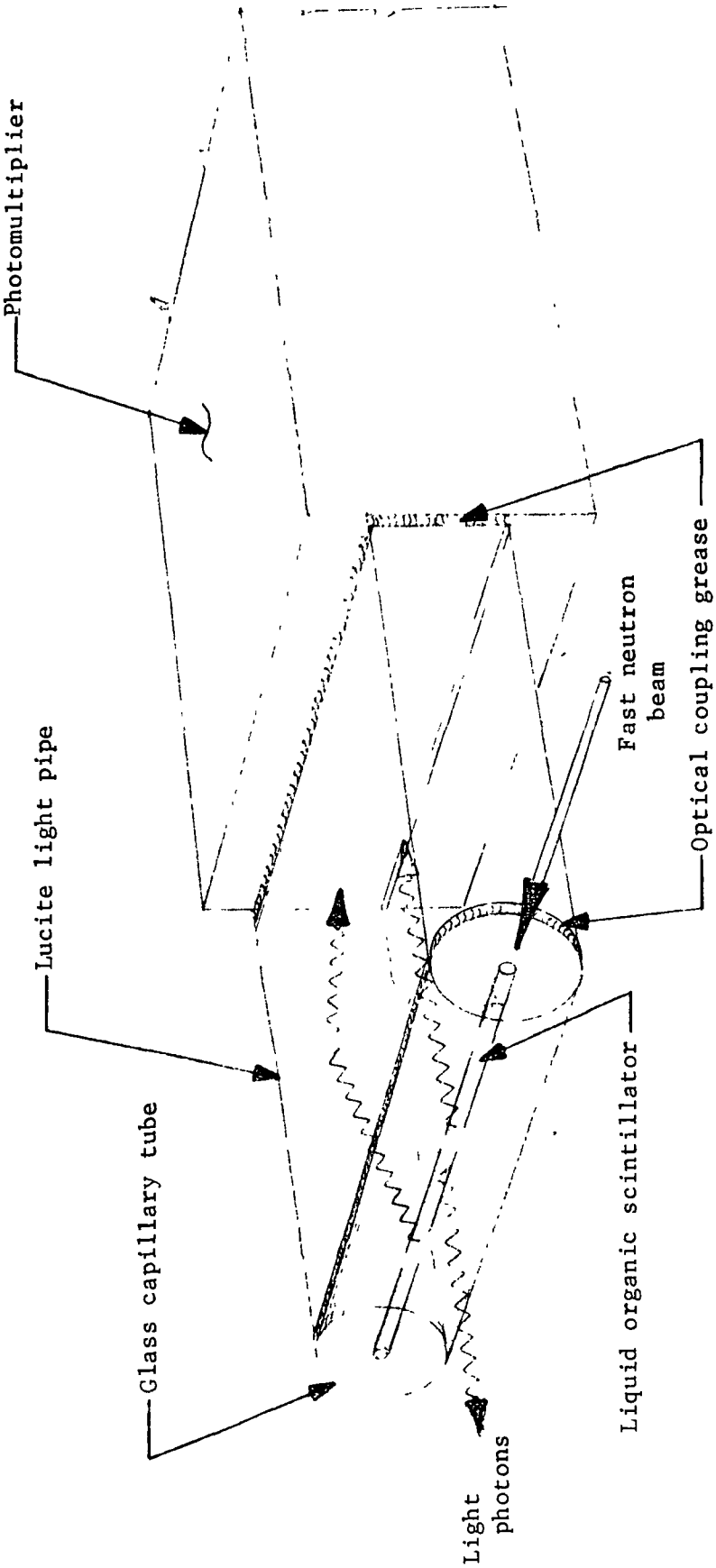

FIGURE 5. SKETCH OF FAST NEUTRON DETECTOR USED FOR EXPERIMENTS

Results of Feasibility Calculations and Experiments. The detector used in the experiments was a 0.63-cm (1/4 in.) diameter by 5-cm long glass tube with a 1.5 mm hole filled with NE-218 (Nuclear Enterprises, Ltd.). Experiments were performed using a weak plutonium-beryllium fast-neutron source.

Originally, light coupling to the photomultiplier was made through a flexible fiber-optic bundle. Sensitivity was disappointing: about 376,000 neutrons were counted in 10 minutes. In addition, photomultiplier sensitivity to neutrons and gamma radiation tended to obscure the desired signal. The use of the solid light pipe, however, improved the sensitivity by greater than a factor of 20.

Calculations were made on the basis of the experimental results to determine the relationship between them and the counting time required to obtain sufficient neutron counts. A pump diameter equal to a source-to-image distance of 51 cm (20 inches) was assumed, and the pump material was taken to be INCO 718. The calculated sampling time for detectors of from 0.4 mm to 2.5 mm in diameter is 40 milliseconds assuming a 100-mg californium-252 source and a gap varying from 0.25 mm to 0.5 mm (0.25 mm = 10 mils vibration amplitude). Sampling time is the total time the counting system would be gated to accept counts; i.e., if the gating interval were 1/10 revolution at 35,000 rpm, the pump would have to rotate about 240 revolutions, or 0.4 second, to achieve the 40 millisecond sampling time. The use of a 10-milligram source would require 2400 revolutions or 4 seconds.

These calculations are only approximate, but give a good idea of the times involved. To obtain real-time measurements with the above example, an intensity 200 times larger, or 20 g, would be needed. Predictions of costs of californium sources for the late 1970's are $2 to $3 per microgram. On this basis, a 10-mg source appropriate for integrated-time measurements would cost about $25,000, a 100-mg source about $250,000, and a 20-g source would be out of reach. On the other hand, the price of today's sources is considerably less than that predicted a few years ago, so real time measurements may someday be feasible. In any case, the technique has definitely been proved feasible for integrated-time measurements.

X-Radiography

The most appropriate X-ray technique for the turbopump application is the use of a pulsed X-ray source, otherwise known as flash X-ray. Commercial units are available with 300 kilovolt, 600 kilovolt, and 2 megavolt energy outputs with a discharge time of about 20 nanoseconds. These units emit X-rays having approximately the energy required to pass through a turbopump with sufficient intensity remaining to expose a photographic film. The lower-energy units have the possibility of using multiple sources, or heads. By using two heads which are pulsed a few milliseconds apart, it appeared possible to make real-time measurements of two successive positions of a vibrating part, thus measuring displacement in a given time interval.

Three basic problems were identified as requiring evaluation to determine feasibility of the X-ray technique: (1) insufficient penetration, (2) the existence of a penumbra (due to a finite X-ray source) may obscure small displacements, and (3) the internal structure of the pump may scatter the X-rays sufficiently to reduce sensitivity below an acceptable level.

With regard to the penumbra problem, recent advances in photography and analysis of prints have occurred which would appear to permit the small displacement to be extracted from the exposed photographic plates. The recent work has actually been done in regard to neutron radiography, so the results apply there as well.

Scattering Experiments

In order to evaluate the scattering problem, a series of simple experiments were conducted using Battelle's 300-kva flash X-ray unit.

These involved the use of a 3.8-cm-diameter mild steel shaft with abrupt reductions in radius of 0.12 mm (5 mils), 0.25 mm (10 mils), and 0.5 mm (20 mils). First a flash X-ray was taken with the source and film about four centimeters from the shaft. Resolution was excellent; the 0.12 mm step was readily apparent on the film negative.

Next, a 2.5-cm-thick aluminum plate was interposed between the source and shaft to simulate scattering by the pump case. Resolution was not reduced significantly.

The final experiment with the stepped shaft involved evaluation of focal point migration with pulse repetition. The shaft (with interposed aluminum plate) was exposed twice at half intensity. No difference was observable with the negative from the previous experiment. The result of this experiment shows that focal point migration in the X-ray tube is insufficient to cause a significant loss of resolution. In addition, it suggests that repetitive pulsing may be a means to increase intensity. Flash X-ray units are available with up to 10 heads for repetitive pulsing.

An additional experiment with a small (15-cm-diameter) electric motor was performed. Radiographs were taken with the motor stationary and running at 1200 rpm. It is not possible to distinguish between the to radiographs without identification. Good definition of wires and components within the motor is apparent. Definition of bearings and components behind thick metal sections is not good, however, suggesting that penetration may be inadequate for the pump section of turbopumps.

The fact that a 0.12-mm step can be detected by the naked eye in the shaft experiments indicates that much smaller variations could be detected by photographic processing and densitometry. The fact that excessive scattering was not observed in the motor photographs suggests that flash X-rays are appropriate for complicated structures.

Experiments with Pump Components

Experiments with J-2 LOX pump components demonstrated that X-rays from the 300 kilovolt unit did not produce sufficient penetration of the pump sections to expose the film. Consequently, feasibility experiments needed to be performed with a higher intensity X-ray apparatus. A 2-megavolt X-ray unit was located at McMinnville, Oregon, and portions of the J-2 pump were taken there for study. These experiments showed that 2-megavolt flash X-rays yielded adequate penetration for the turbopump application. The portions radiographed were the turbine wheel assembly (Figure 6) and the shaft-bearing-seal assembly (Figure 8).

Initially, we found that we were unable to obtain sufficient contrast with the apparatus. The energy (2 megavolts) of the X-rays is so high that very few were abosrbed to expose the photographic film being used. To increase

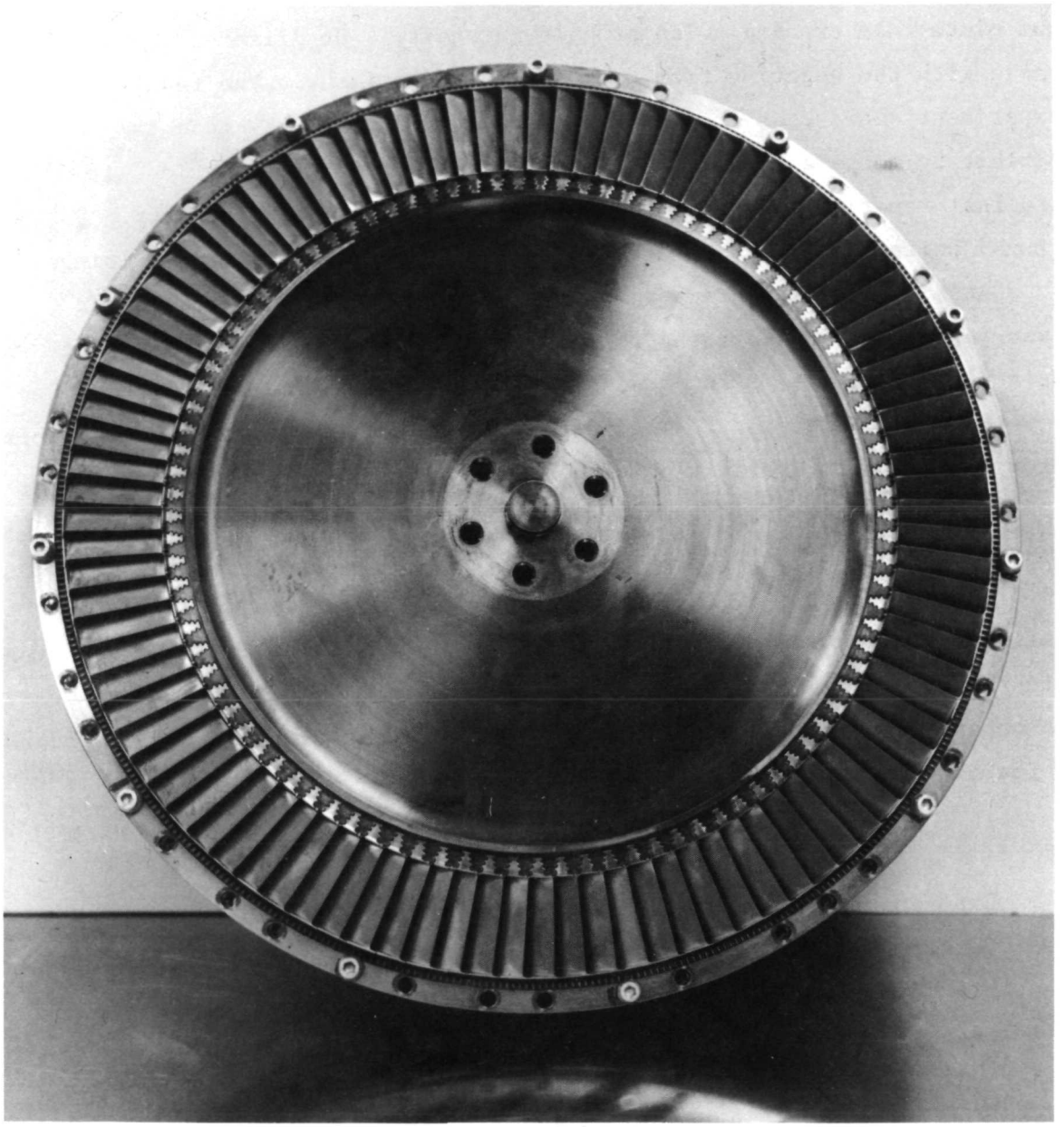

FIGURE 6. PHOTOGRAPH OF TURBINE WHEEL ASSEMBLY

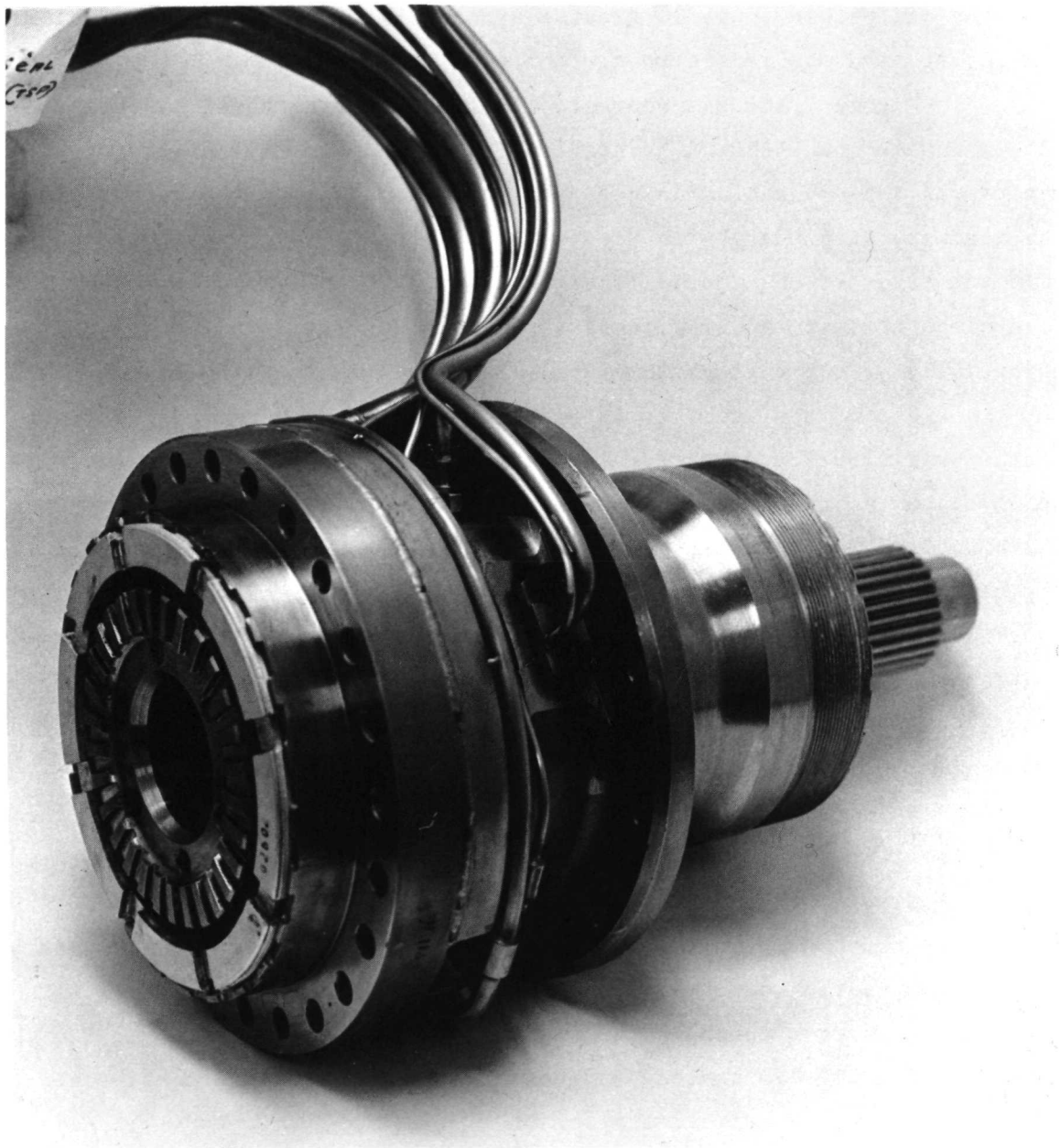

FIGURE 8. PHOTOGRAPH OF SHAFT-BEARING-SEAL ASSEMBLY

exposure, a phosphor plate was placed behind the film. Backscattered radiation from the plate then provided greater exposure; however, the use of backscattering tends to reduce resolution.

Figure 7 shows a radiograph* of the turbine wheel assembly, consisting of two wheels, two sets of rotatable blades, and a set of stationary blades separating the rotatable blades. The radiograph was, of course, taken with the assembly stationary. In Figure 7, the wheel axis is vertical, and the outer diameter of the wheels is at the left. The bright area at the bottom is a piece of lead, so brightness represents absorption. The X-rays were essentially passed through the wheels parallel to the plane of the wheels.

One of the items of interest is the position of the labyrinth seals on the wheels surrounding it. At the upper left of Figure 7, the single-convolution labyrinth seal on the upper wheel is clearly visible. As expected, the honeycomb material around it on the outside is nearly transparent to X-rays. The fuzziness of some of the edges of the turbine blades is undoubtedly due to at least four things: backscattering from the phosphor plate, scattering in the metal components themselves, inperfect alignment of the X-ray beam with the plane of the wheels, and the finite size of the X-ray source.

We were initially puzzled that the relative dimensions of the bottom wheel in the radiograph in Figure 7 did not seem to agree with a cross-sectional drawing of the pump. In addition, the single-convolution labyrinth seal on the bottom wheel is obscured, whereas its counterpart is clearly visible on the top wheel. It seemed almost as if the bottom wheel were upside down. Now, several months later, we have found the explanation. The wheel is upside down. The mounting splines on both sides of the wheel are the same, permitting reversed installation.

---

* It must be emphasized that prints of X-rays are always inferior to the negatives. Negatives can display a much wider range of intensities than do prints. A print is able to display detail for a particular narrow intensity range only. Detail existing on the negative within brighter or darker areas is completely lost on the print.

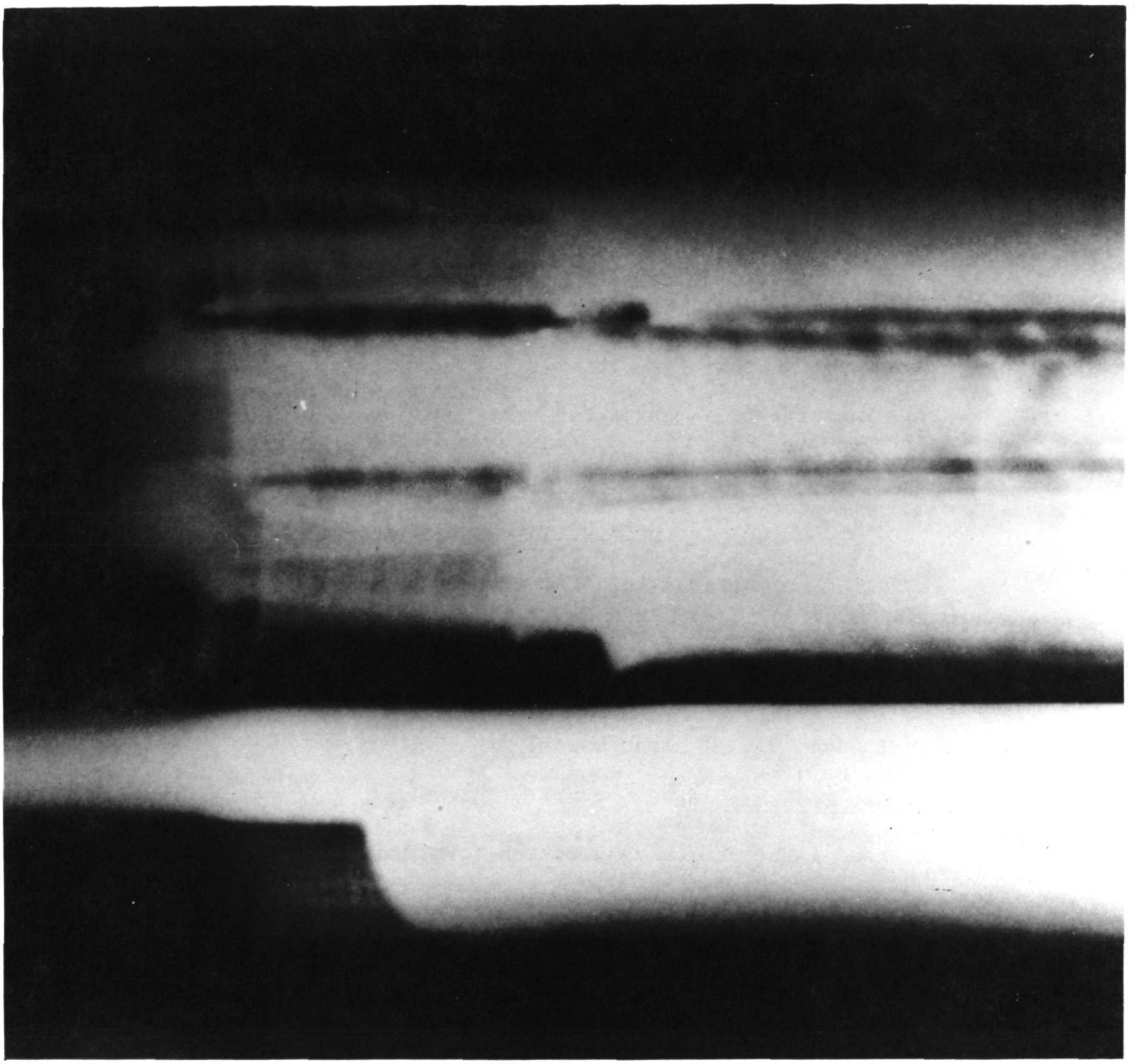

FIGURE 7. FLASH X-RADIOGRAPH OF TURBINE WHEEL ASSEMBLY

- Bright areas represent absorption; dark areas represent transmission.
- Exposure obtained with 2-megavolt X-rays.
- Wheel axis vertical.
- Bright area at bottom of photograph represents a lead block.

Figure 9 shows a flash X-radiograph of the shaft-bearing-seal assembly. The shaft axis is nearly horizontal. The bearing balls are clearly visible as is the thickness of the shaft. Closer inspection also reveals various sets of holes drilled into the shaft and other components (the various features are significantly clearer on the original than on the halftone reproduction in this report). The seal assembly, to the left of the bearing, is only partially represented. Most of the seal components were removed before radiographing. The ring directly to the left of the bearing with a conical surface about 35 degrees to the horizontal is one of the stationary members of the seal.

The experiments demonstrated that the 2-megavolt X-rays are sufficiently penetrating to be useful for the turbopump application.

Optical Techniques

A variety of optical measurement techniques were identified as a result of the literature survey. Each was evaluated for the turbopump application. The light-pipe-reflectance device was selected as the most appropriate. The various techniques are summarized in Table 1. A brief description of each type is given below.

Intensity of Gap Transmission

A broad light source is directed toward a gap separating two surfaces whose relative location is to be measured. An intensity detector measured the transmission of light by the gap. The detector signal is proportional to the size of the gap and hence gives the lateral location of one surface relative to the other.

Edge Gradient Locator

This technique uses an image scanning device such as a flying spot scanner to give the lateral location of a surface by the difference in image contrast across an edge. The edge can be an actual discontinuity in the surface or can be a painted or etched pattern having a sharp boundary between areas of differing luminance.

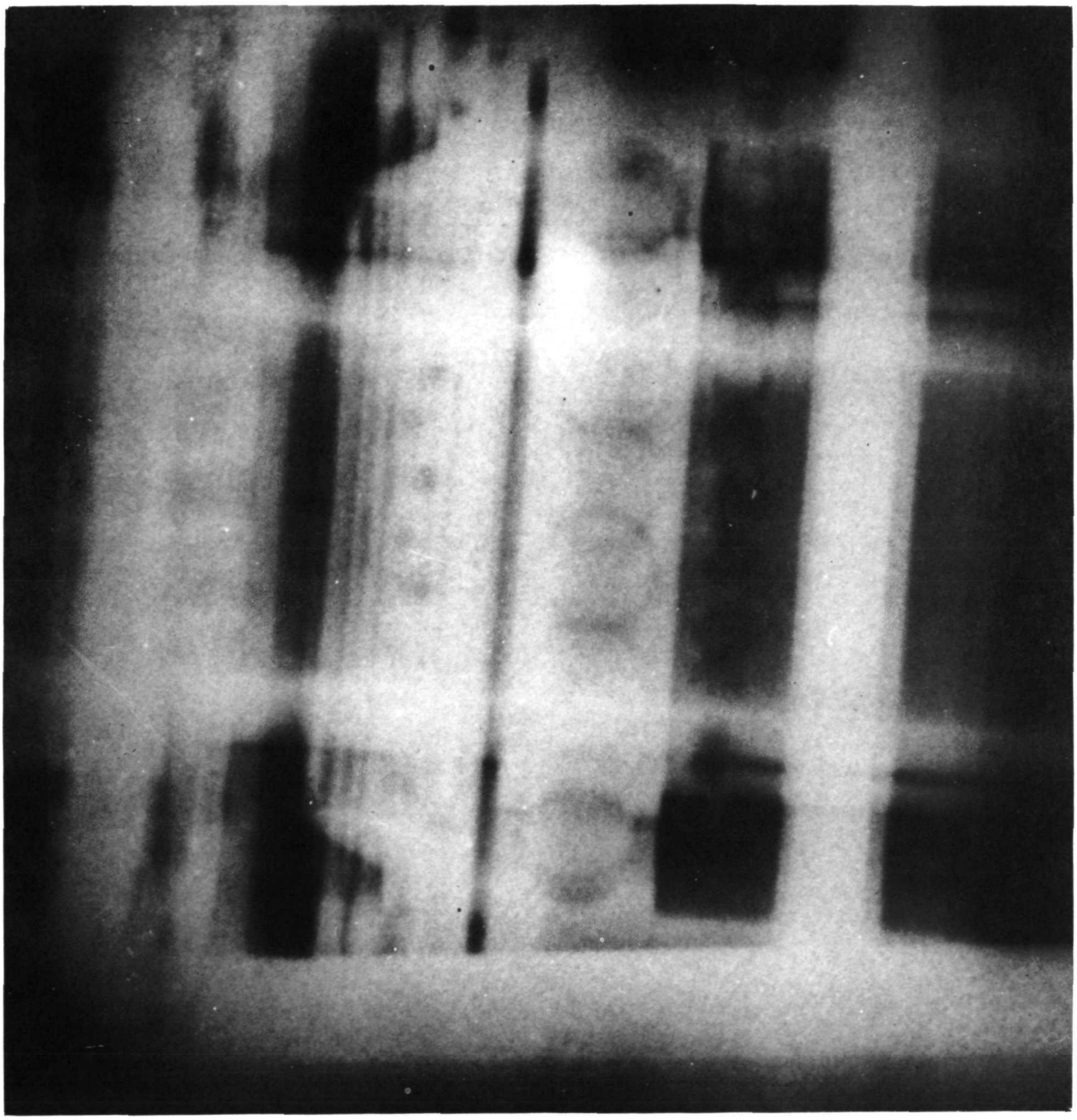

FIGURE 9. FLASH X-RADIOGRAPH OF SHAFT-BEARING-SEAL ASSEMBLY

- Bright areas represent absorption; dark areas represent transmission.
- Exposure obtained with 2-megavolt X-rays.
- Shaft axis horizontal.

TABLE 1. ESTIMATED CAPABILITY OF VARIOUS OPTICAL APPROACHES TO MEASURING VIBRATION

Type of Technique	Parameter Measured	Estimated Performance		
		Range in mm	Resolution in mu	Frequency Limit in cpm
Intensity of gap transmission	Displacement	12.70	38.1	10^4
"	"	0.25	0.03	n.a.(a)
"	"	1.02	33.0	10^9(?)
"	"	6.35	63.5	10^2
Edge gradient locator	"	6.35	33.0	10^6
"	"	6.35	25.4	10^6
"	"	6.35-0.40	63.5-0.51	10^6
"	"	6.35-0.48	1.5-0.76	n.a.
"	"	19.05	5.1	$> 10^5$
"	"	2.03	12.7	10^2
Surface triangulation	Displacement	1.03-0.02	10.2-0.10	10^6
"	"	0.30	0.10	n.a.
Interferometer	"	0.01	0.10	3,000 to $2x10^6$
"	"	12.70	0.13	$6x10^5$
"	"	5.08	1.27(?)	$6x10^5$
Light pipe/ reflectance	"	3.18	63.5	$2x10^6$
"	"	1.02	25.4	n.a.
Diffraction by a gap	"	3.18	38.1	$3x10^6$
"	"	0.18	0.25	$6x10^5$
(unknown)	"	5.08	25.4	n.a.
"	"	0.25	2.54	10^5(?)
Laser/speckle	Speed	(Resolution ~ 1%)		$3x10^4$ to $3x10^5$
"	"	160 meters/sec	± 1.4%	n.a.
Mirrors on twisted shaft	Torque	(Accuracy of 1% of full load 50,000 rpm)		

(a) Indicates not available.

Surface Triangulation

This method uses a light source to project a spot or line of light at an angle to a surface normal. A detector system is used to determine the size or location of the illuminated area on the surface. This gives a longitudinal location of the reflecting surface relative to the source detector system.

Interferometer

This method measures the relative longitudinal location of two surfaces by using the interference of coherent waves reflecting from the surfaces. The surfaces must be nearly optically flat in order for the interference pattern to be simply detected and analyzed. Holography has been used within the last decade to circumvent the requirement for optically flat surfaces, but suffers drastically from a lateral shift of the surface relative to the hologram.

Light Pipe Reflectance

One end of a fiber light pipe is placed in proximity to a surface whose relative longitudinal displacement is to be measured. Light is directed down a portion of the bundle of fibers and scatters from the surface being measured. Some of the scattered light will impinge on the remaining fibers of the light pipe and be conducted out through the bundle to an intensity detector. If the active end surface of the light pipe is flat against the surface to be monitored no light gets back to the detector. As the surfaces are separated the detector signal increases up to a maximum. After the maximum is reached, the signal drops slowly as the separation is increased further. This dual behavior provides the potential for measuring either small separations with high resolution or large separations with low resolution.

Diffraction by a Gap

If coherent light is restricted by a slit or small gap, diffraction is the "self-interference" of the wave front passing through the gap. At a

reasonably long distance from the gap the pattern produced by the interference is relatively simple and bears an inverse size relationship with gap size and hence provides an indirect means of measuring relative lateral displacement.

Two optical methods have been uncovered that measure the velocity of surfaces.

Doppler Shift

Plane wave fronts reflected from two optically flat mirrors are cause to interfere with each other. An intensity detector is located to monitor the relative phase between the two waves. As one mirror moves the phase then varies repetitively and a frequency is generated that is proportional to the relative longitudinal velocity between the surfaces.

Laser/Speckle

A speckle pattern of light and dark results when highly coherent laser light reflects from an unpolished surface. This pattern is a complex interference pattern between wave fronts originating all over the illuminated area of the surface. If the surface moves, then this complex pattern moves and scintillates. If a detector receives light from this pattern through an appropriate grid then a fluctuating signal is generated whose frequency is directly proportional to the lateral velocity of the surface relative to the grid.

Overall Evaluation of Optical Techniques

A brief evaluation of each technique is given in Table 2. The light-pipe-reflectance method was selected as the best optical approach for the turbopump application.

There are two areas that limit the applicability of most of the optical techniques. These are the needs for one or more clear windows at each measurement region of interest and the necessity for one or more of the surfaces being measured to be optically flat. It is frequently difficult to provide these even for room temperature and atmospheric pressure applications except in experimental systems where the overall device design can be tailored specifically for the optical measurement. The light pipe/reflectance method, however, does not suffer from either drawback and should be generally applicable. The light pipe itself acts as the combined window and light guide

TABLE 2. EVALUATION OF OPTICAL TECHNIQUES

Type of Technique	Parameter Measured	Brief Critique
Intensity of gap transmission	Displacement	Required straight-line path through pump for each measurement site is difficult to provide. Requires two optical quality windows. No surface preparation necessary.
Edge gradient locator	"	Same as above
Surface triangulation	Beam area	One large window or two small windows of high optical quality at each measurement side are difficult to provide along with the straight-line optical path to the pump exterior.
Interferometer	Displacement	Capable of very high accuracy but high quality optical window is a problem. Straight-line path to pump exterior is needed. Optical flatness needed on surface to be measured is not likely to be available on turbopump components.
Light pipe/reflectance	"	No surface preparation needed. Torturous optical path capability is inherent because of flexibility of fiber bundle. "Window" is provided by the light pipe itself. Source and detector exterior to pump.
Diffraction by a gap	"	Same as for gap transmission
(Specific operating principal not known)	"	Insufficient information available to evaluate beyond the necessity for optical quality windows.
Laser/speckle	Speed	Indirect method of measuring vibration although perhaps providing valuable information about nonrotating surfaces.
Mirrors on twisted shaft	Torque	Developed for cryogenic pump torque measurement but not a method for measuring vibration.

which should permit optical entry from external sources and detectors to internal regions of interest through somewhat torturous paths. The reflectance technique itself depends upon diffuse scatter from the surface being measured and therefore works well with ordinary "engineering" surfaces. Furthermore, it is very possible that the use of a light pipe could be used to measure the vibration of a nonrotary surface such as a seal stator. This would be an adaptation of the laser/speckle approach to lateral velocity measurement. Although this idea is unproven the concept would be to use part of the fiber bundle to convey the laser illumination to the surface being measured. The speckle pattern would impinge upon other fibers in the bundle to convey light back to an external intensity detector. If the detector fibers can be scaled and arranged suitably then they may behave much like the detector grid does in the conventional lasser/speckle approach.

Radioisotope and Gamma Ray Devices

Gamma ray devices are inherently attractive because it is relatively easy to locate a gamma source on the surface of internal moving parts by diffusing small amounts of a radioisotpoe into surface material. The basic problem to be faced is the development of a detection scheme which will indicate vibration and displacement of the source. The only potential detection technique* identified was Mössbauer absorption. This technique was considered carefully as described below, but it was found not feasible for the turbopump application.

Mössbauer Detection

The Mössbauer effect, first observed in 1957 by R. L. Mössbauer, involves resonant absorption of gamma radiation by atomic nuclei. The effect is exhibited by certain radioisotopes with extremely narrow line width. A common Mössbauer radioisotopic source is Co^{57}. This isotope decays by the nuclear capture of a K-electron to form an excited nuclear state of Fe^{57}. The excited Fe^{57} nuclei then drop to the ground state by one of two routes:

---

* Gamma radiography was considered to be the same as X-radiography.

emission of a 137 kev gamma photon, or emission of a 123 kev gamma photon followed by the emission of a 14.4 kev gamma photon. Approximately 91 percent of the excited Fe^{57} nuclei decay by the latter scheme. If the original Co^{57} metal is in a crystalline form, then approximately 10 percent of the nuclei emitting 14.4 kev gammas will be constrained by the crystal lattice such that the nuclei will not recoil. The resulting recoil-free gammas will have a very narrowly defined energy, or frequency. The frequency of the gammas emitted by nuclei which are free to recoil will be Doppler-shifted by various amounts corresponding the the recoil energy of the nuclei.

The existence of recoil-free gamma irradiation leads to the possibility of detecting motion of the source. In the case of a Co^{57} source, if an absorber of Fe^{57} is interposed between the source and the detector (Figure 10), then resonance absorption of the 14.4 kev gammas will occur so long as the gammas have exactly the required energy to raise Fe^{57} nuclei to the 14.4 kev excited state. This will occur only if the source and absorber are metallurgically the same and at rest with respect to each other. If relative motion exists, the gamma energy will be Doppler shifted and resonant absorption will not occur. The effect of source velocity on transmitted intensity through the absorber is shown in Figure 11. As can be seen, the width of the absorption peak is approximately ± 10 mm/sec.

Recently, it has been shown that Mössbauer resonant absorption can be used directly to measure a mean square amplitude. First, the count rate of the radiation passing through the absorber is determined while the source and absorber are stationary. The count rate is again taken with the source in motion. The change in the count rate determines the mean square velocity of the source. For Fe^{57}, however, the relative velocity cannot exceed 10 mm/sec, as illustrated in Figure 11. For a turbopump rotating at 35,000 rpm, a velocity of 10/mm sec corresponds to about 15 micron vibrational amplitude. Amplitudes much greater than this are anticipated from shafts, turbine wheels, and blades. Thus, apart from all other considerations, it appears that this detection method with a Co^{57} source is not capable of dealing with many of the amplitudes of interest.

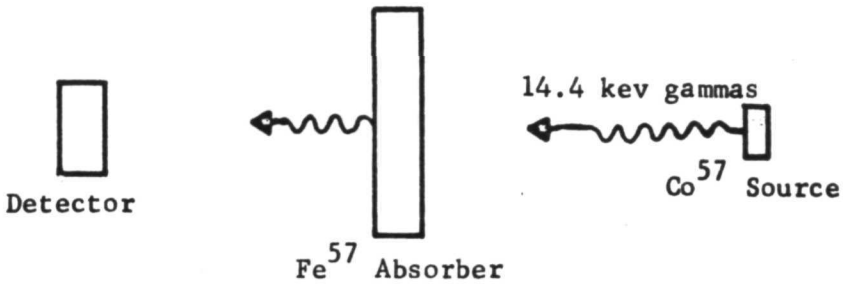

FIGURE 10. MÖSSBAUER DETECTION SCHEME

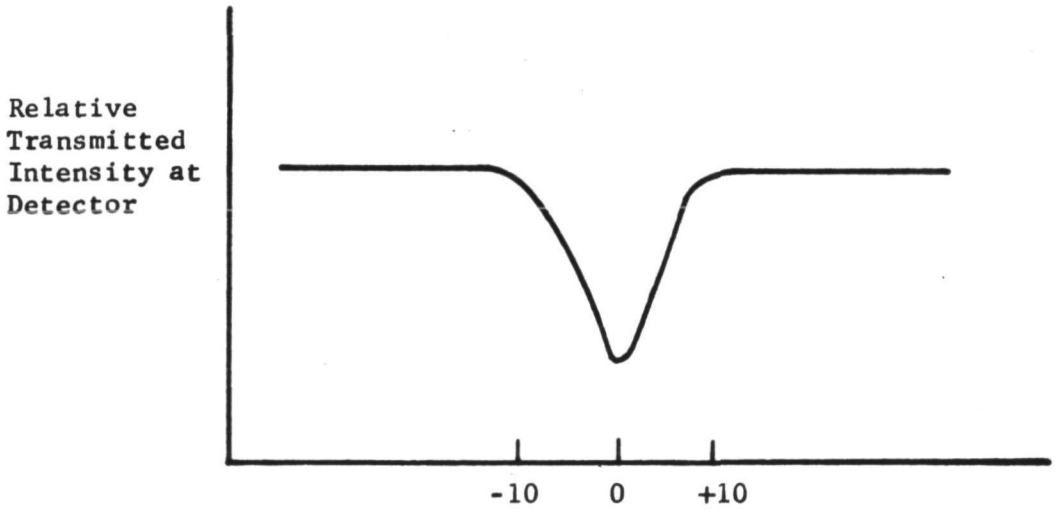

FIGURE 11. EFFECT OF VELOCITY OF SOURCE ON TRANSMITTED INTENSITY FOR Co^{57}-Fe^{57}

The other Mössbauer elements were evaluated with respect to the turbopump application, and it was determined that, by reasons of temperature sensitivity, insufficient half life, insufficient recoil-free gamma intensities, etc., they are less desirable than Co^{57}.

Absorber Movement Schemes

Detection schemes capable of sensing sufficiently large relative velocities by vibrating the absorber were considered. In these cases, frequency modulation of the absorber vibration by the source might permit both amplitude and frequency of the source to be determined. There would appear to be at least two possibilities associated with moving the absorber. The first would involve synchronizing the absorber with the source vibration. The fact that the source may vibrate at several frequencies characteristic of critical frequencies of, say, the turbine wheel, would appear to make the synchronizing system prohibitively complex. The second possibility involves vibrating the absorber at a high frequency and allowing the Doppler-shifted signal from the source to, in effect, frequency-modulate it. Our calculations show, however, that the range of Doppler velocities to be anticipated will result in numerous side bands, spreading the vibration information over such a wide range of frequencies that the inference of vibration magnitudes and frequencies may be impossible. Simply stated, Mössbauer analysis is a much too sensitive measuring technique for something as large as a turbopump.

No other detection scheme was conceived which offered a good possibility of using gamma rays.

Conventional Displacement Sensors

Basically, three kinds of techniques were evaluated in this category: magnetic sensors, capacitance sensors, and signal transmitters which do not use slip rings. Magnetic techniques evaluated included sensors measuring changes in inductance, and eddy-current sensors using either coils or Hall elements for detection. The Bentley inductance probe is currently used to measure deflections of turbopump components and, as such, can be considered as the state of the art. Application of Bentley probes requires substantial modification of a turbopump to locate the probes near the parts to be measured.

During the literature search and interviews with manufacturers, emphasis was placed on attempting to discover techniques which could be applied without substantial modification of the turbopumps. With the possible exception of FM signal transmitters, no such techniques were uncovered. The Bentley probes currently in use are, in our opinion, representative of the state of the art of magnetic and capacitance probes as applied to turbopump measurements.

Magnetic and Capacitance Techniques

Two kinds of magnetic sensing devices are available commercially. Inductive probes measure the change of inductance in a coil as the gap between the coil and the moving part changes. These require a high-conductivity material on the moving part. Eddy-current probes measure the impedance of a coil as influenced by eddy currents set up in the moving part. In some eddy-current devices, a Hall element is used in place of a coil. Capacitive devices essentially sense the change in electrical capacitance of the separating gap between a probe and the component being measured.

Both magnetic and capacitive techniques share one advantage. There are probes in each category which are highly developed and have been applied to a wide range of applications with a wide range of environmental conditions. One commercial capacitance probe made by Dynamic Data Corporation has actually been in successful service at temperatures above 2000 F. Also one type, F. W. Bell Inc.'s Hall-Pak Generators (inductive), have demonstrated successful operation at cryogenic temperatures. Several of Dynamic Data's high-temperature capacitance probes were recently operated at liquid nitrogen temperatures and apparently performed well and also did not suffer any permanent damage. It must be borne in mind, however, that the capacitance method is only feasible if no changes in the dielectric occur in the gap. This could be a limitation if the gap contains alternately liquid and gas or a mixture of these. This could pertain if cavitation occurs. A capacitive transducer face consists of concentric electrodes separated by an insulating material; because these materials are of different hardnesses there is the likelihood of differential wear in the event of cavitation or simply the erosive action of the high

velocity fluid. Such wear would be likely to change the contour of the probe face, and to some extent alter the calibration of the system. In addition, any roughening of the surface would be apt to increase the tendency for turbulence and more violent cavitation. Such a situation is self-aggravating and must lead to premature, and possibly rapid failure of the transducer. Overcoming this difficulty would involve a judicious selection of materials for probe components and/or coating the sensing face with a durable dielectric film--e.g., a sprayed-on ceramic. Another problem would be sealing of the probe and its concentric electrodes against leakage of the 48 MN/m^2 cyro-fluid. This also requires proper materials selection plus possible design improvements to produce an adequate strength as well as a minimum elastic deformation under pressure.

The inductive techniques are inherently more attractive because measurements are not affected by changes, such as cavitation, in the gap region being measured. Even the presence of a medium of low conductivity in the gap can be tolerated. One manufacturer, F. W. Bell, produces Hall effect magnetic field sensors which can be used to - 269 C; apparently other manufacturers have not yet attacked the cryogenic applications. In any event the selection of materials having low coefficients of conductivity and of permeability at cryo temperatures appears quite feasible. The other problem--differential thermal expansion effects--should prove somewhat less difficult to overcome than was the case for development of transudcers capable of operation at high temperatures. The Hall-effect type of pickup cannot be exposed to temperatures in excess of $\sim$ 150 C; in fact, they begin to lose calibration above $\sim$ 105 C. Other conventional types of inductive transducers have been applied in ambient temperature fields up to $\sim$ 1500 F.

Mechanical Technology, Inc. have designed and successfully operated transducers using ceramic insulated gold wire wound on a ceramic form. These coils have been subjected to many temperature cycles to 1500 F with no detectable degradation in the coil electrical properties. The subsequently manufactured transducer was fully encapsulated with all welded joints. This points up an inherent advantage to employing inductive transducers, the sensing function can be accomplished through a metallic sheating or bulkhead.

Thus, no roughening or differential wear or erosion rates need to be anticipated (the situation described above for the capacitative types). This construction feature also protects the internal transducer parts from the high-pressure environment. The presence of pressure-produced mechanical deflections which would change transducer calibration might pose a problem for the hermetically sealed capsule design. Application over a broad temperature range could also be expected to produce calibration changes, but optimization should be feasible.

Signal Transmission Without Slip Rings

Heretofore, consideration has been limited to sensing techniques which do not require contact with the moving part under surveillance. A more common approach, used in the past, is the application of accelerometers, strain gages, and thermocouples to the moving part. Transmission of the low power output signals from these sensors through slip-ring contacts, however, has been unsatisfactory for high-speed rotating machinery because of wear and unreliable performance of the slip rings. Recently, telemetry hardware has been developed for application to high-speed rotating equipment. An example of the refinement attained for such equipment is evidenced in the Aerotherm Corporation telemetry systems. Tiny transmitters potted to withstand 30,000 g at 125 C, are fitted into compartments in a hollow shaft or rotating support ring. The transmitters are powered by a transformer or batteries, and communicate via a modulated carrier wave to a stationary (and circular) antenna mounted about 1/8 inch away. These low-level signals are carried via co-ax cable to the receiver-amplifier and hence to a data readout or recording device. At present, transmitters are cylindrical, 15.75 mm x 28.35 mm in diameter; or rectangular, 14.15 mm square x 34.65 mm long. One transmitter is used for each signal; however, the manufacturer is currently developing a multiplexing system which will handle eight signals simultaneously.

The use of a signal transmitter appears to us to be an attractive way to do away with the disadvantages of contact-type slip rings. For best results, however, the use of a system in which the rotating and stationary components are very close together would be required. In the case of a turbopump, this would imply that the turbopump design should allow a stationary

pickup to fit inside a hollow pump shaft. Such a requirement might be a severe restriction on pump design. In any case, the use of a signal transmitter solves only half the problem. Sensors must still be located at the points of interest.

Phase I Conclusions

The feasibility study of Phase I resulted in four techniques found feasible for the turbopump applications.

(1) Ultrasonic Doppler

(2) Flash X-ray

(3) Light-pipe reflectance

(4) Fast neutron detector.

It is clear that none of the four techniques will be able to make all the measurements of interest in a prototype pump. An ultrasonic Doppler device is limited to applications where a solid or liquid path can be devised into the part to be measured from the source. This appears to remove the turbine section from its capability, because of cooling channels around the blades. On the other hand, the flash X-ray appears capable of measurements in the turbine section where metal sections are thin but the use of the 2-megavolt unit is somewhat cumbersone, and sensitivity is not so great as is that for the ultrasonic technique in the pump section where heavy metal sections exist. The fast-neutron technique may not be appropriate to thin metal sections, but it would be able to sense motions in the pump section. The fast-neutron technique is probably the most sophisticated of the four, requiring the greatest effort to develop and the highest cost to apply to turbopumps. The light-pipe-reflectance device appears somewhat limited in high-temperature capability; therefore, it would not be expected to be applicable to the turbine blades (although it is probably applicable at turbine-wheel temperatures). In addition, it requires somewhat more pump modification than do the others.

It is possible, therefore, that a combination of the various techniques might be desirable. For instance, a flash X-radiograph might be taken first to obtain diagnostic information regarding several turbopump components. Subsequently, one or more ultrasonic or optical sensors might be fitted on the pump to measure only the most critical components.

PHASE II. DEVELOPMENT OF THREE TECHNIQUES

Three techniques were selected by NASA-MSFC for development in Phase II.

(1) Ultrasonic Doppler technique

(2) Flash X-radiography

(3) Light-pipe reflectance

Specific experiments and calculations were carried out to develop each technique to a breadboard stage. To assist development, a J-2 LOX turbopump was furnished by NASA-MSFC. The pump was mounted on a test stand (Figure 12) with an external 1000 rpm drive. Measurements of vibration or runout were made on the J-2 pump with the three approaches under development. During the measurements, the pump was filled with oil or kerosene to simulate the cryogenic fluid being pumped.

Each development effort is described separately below.

Ultrasonic Doppler Technique

The Doppler Effect

When the distance that a sound wave travels between a source and a receiver varies during the time of travel, the number of wave-fronts arriving at the receiver within a given period of time differs from the number of wave-fronts emitted during a similar period of time. The pitch of the wave detected by the receiver is either higher or lower than the pitch of the emitted wave depending upon whether the travel distance is decreasing or increasing respectively during the time of travel. The change in pitch is called a Doppler effect and the difference between the transmitted and received frequencies is called Doppler frequency. The change in path length may be caused by relative motion between the source, the receiver, and reflecting surfaces along the path of the sound beam.

When the sound source and the receiver are located side-byside in a stationary position (monostatic arrangement) so that they may be considered as though they occupied the same position, the Doppler frequency caused by a single reflecting surface moving parallel to the path of the sound beam is

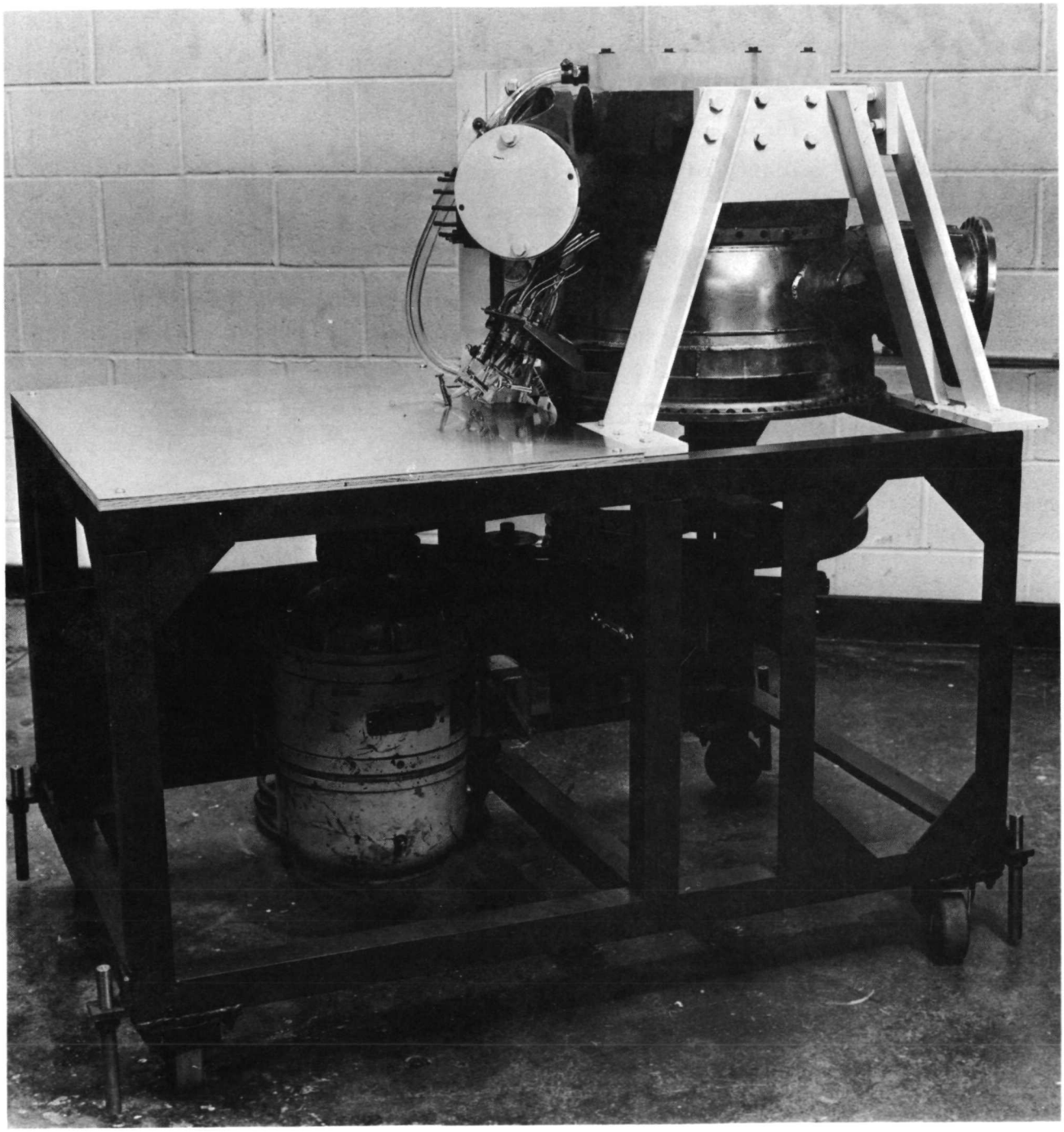

FIGURE 12. PHOTOGRAPH OF PUMP-TEST STAND

$$f_D = \frac{-2v}{c} f_o \quad , \tag{4}$$

where

v = the velocity of the reflecting surface

c = the velocity of sound in the medium in which the reflecting surface is located

f_o = the frequency of the emitted wave, or carrier frequency.

The velocity v is a function of time, and for a vibrating surface it depends upon the nature of the vibration. In the case of a sinusoidal vibration parallel to the direction of beam travel, Equation (4) may be rewritten as follows

$$f_D = \frac{-2V\cos\omega t}{c} f_o = \frac{-2\xi\omega\cos\omega t}{c} f_o \quad , \tag{5}$$

where

V = maximum velocity

ω = angular frequency ($=2\pi f_v$)

f_v = the frequency of vibration

ξ = the maximum amplitude of vibration.

A positive or negative f_D indicates that the received signal has increased or decreased from the carrier frequency. If the Doppler variation for which Equation (5) is applicable were extracted by comparing the received signal with the carrier frequency, the observed frequency amplitude would vary between zero and the maximum value regardless of the direction of motion of the reflecting surface. A plot of the magnitude f_D through a full cycle of vibration would be a full-wave rectified wave. If the received wave is compared with another constant frequency (intermediate frequency) which differs from the carrier frequency by an amount greater than the magnitude of f_D, the difference, or beat frequency, will not pass through zero. A plot of the magnitude of the difference between the frequency of the received signal and the intermediate frequency is of the form

$$A = B + C\cos\omega t \tag{6}$$

and $C\cos\omega t$ is a true representation of the implied f_D given by Equation (5).

Since the only variables in Equations (4) and (5) are those corresponding to velocity of vibration and the dependent variable f_D, Equation (4) may be rewritten

$$f_D = kv \quad , \tag{7}$$

where

k = a constant.

Thus, a plot of f_D derived from Equation (6) represents a plot of v. Since

$$v = d\xi/dt \tag{8}$$

then

$$\xi = \int v\, dt \quad . \tag{9}$$

For a purely sinusoidal vibration at a known constant frequency, the curve of f_D can be calibrated directly in terms of displacement.

These principles are applied in the ultrasonic system developed for measuring vibrations of rotating parts in turbopumps.

Influence of Ultrasonic Wave Propagation Characteristics on Effectiveness of the Doppler Method

It is important in the application of the ultrasonic Doppler method to provide for the impingement of the ultrasonic energy upon the surface to be measured and for the return of at least a portion of the reflected energy to the receiver. A consideration of ultrasonic wave propagation characteristics will aid in the selection of probe locations and orientations or modifications in turbopump designs to aid the effectiveness of the ultrasonic method.

Ultrasonic waves can be made to travel in directional beams in homogenous media. The directionality of the beams depends upon the ratio of the cross-sectional dimensions of the source to the wavelength, except in the special case of wave guides in which the boundaries of the guides limit the spreading of the beam.

Ultrasonic waves obey the same laws of reflection and refraction that apply to other types of wave motion, for example Snell's law of reflection and refraction. The angle of reflection from a boundary between two media is equal to the angle of incidence. The angle of refraction at a boundary between two media is determined by the following equation.

$$\frac{c_1}{c_2} = \frac{\sin \theta_1}{\sin \theta_2} \quad , \tag{10}$$

where

c_1 = the velocity of sound in the medium of the incident wave
c_2 = the velocity of sound in the second medium
θ_1 = the angle of incidence
θ_2 = the angle of refraction.

Figure 13 shows schematically how the principles described previously can be applied to detect and measure vibrations of a remote surface.

Figures 13a and 13b were demonstrated experimentally during Phase II. Since the primary consideration is to direct an incident beam onto the desired surface and to direct a portion of the incident energy to the receiver, the other arrangements are given for design purposes only. Obviously, Figures 13b, 13c, and 13d are simplified.

A knowledge of the exact path of the ultrasonic beam is important to the proper installation and calibration of the ultrasonic Doppler system. By applying the simple principles described previously in this section, the turbopump designer could provide a slight boss on the exterior of a pump housing which would identify a location for the ultrasonic transducers. These bosses would imply that the ultrasonic beam has an unobstructed path to and from the surface of interest. Air pockets, packings, and similar asperities in the path of the beam interfere with the transmission of ultrasound and could render the method ineffective.

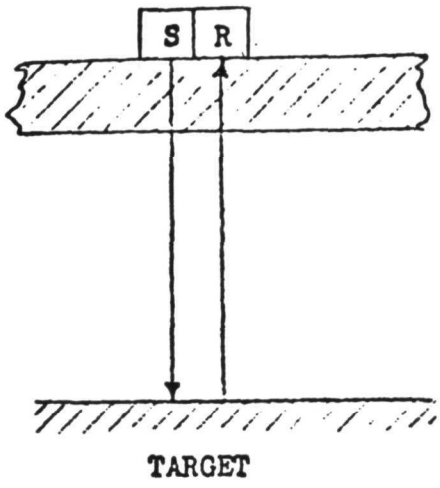

a. Direct Path

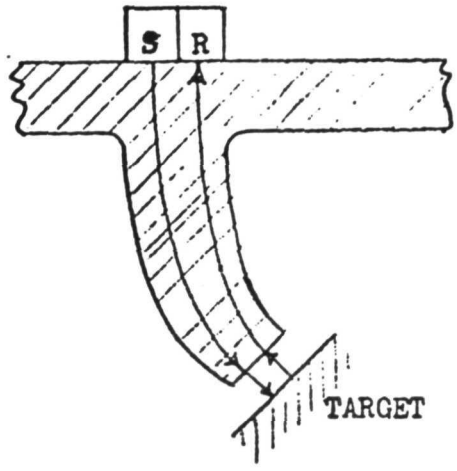

b. Wave Guide

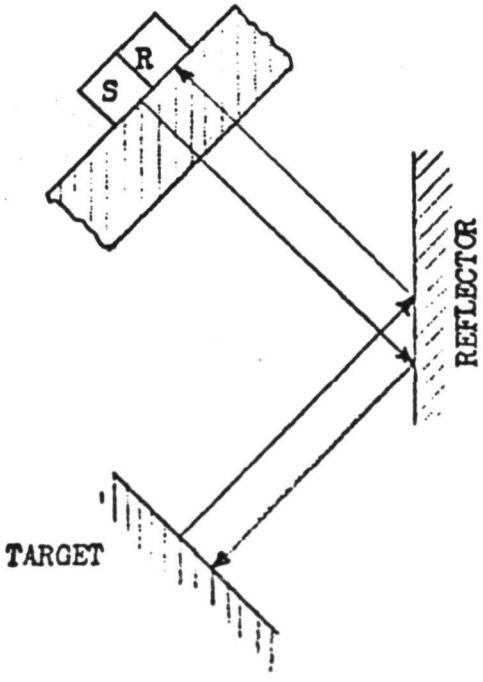

c. Intermediate Reflector

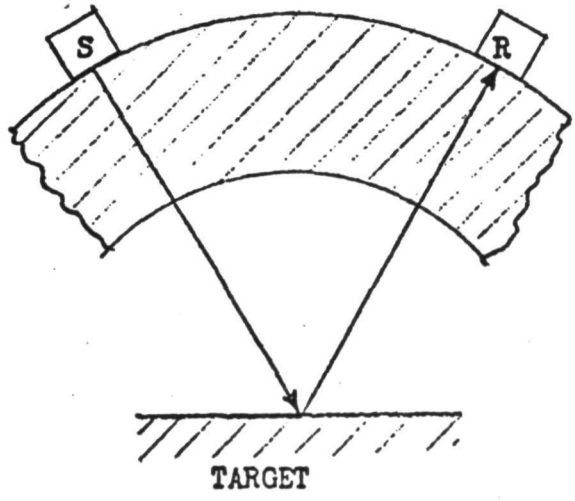

d. Bistatic arrangement for use where operation at normal incidence is not possible.

FIGURE 13. ARRANGEMENTS OF SOURCE S AND RECEIVER R THAT CAN BE APPLIED TO DETECT AND MEASURE VIBRATIONS OF A REMOTE SURFACE

Low frequencies are less directional than high frequencies. They also suffer less by attenuation. In some areas this might be an advantage, for instance in the turbine region. However, lower frequencies would be less sensitive to low amplitudes of vibration. If they are too low, they are more sensitive to normal displacements such as the movement of impellor blades or turbine buckets. These possibilities must be considered in the design of low frequency systems.

Reflection and Transmission at a Boundary Between Two Media

The intensity of the energy reflected from and transmitted across a boundary between two media also are important to the effectiveness of the ultrasonic Doppler method. The transducers used in the system developed during the present research program are sensitive to ultrasonic pressure.

At normal incidence, the equations for determining the pressures of the reflected wave and the transmitted wave relative to the pressure of the incident wave are

$$\frac{P_R}{P_i} = \frac{Z_2 - Z_1}{Z_1 + Z_2} \quad , \tag{11}$$

and

$$\frac{P_T}{P_i} = \frac{2Z_2}{Z_1 + Z_2} \quad , \tag{12}$$

where

P_R = the acoustic pressure of the reflected wave
P_T = the acoustic pressure of the transmitted wave
P_i = the acoustic pressure of the incident wave
Z_1 = the complex acoustical impedance of the medium containing the incident wave
Z_2 = the complex acoustical impedance of the medium containing the transmitted wave.

The values of Z_1 and Z_2 depend upon the location of the point within the wave at which the impedance is measured. If the two media are effectively semi-infinite, i.e., no standing waves are possible, Z_1 and Z_2 in Equations (11) and (12) may be replaced by their corresponding characteristic acoustical impedances $\rho_1 c_1$ and $\rho_2 c_2$. On the other hand, for the special case of a wave at normal incidence on a thin section one-half wavelength thick, no reflection occurs and the wave is transmitted through the section suffering only those losses associated with the internal damping properties of the section. If the section is a quarter wavelength thick, the wave is completely reflected.

The ultrasonic properties of the cryogenic materials LOX and LH_2 are similar to those of typical liquids at room temperatures. The important characteristics are tabulated in Table 3.

TABLE 3. ACOUSTICAL PROPERTIES OF LOX AND LH_2

Material	Temperature, C	ρ, g/cm^3	c, 10^5 cm/sec	ρc, 10^5 g/cm^2-sec
Oxygen	-183.6	1.143	0.911	1.042
	-210	1.272	1.130	1.437
Hydrogen	-252.7	0.355	1.127	0.400
Fresh Water	20	0.998	1.483	1.48

The acoustical properties of aluminum alloys at these temperatures are not available. However, a reasonably good estimate, at least for the purpose of evaluating the effectiveness of the ultrasonic Doppler system for measuring vibrations of remote surfaces, can be obtained by using room temperature data. A typical value of ρc for aluminum alloys is 1.75×10^6 g/cm^2-sec. From Equations (11) and (12), typical ratios of P_R/P_i and P_T/P_i at an aluminum/liquid interface are given in Table 4.

TABLE 4. REFLECTION AND TRANSMISSION OF ULTRASONIC ENERGY AT AN ALUMINUM/LIQUID BOUNDARY

Liquid	Temperature, C	P_R/P_i	P_T/P_i
LOX	-183.6	-0.8875	0.1125
	-210	-0.848	0.152
Hydrogen	-252.7	-0.955	0.0447
Fresh Water	20	-0.844	0.156

Values for fresh water at 20 C are included in Tables 3 and 4 for purposes of comparison. Transmission of ultrasonic energy from aluminum into water has often proven to be sufficient for the detection of reflecting surfaces located in the water. The energy transfer properties of both LOX and LH_2 appears to be more than adequate for the use of the ultrasonic Doppler measurement technique.

Advantages of the Doppler Method Over Other Ultrasonic Methods

In a system with as complex acoustic paths as a turbopump, an ultrasonic beam encounters many reflecting surfaces which may reflect more energy to an ultrasonic receiver than would be expected from the surfaces of interest. Although these surfaces probably are stationary, signals reflected from them would obscure the desired signals and make an accurate measurement impossible.

The Doppler method is inherently a type of correlation technique in which motion signals are separated from static signals. Only those signals within a narrow range of the carrier frequency can enter the detector system through the narrow bandpass input filter. By virtue of the means of processing the signal, only those signals which modulate the carrier (or the i-f) are eventually displayed unless the processing system develops excessive internal noise. Thus, the Doppler method provides an effective means of measuring vibrations at remote locations within an inherently noisy environment. At high frequencies, the ultrasonic beam is directional. The most

important requirement is that an acoustic path be provided for transmission of the waves to the target area and for the return of the reflections to the receiving transducer.

Apparatus Developed for Measuring Vibrations by the Doppler Method

Electronic Circuitry. Figure 14 is a block diagram of the electronic circuitry required for the displacement measuring device based upon the ultrasonic Doppler principle.

Referring to Figure 14, the power supply, R.F. oscillator 1 and amplifier are the driving source for the transmitting transducer. A laboratory model CW power oscillator was used for this purpose during the present research program.

The transmitting transducer is a piezoelectric plate. A narrow bandpass type of transducer is preferred for this function; however, during Phase II, we were able to show that good results are possible using either a broad-band or a narrow-band transducer. A narrow-band transducer with feedback control of frequency is recommended.

If the side branch consisting of low-pass filter, amplifier, and detector, is used, the receiving transducer should have sufficiently broad-band response to provide a flat response over the range of the low-pass filter. If the side branch is not used, the transducer can have a band-pass characteristic similar to that of the band-pass filter that follows it. The band pass of the receiver should slightly exceed the maximum frequency modulation anticipated. For example, if the maximum amplitude to be measured is 0.318 mm (0.635 mm total displacement) in LH_2 at -252.7 C, the maximum Doppler frequency obtained for a shaft rotation of 36,000 rpm and a carrier frequency of 5 MHz is 10,650 Hz. The band pass of the filter and transducer should extend at least from 4,989,000 to 5,011,000 Hz.

The receiving amplifier amplifies the received signal to a level suitable for operation in the mixer. An intermediate frequency is also produced in the mixer to provide a biasing frequency for the FM or Doppler

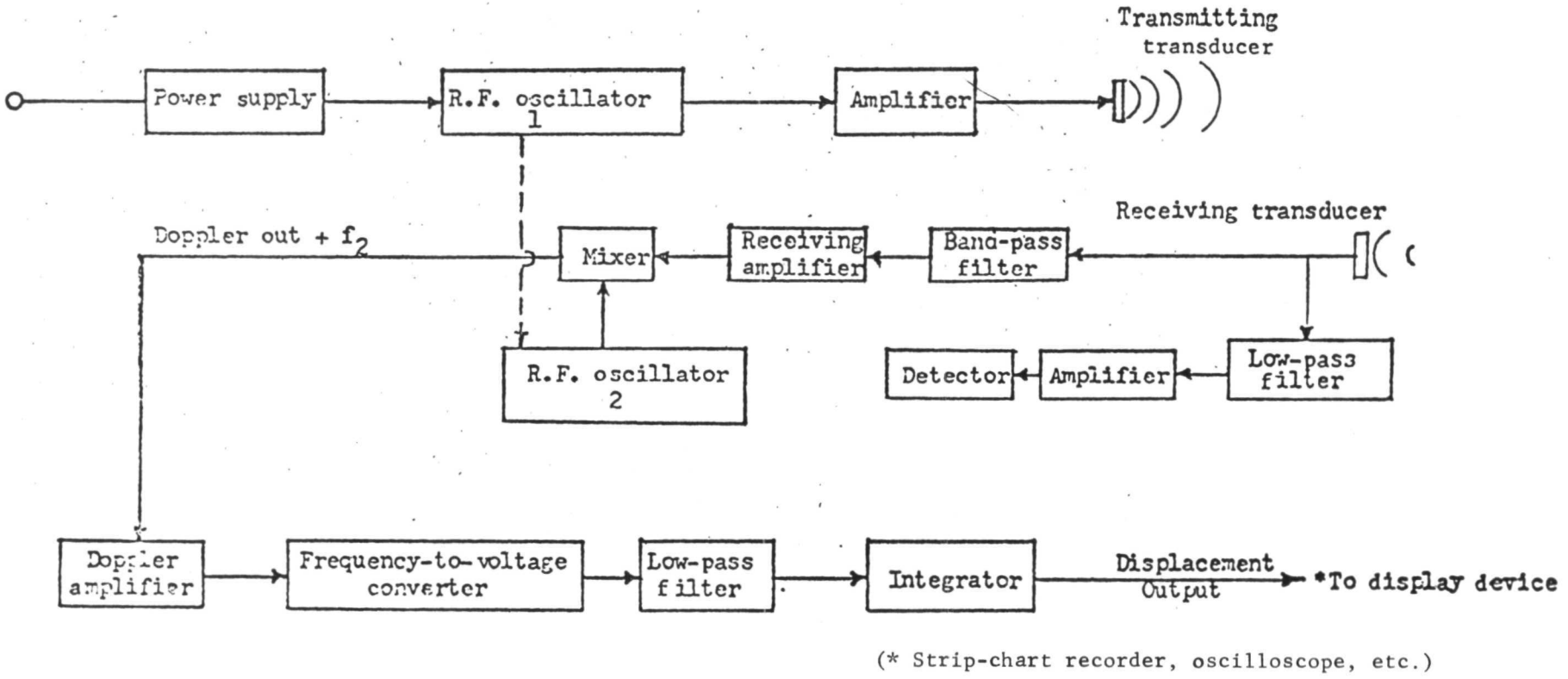

FIGURE 14. BLOCK DIAGRAM OF ULTRASONIC DISPLACEMENT MEASURING DEVICE

signal. The i-f is necessary to prevent full-wave rectification of the Doppler signal in the frequency-to-voltage convertor, which has no other means of determining whether the Doppler frequency represents a shift above or below the carrier frequency. The i-f is the difference between the carrier frequency and the output frequency of R-F oscillator 2 and this difference is held constant at a level exceeding the maximum Doppler shift. The mixer extracts both the i-f and the Doppler frequency. These components are amplified as needed in the Doppler amplifier and fed into the frequency-to-voltage convertor.

The output of the frequency-to-voltage convertor is a voltage signal corresponding to the frequency swing of the input signal. It contains two components: the i-f component at the intermediate frequency and the modulation component at the vibration frequency. The i-f is removed by the low-pass filter. The output from the filter is a voltage signal with an amplitude corresponding to the velocity of vibration and a frequency corresponding to the frequency of vibration. The integrator converts the velocity signal to an amplitude signal. The integrator is not essential if the vibration is sinusoidal.

For the experimental studies conducted during the present project, the receiver circuit including the band-pass filter, amplifier, R-F oscillator 2, mixer, and Doppler amplifier were incorporated in a commercially available device: a Hammerlund HQ100A receiver (amplifier, heterodyne oscillator, mixer, filter).

A constant-frequency difference between oscillators No. 1 and 2 was maintained manually by taking advantage of the characteristics of the equipment. The transmitting transducer was tuned to resonance (5 MHz). The Hammerlund receiver has an intermediate frequency of 455 kHz and a band-pass filter which permits a swing of approximately 3000 Hz to either side of 455 kHz.

Only the tunable r-f amplifier, local oscillator (heterodyne oscillator) and the i-f amplifier circuits of the Hammerlund receiver were used. The output signal was taken from the secondary winding of the last

i-f transformer. The audio detector tube was removed from its socket. The signal from the i-f amplifier in the HQ100A receiver was fed to the input of the GR1142-A discriminator.

The frequency-to-voltage convertor was supplied by a General Radio frequency meter and discriminator, type GR1142-A.

The output of the frequency-to-voltage convertor (GR1142-A) was fed into a tunable filter Type GR1232-A. This filter removed the i-f signal and presented the Doppler signal to the display device, which was a Tektronix oscilloscope. A Tektronix Type 565 oscilloscope was used generally for displaying the output signal.

Function of the Supplementary Circuit. The extra circuit consisting of low-pass filter, amplifier and detector is optional. This circuit utilizes the same receiving transducer that is used for the Doppler measurements to provide passive monitoring of the operation of the turbopump. Obvious anomalous operation of the turbopump would produce corresponding signals that might be detected early enough that catastrophic failure could be prevented. The amplifier could be a relatively inexpensive unit with band-pass characteristics extending through the audible range and into the low ultrasonic range. The cutoff frequency of the filter also could be a low ultrasonic frequency.

Transducers. Experiments during the program have shown that certain precautions are necessary in the design and use of ultrasonic transducers for applying the Doppler principle to the measurement of vibrations in the moving elements of turbopumps. Perhaps the best combination of transmitter and receiver would consist of a narrow bandwidth transmitter and a broad bandwidth receiver. Our experiments have proven that this is not a rigid requirement, however. The philosophy of using a narrow-bandwidth transmitter is that such transducers are easily adapted to controlling the frequency of the power oscillator and thus maintaining the frequency and amplitude of the transmitted (carrier) signal at reasonably constant levels. On the other hand, a broad-band transmitter provides less loss of signal amplitude with drift in frequency when manually adjusted oscillators are used.

The transmitter and receiver may be assembled in a common, compact housing thus comprising a dual-element probe. Operation in this manner is called monostatic. The primary precaution to be observed in designing a dual-element probe is to prevent both electrical and acoustical cross-talk. If cross-talk occurs, the magnitude of the cross-talk signal is so much greater than the signal from the vibrating surface that the Doppler signal is completely overcome.

Cross-talk was prevented during the experimental work with dual element probes used on Phase II by completely encapsulating each element separately in its own electrically conductive housing. The two units were then mounted together in a common housing in which they were acoustically isolated. However, during Phase III a new compact dual-element probe was developed which contained both the transmitting transducer and the receiving transducer in the same epoxy block. The two elements were both electrically and acoustically isolated within the block.

Dual-element probes are available commercially for measuring thicknesses by pulse-echo (pitch-catch) means. For such measurements, cross-talk presents no problem. Experiments using one of these commercial probes for Doppler measurements showed excessive cross-talk. However, excellent results were obtained when only one of the elements was used as a transmitter and a second small, commercial probe was used as a receiver. No acoustical or electrical cross-talk was possible with these probes because they were completely shielded electrically and they were acoustically isolated.

In some situations, it may be possible to transmit the incident wave from one location but the angle of incidence in the vibrating surface may be such that it is necessary to detect the reflected wave at another location. This arrangement of separated transmitter and receiver is called a bistatic arrangement. Such an arrangement increases the versatility of the ultrasonic Doppler method. Transducers for bistatic arrangements are immune to cross-talk if they are properly shielded.

Broad-band transducers are recommended for the receiver with the center-frequency equal to that of the carrier frequency. The output signal is then a reasonably good reproduction of the received signal, being able to follow the frequency modulation. Broad-band transducers are obtained by backing the piezoelectric element with a damping material.

Our studies showed that miniature transducers containing elements as small as 6.35 mm in diameter or 6.35 mm square would be adequate for the turbopump application. The beam-spread of a 6.35 mm diameter, 5 MHz beam in aluminum is approximately 22 degrees. It is approximately 5 degrees in typical liquids. If greater directionality is required and if no liquid or solid structure is available which is suitable for use as a wave-guide, collimation can be improved by increasing the area of the radiating surface.

The beam spread of a round piston-type source is given by

$$\sin \theta/2 = 1.2\lambda/D \quad , \tag{13}$$

where

θ = the angle of beam spread

λ = the wavelength of sound in the transmitting medium

D = the diameter of the radiating surface.

For square transducers

$$\sin \theta/2 = \lambda/b \quad , \tag{14}$$

where

b = the length of one side.

Coupling Transducers to the Turbopump. The acoustical impedance of air is very low compared with the impedance of solids. For this reason nearly 100 percent of the energy of an ultrasonic wave incident on an air/metal or metal/air interface is reflected from the interface with little or no transmission across the interface.

There are special techniques for improving the impedance match between gases and solids. For example, coupling across a half-wave air gap takes advantage of the distributed, complex impedance of the gap to obtain a match. The extremely close tolerances required at MHz frequencies makes such coupling impractical for the turbopump application. At lower frequencies, good coupling into gases is accomplished by increasing the radiating surface by attaching small energizing elements to diaphragms of relatively large area (i.e. relative to the cross-section of the energizing element). This method is not adaptable to the pump section but, conceivably, it could be applied

in the turbine section. In the turbine gases, a frequency of 100 KHz would produce wavelengths of approximately 3 mm. A displacement of 0.025 mm would produce a Doppler shift of 57 Hz.

Research on the ultrasonic Doppler method was restricted to the pump section during the present research program.

Transducers used in the experimental research were coupled to the test apparatus by means of lubricating oil or by cementing the transducer to the part. Other oils or greases, such as silicone stop-cock grease, are also suitable couplants. For permanent installations, the transducers may be bonded to the test apparatus. Several epoxy materials are suitable for this purpose. The mating surfaces must be free of grease and dirt and the epoxy must be free of gas bubbles to insure a good bond over the entire radiating surface.

Operation of conventional transducers at cryogenic temperatures requires thermal protection for the active elements. Methods of preventing damage due to differences in thermal expansion could include provisions designed into the transducer for locally heating the active elements or attaching a short transmission line to the transducer or to the housing of the pump so that the end to which the transducer is attached can be warmed without effectively heating the cryogenic material inside the pump.

During Phase III, a new transducer was fabricated and tested that withstood tests at liquid nitrogen temperatures with no obvious adverse effects. The active elements were potted in Armstrong A-31 epoxy. From the test results with this transducer, it appears that it can be cemented safely to the turbopump.

Flash X-Radiography

The results of Phase I indicated that the flash X-ray technique was capable of sensing the position of components inside turbopumps. In order to develop the technique, further experiments were undertaken using a 2-megavolt unit and the entire J-2 pump mounted on the test stand. The

purpose of the experiments was to determine how to optimize the technique with respect to shielding against scatter, orientation of local areas in the pump with respect to the X-ray source, source-to-object distance, source aperture, film type, and the use of film screens and filters. Because the 2-megavolt unit at McMinnville, Oregon was tied up, the 2-megavolt unit used for Phase II was that at the National Bureau of Standards Laboratories (NBS) at Gaithersburg, Maryland, where we could secure a significant block of time.

Static Experiments

Flash X-ray photographs for the assembled J-2 pump were undertaken primarily to uncover unforeseen difficulties with the technique. The pump and an electric drive system were mounted in a heavy mobile stand as illustrated in Figure 15. During the first effort, means for accurately positioning this assembly with respect to the X-ray tube, which would not be moved, were not available. As a result, no radiographs of the turbine section were attempted. Screw jacks were provided to allow for accurate height adjustment during the experiments which were carried out during the second visit.

Some of the initial radiographic results at NBS are reproduced in Figures 16, 17, and 18 for the shaft-bearing-seal assembly. These should be viewed as raw data since a great deal of experimental refinement is possible--as will be revealed below. The contrast is less than that shown in Figures 7 and 9, because of the additional scattering produced by the pump case and other components in the assembled unit. Again, it must be emphasized that the prints in this report are only a crude reproduction of the actual radiographic negatives. Figure 16, of obviously insufficient quality for practical use, resulted from an already refined technique: the use of a pair of Radlin TI-2 fluorescent screens and a 1.02 mm-thick lead scatter-attenuator in combination with Kodak Royal Blue film. Figure 17 illustrates the improved result obtained by masking out "forward scatter" by means of a lead-brick wall in front of the pump. This is shown in Figure 19--a minimum sized opening is aligned with the pump region of interest. This removes unneeded radiation from the field of the pump and, consequently, eliminates much of the contrast-reducing forward scatter. An additional optimization

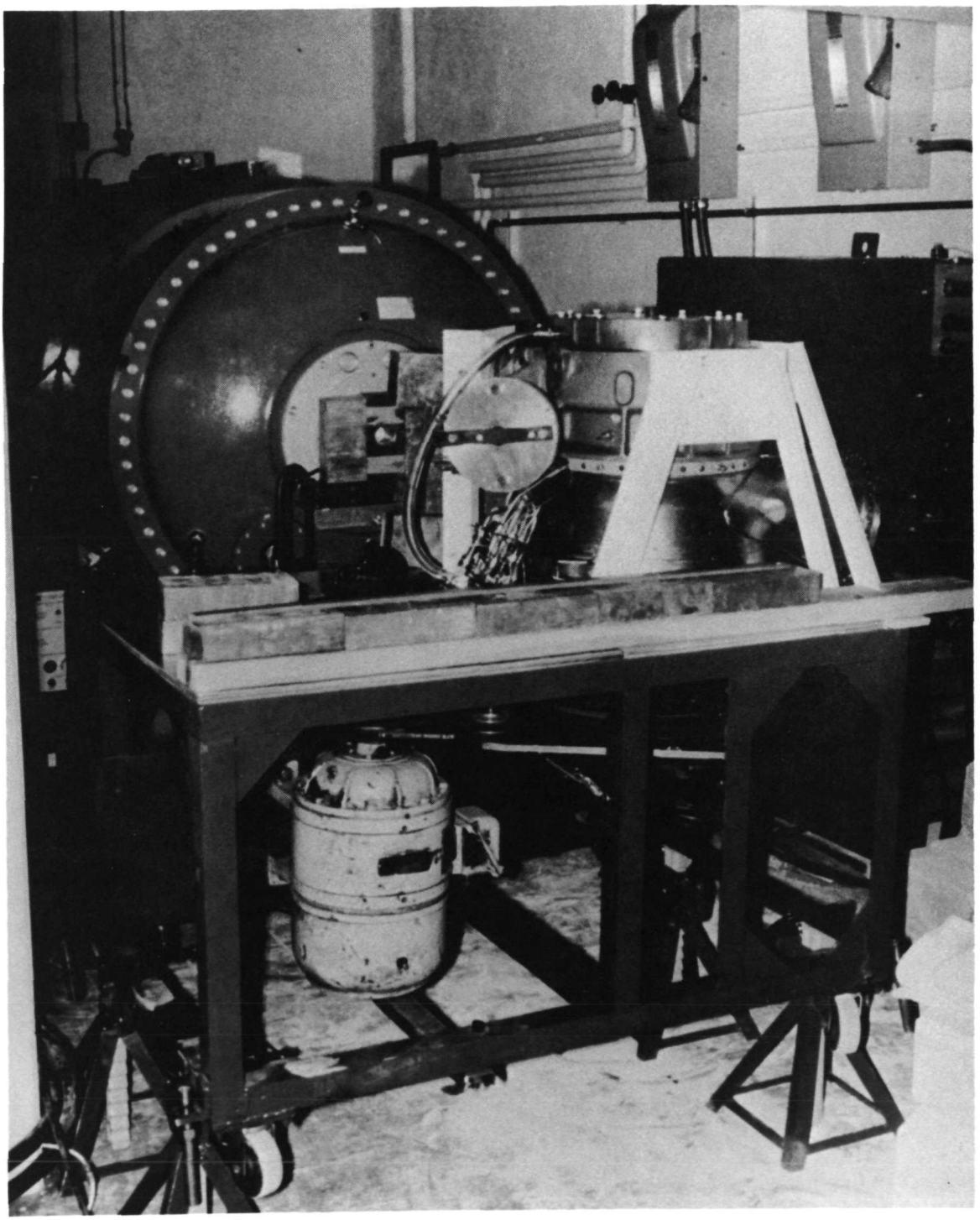

FIGURE 15. EXPERIMENTAL ARRANGEMENT OF PUMP WITH MOTOR DRIVE AND STAND ON ADJUSTABLE JACKS

X-Ray Unit in Background.

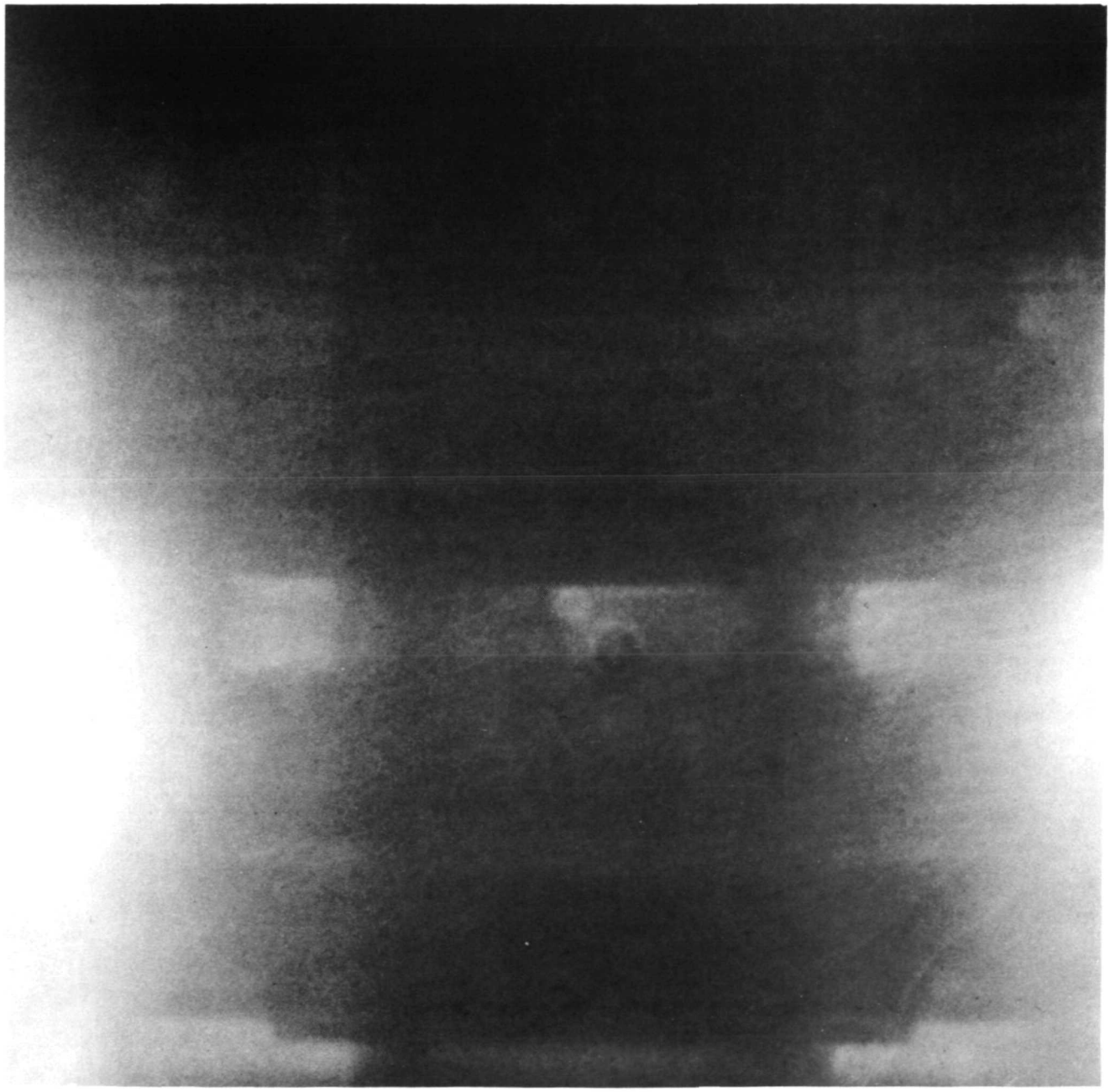

FIGURE 16. RADIOGRAPH OF BEARING ASSEMBLY THROUGH HOUSING: STATIC PUMP, NO MASKING, NO APERTURE

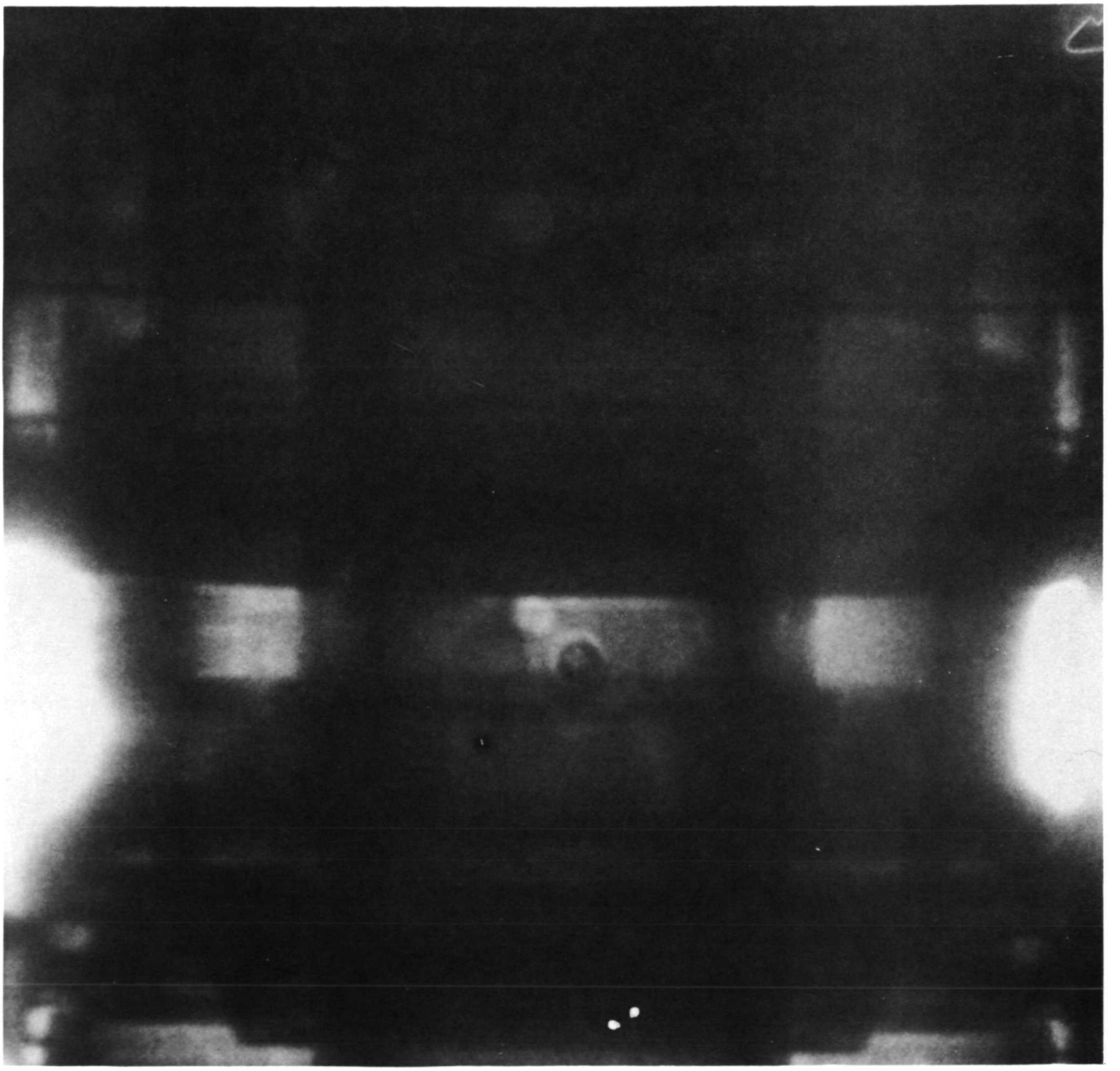

FIGURE 17. RADIOGRAPH OF BEARING ASSEMBLY USING MASKING

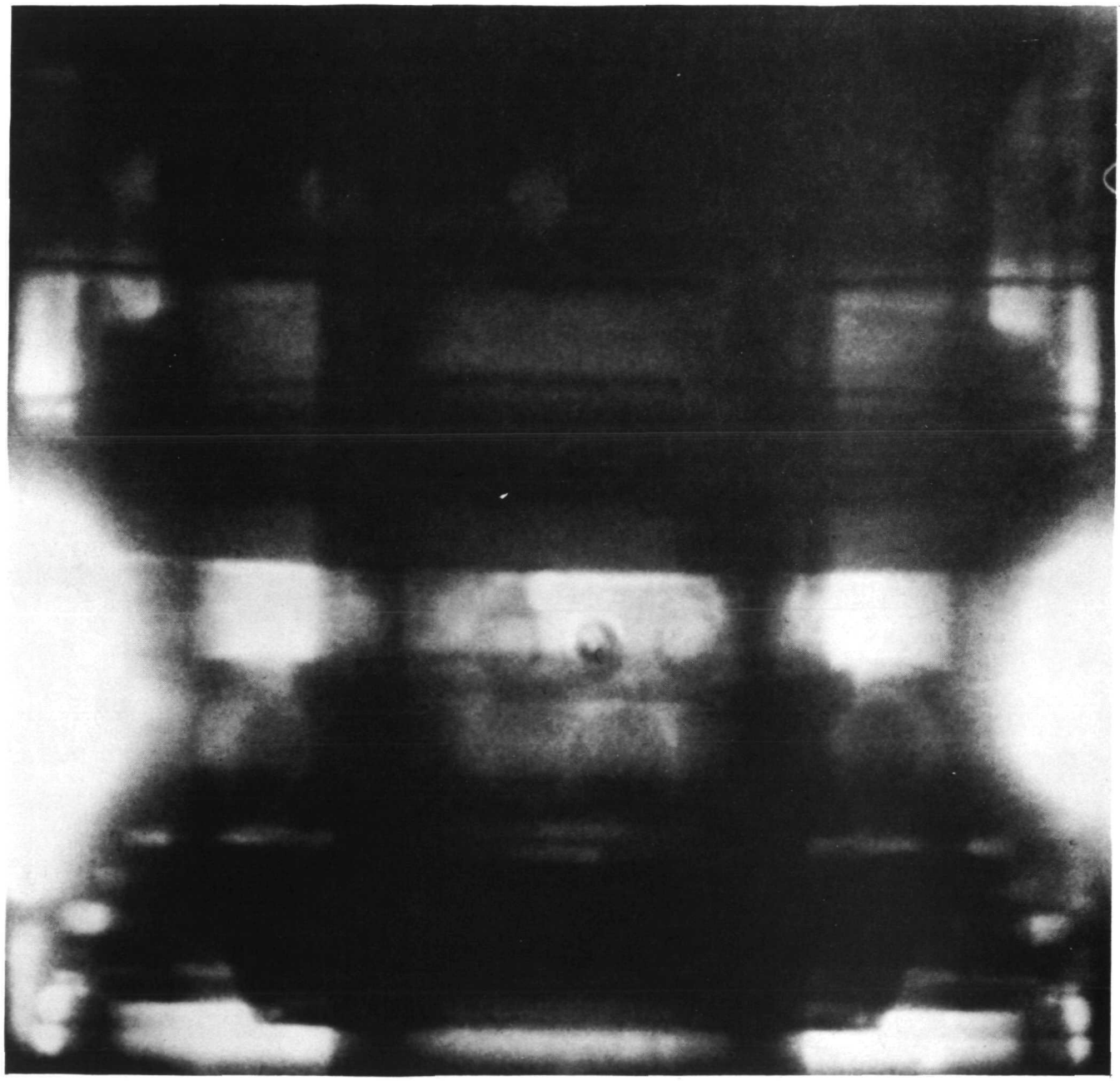

FIGURE 18. MULTIPLE-EXPOSURE RADIOGRAPH OF BEARING ASSEMBLY

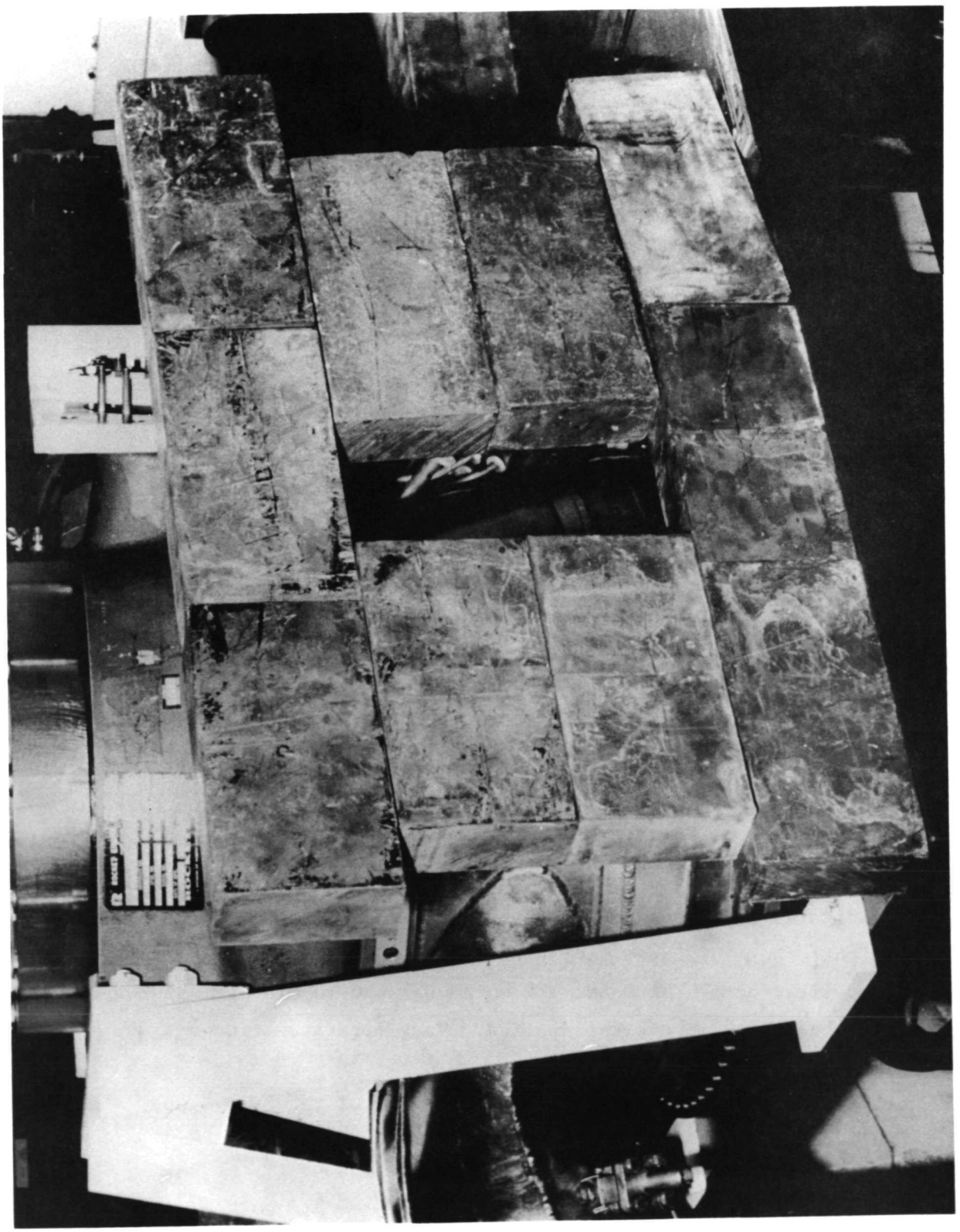

FIGURE 19. MASKING ARRANGEMENT FOR LIMITING BEAM SCATTER

applied to obtain the results shown in Figure 17 involved the use of an unapertured source. This produced unexpectedly better results than did an apertured source. The additional improvement resulting from the use of multiple exposures is shown in Figure 18. Four flash exposures spaced at approximately 45-second intervals* were applied to obtain the result shown. The improvements in contrast and definition are, of course, considerably more obvious in the original radiographs. It should be noted that optimization of the technique described above was not attempted. Also, other known refinements were not applied because of the program guideline schedules and objectives. On the other hand, the encouraging results indicated that dynamic experiments should be undertaken.

Dynamic Experiments

Efforts toward optimization of the X-ray aperture geometry were planned, as well as several as yet untried techniques for contrast enhancement. There were (1) simultaneous exposure of several X-ray films contained in a stacked array, and (2) use of persistent-fluorescence type screens. The dynamic experiments were successfully carried out during the second visit to the NBS installation at Gaithersburg, Maryland. Each of the suggested potential methods of effecting improved images was evaluated and the results are discussed below.

A tapered collimator (aperture) was constructed as illustrated in Figure 20. The effect of applying this modification is illustrated in Figure 21. Comparison with Figure 16, which is a radiograph of the same shaft-bearing section, indicates improvement--although fogging due to scatter is still very prevalent. Both of these radiographs were taken when the shaft was static. Modification of the lead mask which is used to minimize "forward scatter" was the next improvement applied. Very accurate alignment was

---

* The 45-second interval is required for gettering of the X-ray tube. The 2 megavolt units do not, as yet, have multiple-head capabilities as do the lower-power units.

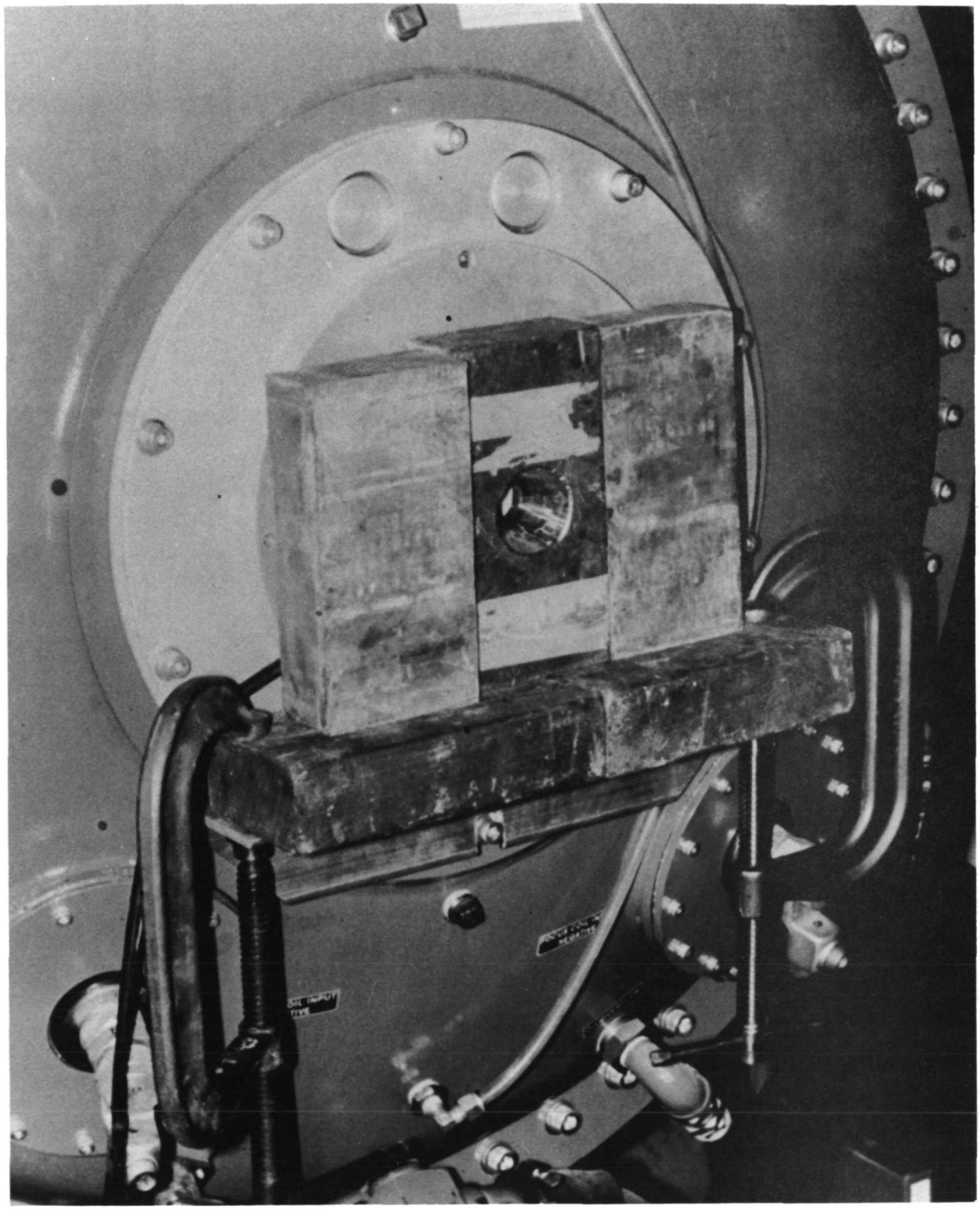

FIGURE 20. X-RAY TUBE APERTURE DESIGN

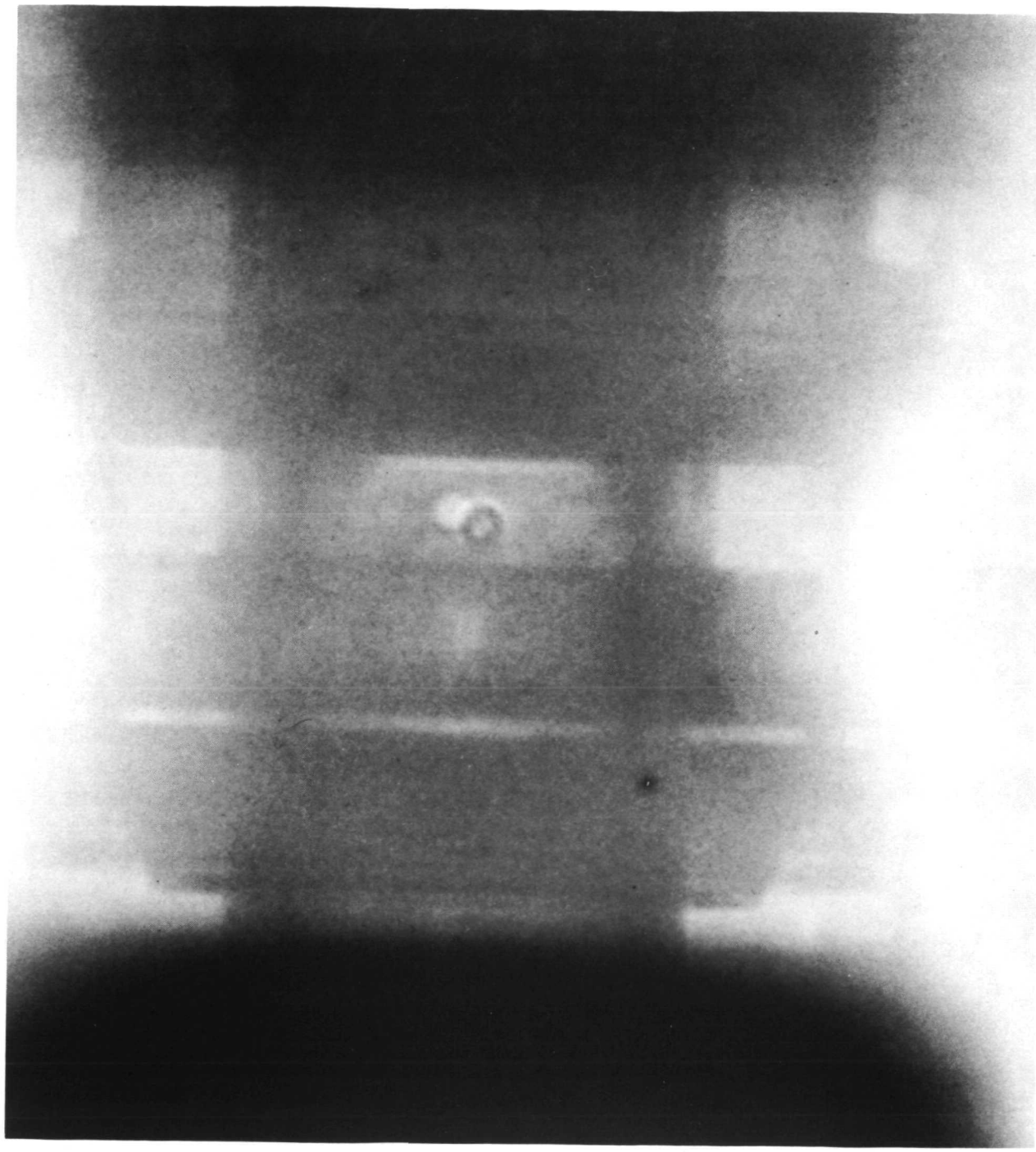

FIGURE 21. RADIOGRAPH OF BEARING ASSEMBLY WITH COLLIMATOR MASK IN USE

applied including tapering of the lead walls (see Figure 19) to obtain the results reproduced in Figures 22, 23, 24, and 25. Figures 22 and 24 show the system after it received single-pulse exposures; Figures 23 and 25 resulted from double-pulse exposures. Also, Figures 24 and 25 are dynamic, i.e., the shaft was being rotated at approximately 1000 rpm. A simple cam-operated microswitch was used to trigger the X-ray pulse. The resulting radiographs indicate that exact registry of the multiple images was obtained in all cases. Also, there was no degradation of the image resulting from shaft rotation. As expected, uncoupled components (notably the bearing balls) were not imaged in registry during the double exposures (Figures 24 and 25). It is also apparent that the contrast-reducing beam scatter is not increased as a result of the movement of imaged components.

Reorientation of the shaft-mounted cam (a simple adjustment) facilitated the making of radiographs for any chosen angular shaft position. Figure 26, also a double-pulse exposure, illustrated a radiograph from a position 180 degrees from that shown in Figures 22 and 25. No differences were expected between the radiographs of the two positions, and none are apparent. Shaft displacement, in particular, would not be expected at this speed. Note that each of the illustrated radiographs displays a row of several "hole" images running horizontally, well above the bearing. These are in the outer casing and are fixed with respect to shaft or other possible displacements. Displacement measurements could be indexed from these images. Similar reference points will probably exist for any anticipated pump design.

Radiographing the turbine section required a different geometric setup. The central beam of the incident X-rays was aligned tangentially with the turbine wheel. Film placement, masking, centering, etc., were adjusted accordingly. However, radiographic access to the turbine section was not entirely satisfactory due to the pump support (the platform on which the pump is mounted). In spite of this, successful results were achieved, as shown in Figures 27, 28, and 29.

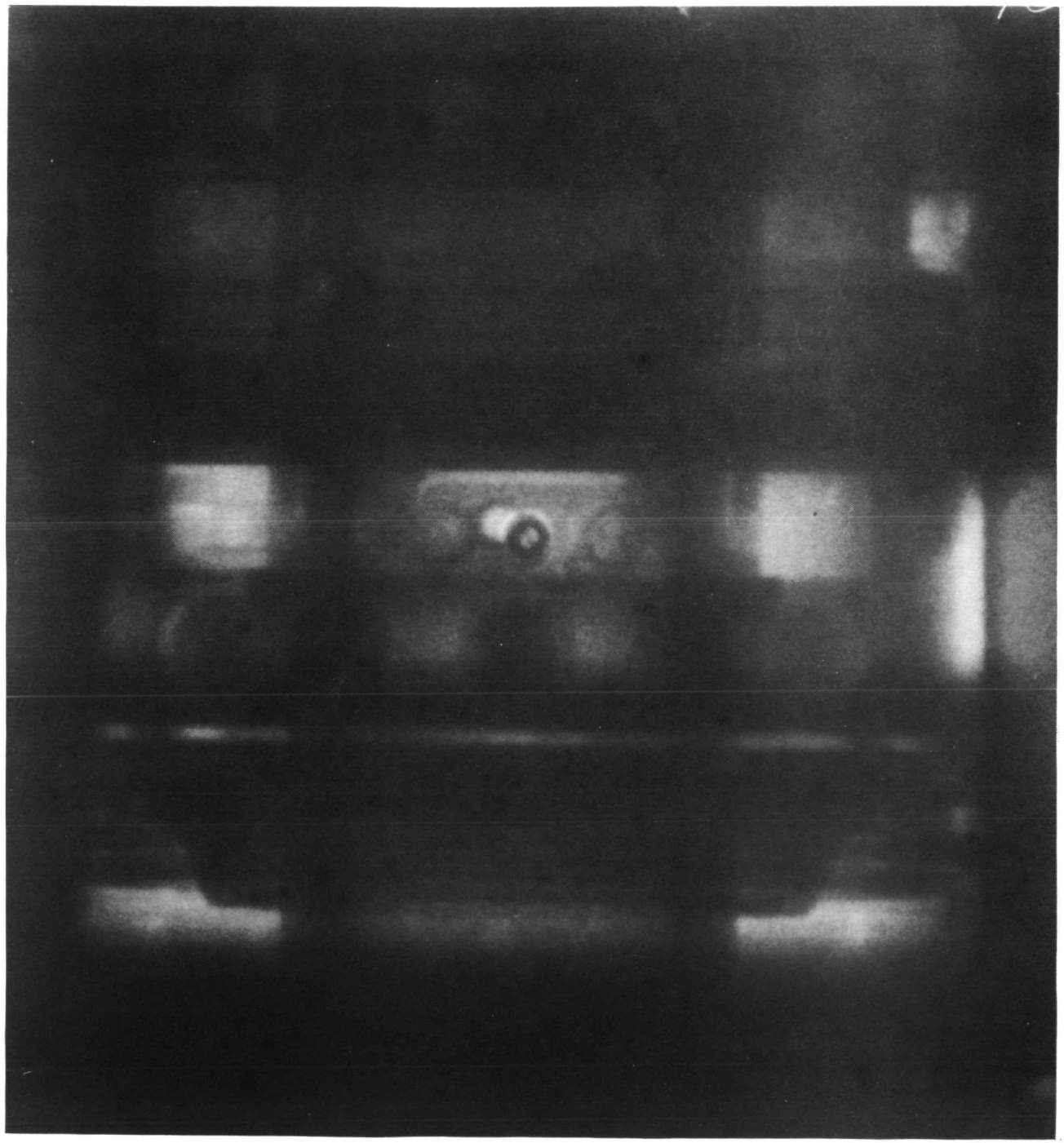

FIGURE 22. RADIOGRAPH OF BEARING ASSEMBLY USING A REFINED MASK DESIGN; STATIC PUMP, SINGLE-PULSE EXPOSURE

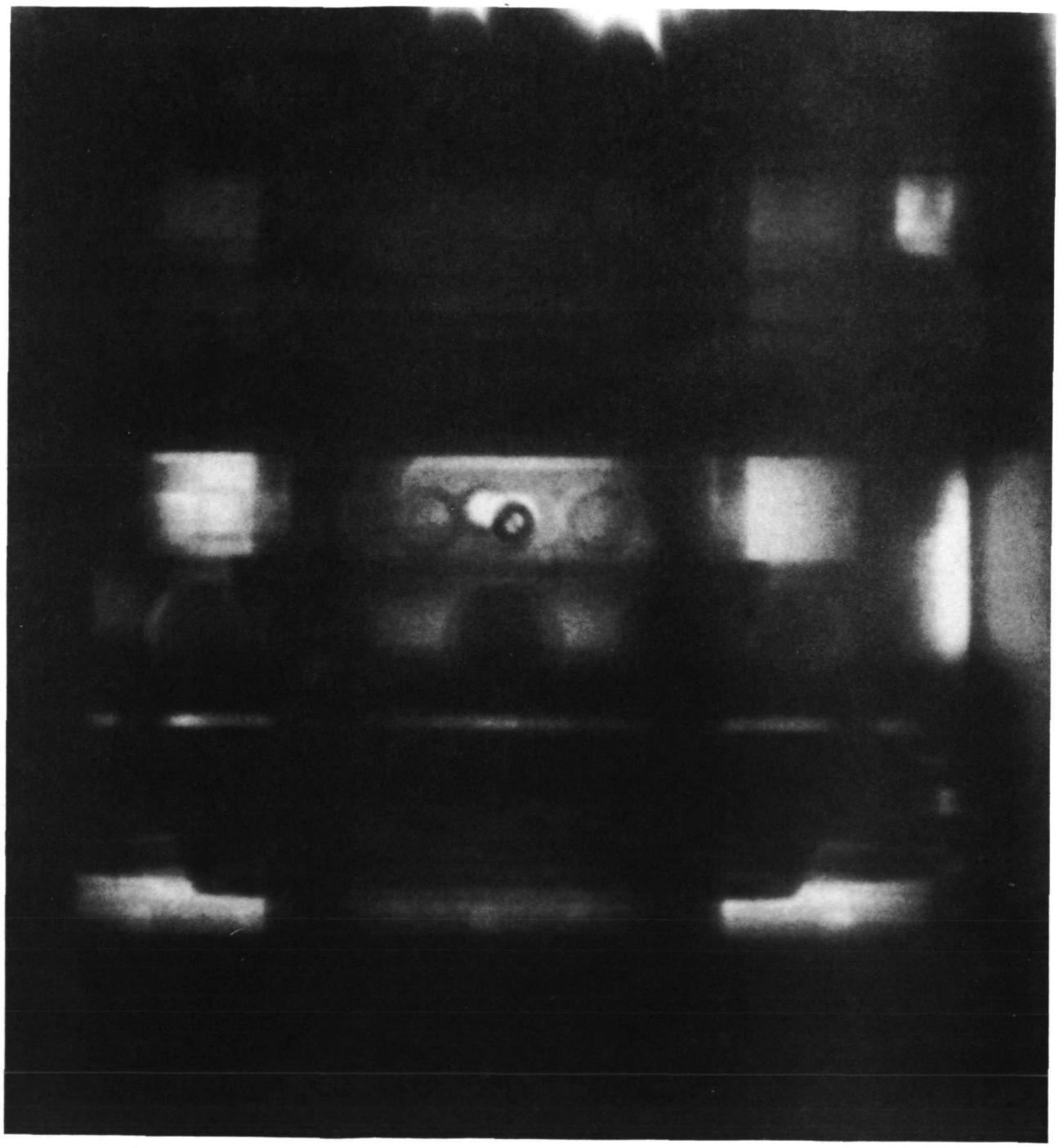

FIGURE 23. RADIOGRAPH OF STATIC SHAFT USING A DOUBLE-PULSE EXPOSURE

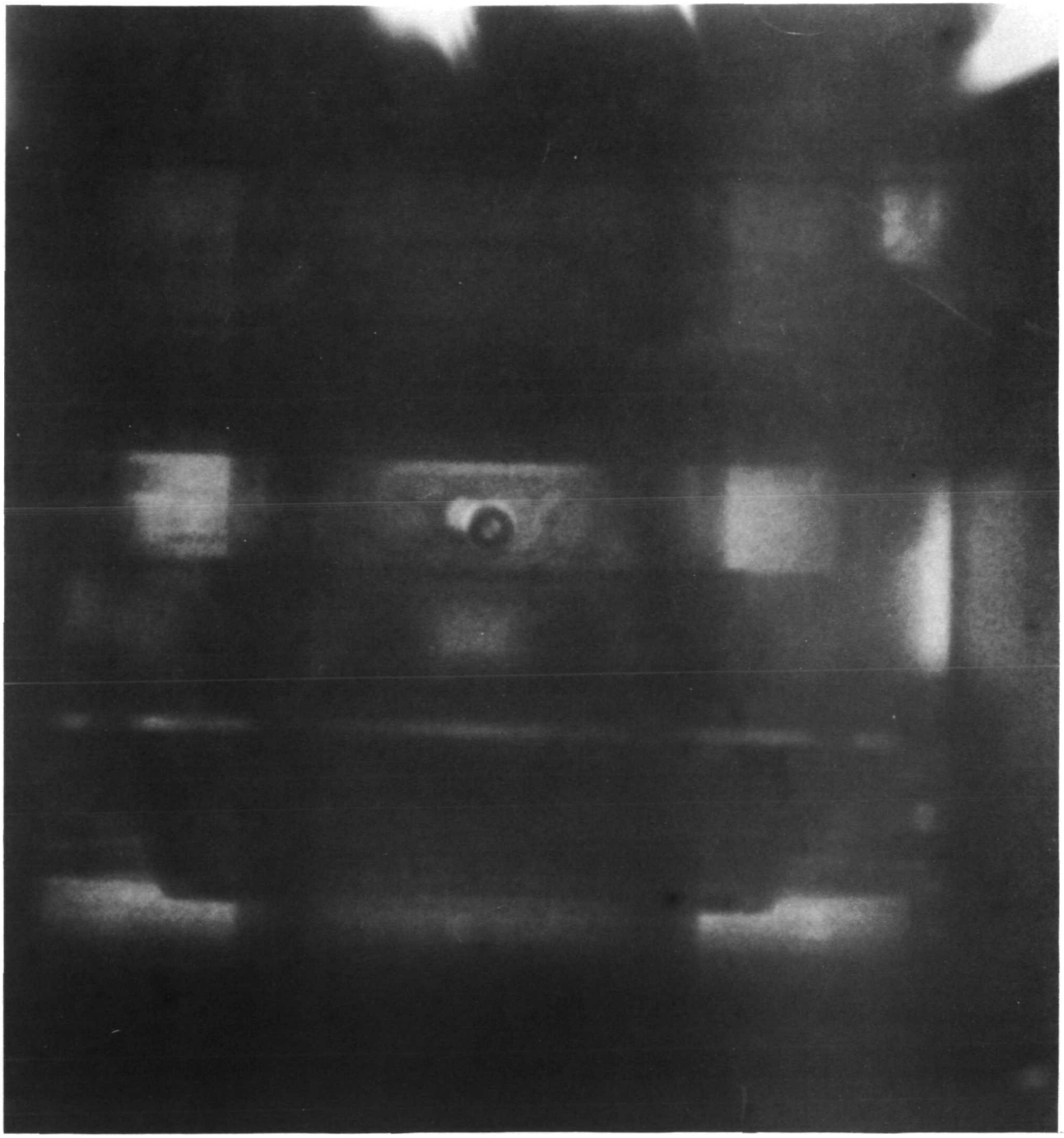

FIGURE 24. RADIOGRAPH OF ROTATING SHAFT (1000 RPM); MASKING, APERTURE, AND SINGLE-PULSE EXPOSURE

FIGURE 25. RADIOGRAPH OF ROTATING SHAFT USING DOUBLE-PULSE EXPOSURE

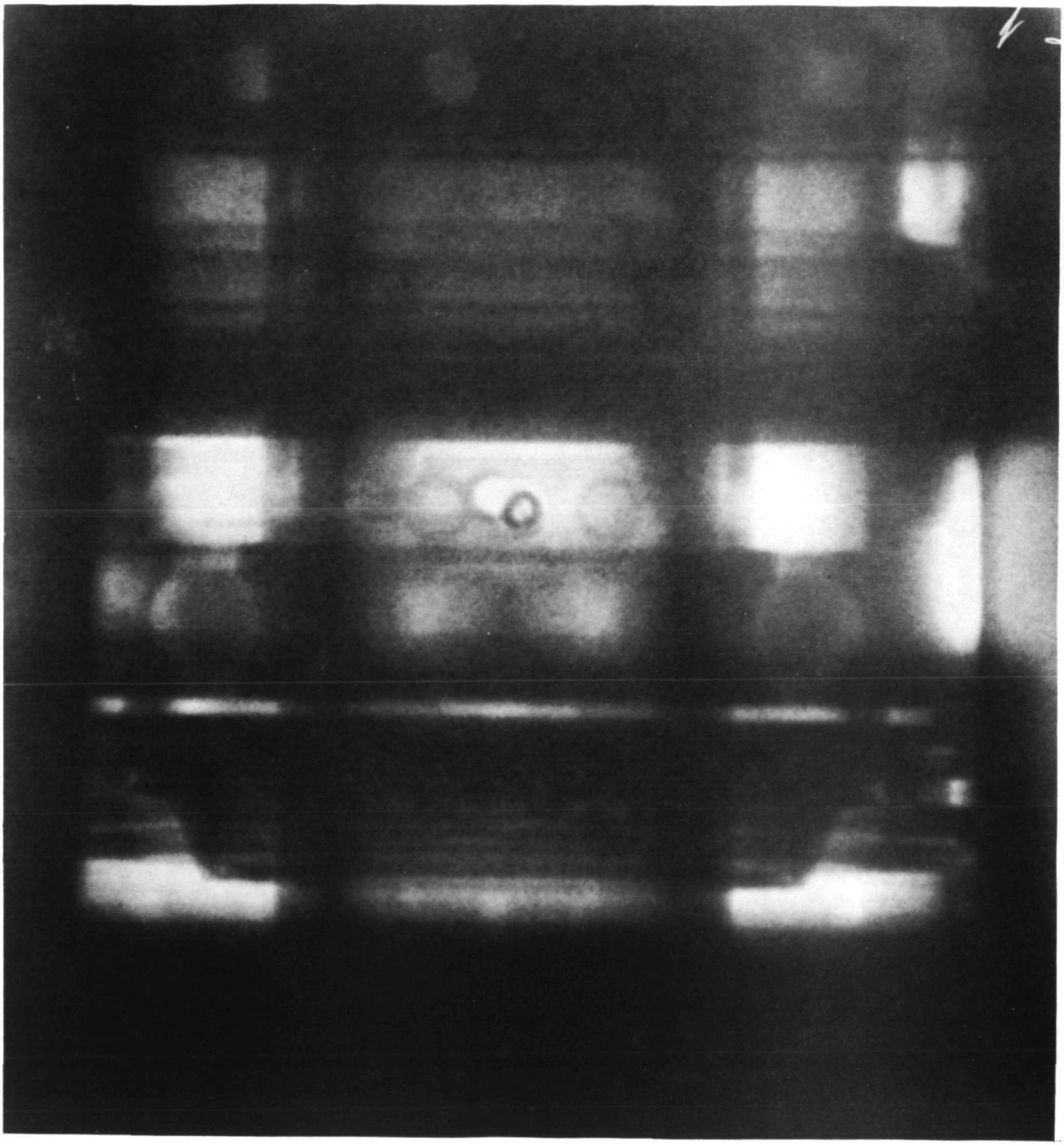

FIGURE 26. RADIOGRAPH OF ROTATING SHAFT SAME AS FIGURE 25 BUT AT 180 DEGREES ANGULAR SHIFT

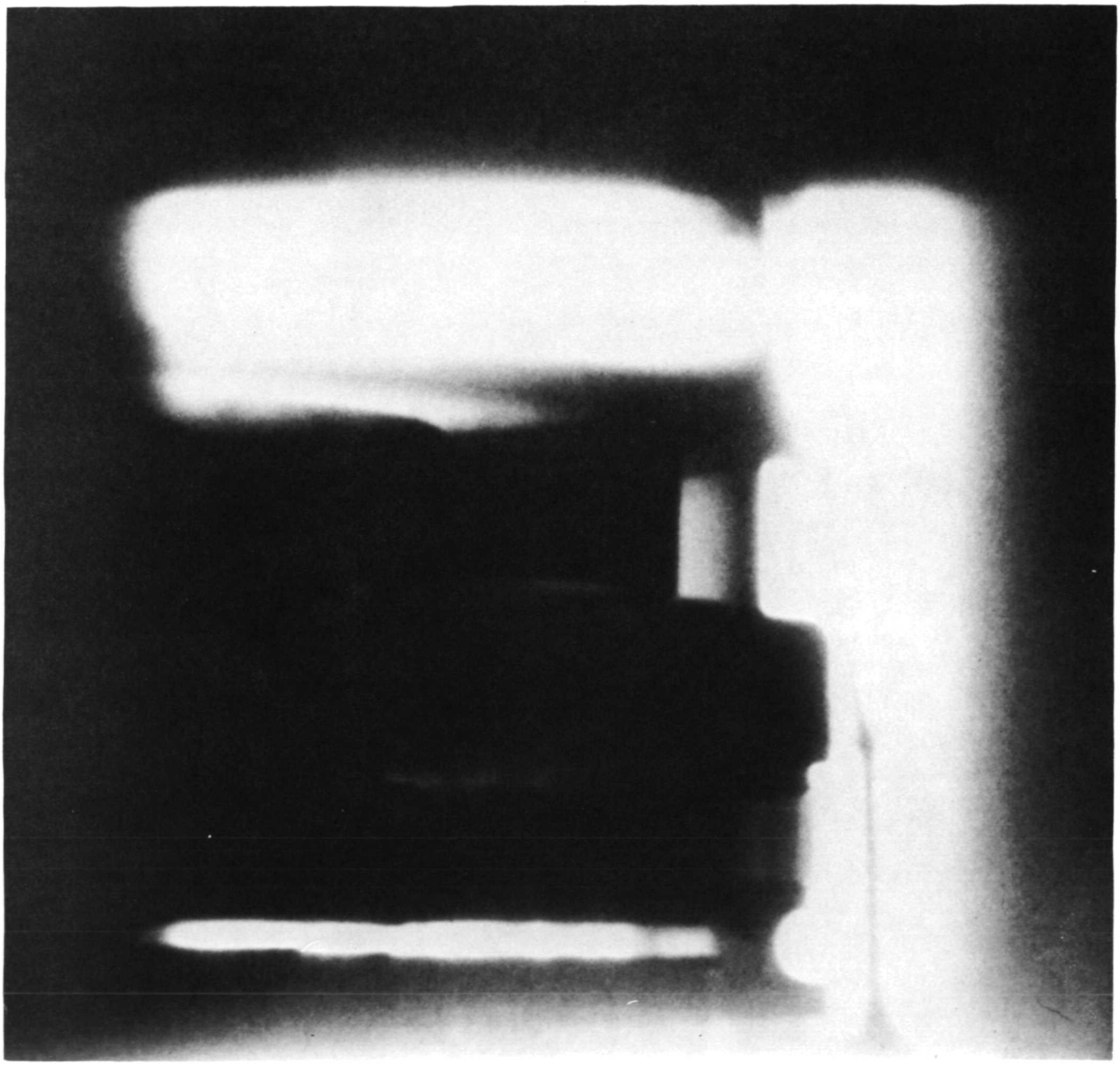

FIGURE 27. RADIOGRAPH OF TURBINE SECTION: STATIC, SINGLE-PULSE EXPOSURE

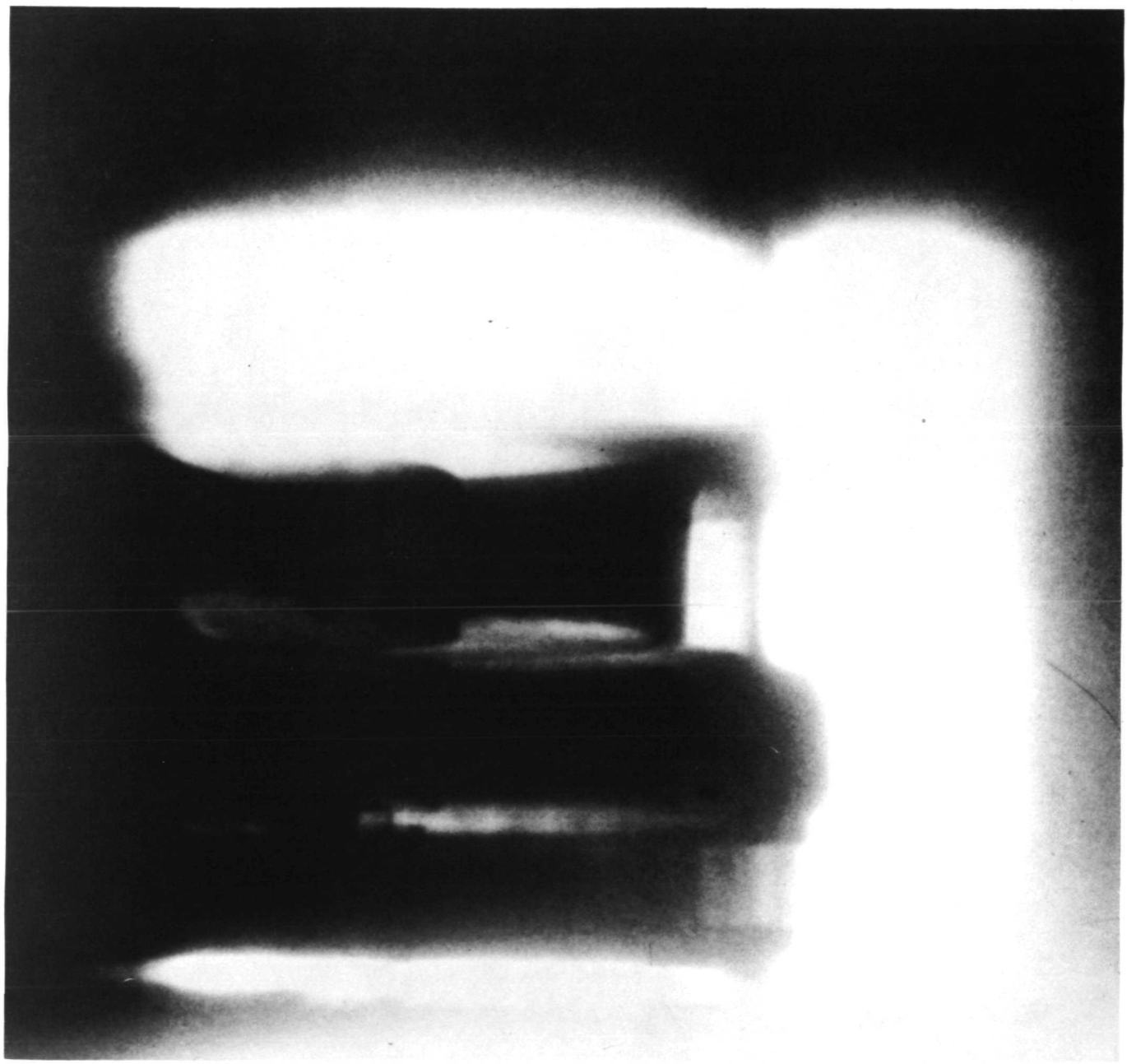

FIGURE 28. RADIOGRAPH OF TURBINE SECTION: STATIC, DOUBLE-PULSE EXPOSURE

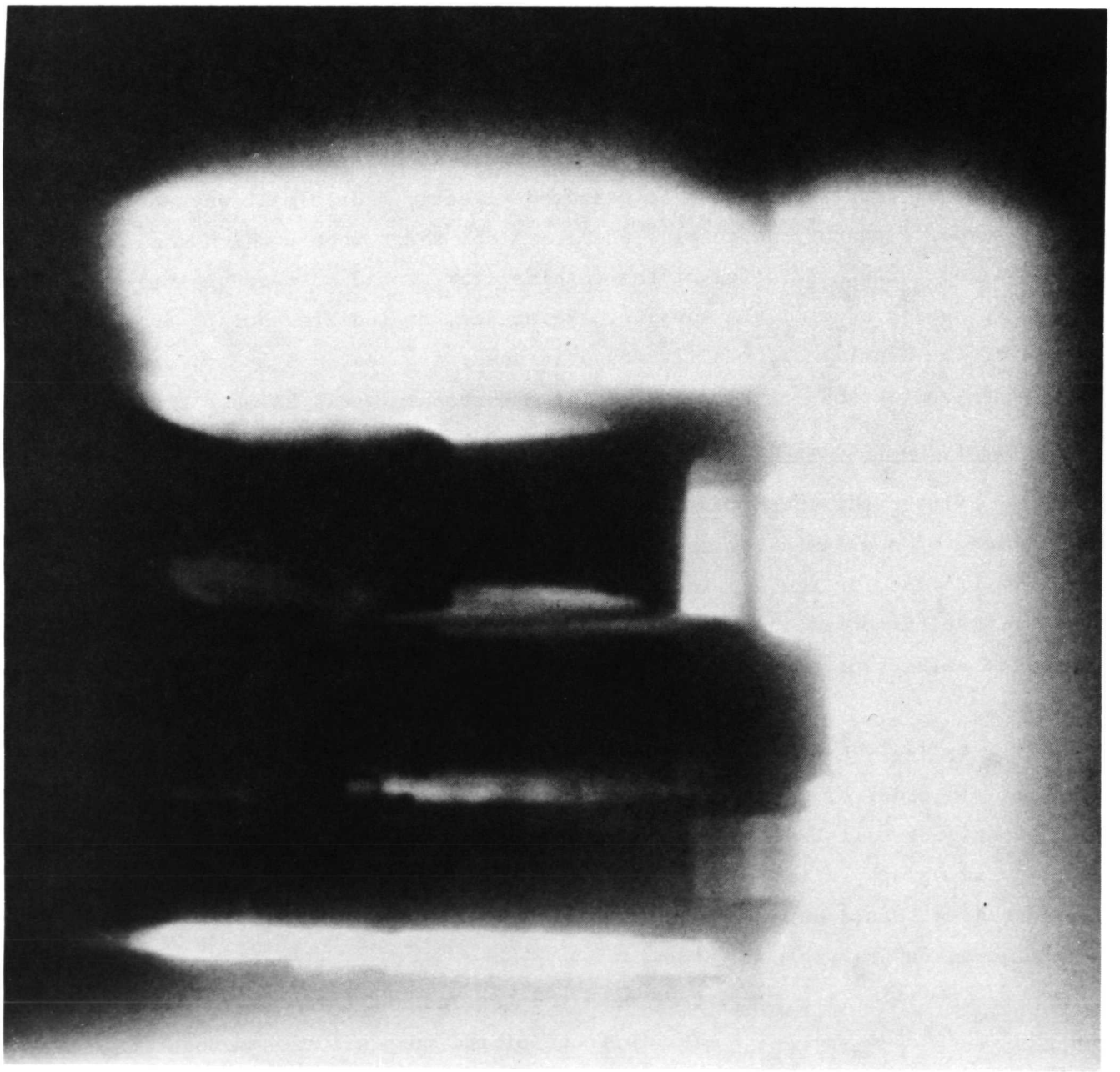

FIGURE 29. RADIOGRAPH OF TURBINE SECTION: TURBINE ROTATING AT APPROXIMATELY 1000 RMP

The pump was static for the single X-ray pulse used for the exposures of Figure 27 and the double pulse of Figure 28. Figure 29 was taken under dynamic conditions with a double pulse. Since all moving parts in Figure 29 are coupled, the imaging in this photo is identical in the last detail to Figure 28. Again, no motion effects are apparent, nor were they expected. For an actual vibration diagnosis, radiographs of similar sections need not show more detail than the shadowgraph-like features displayed here. For example, axial displacement can be measured directly from almost any point on the shadow image of the turbine wheel. Also, shaft wobble which should be amplified through nutation of the turbine disk, would be made visible at the sharp shadow edge of the turbine. Reference, or indexing points from images of the housing are readily found in these figures, and it appears that flash radiographs of this section of a turbopump would be most fruitful.

Conclusions and Recommendations

Flash radiography was studied as a technique for sensing vibrations in sections of a dynamically operating J-2 turbopump. The radiographs show decisive promise for the application of this technique to prototype pumps under operating conditions. A 2-megavolt, commercial, flash X-ray unit exhibited sufficient penetration of the pump to assure adequate radiographic exposures.

At X-ray energies of 2 megavolts, the main concern is scatter and its control. In order to minimize scatter for future applictions, attention to good techniques will be necessary. Otherwise, straightforward techniques of applied radiography will provide good results. The successes achieved during these studies should carry over for the anticipated higher pump speeds and more rigorous operating conditions.

Specifically, the use of both the tapered aperture collimator at the source and the lead-wall mask in front of the pump are recommended. A lead open-faced box for holding the film cassette is also recommended as an additional means for reducing backscatter.

Concerning the film, filters, and screens, the use of Kodak Royal Blue, 1.02 mm of lead, and two Radlin TI-2 screens are suggested. We found that this combination gave excellent results. The long-decay fluorescent screens which were tried, were judged too grainy to permit the measuring accuracy required. The technique of using stacked film was tried but judged undesirable since no marked image improvement resulted. Thus, a fairly straightforward radiographic technique is indicated.

Application of flash radiography to operating speeds of 36,000 rpm and turbine gas temperatures of 2000 F are not expected to present any additional difficulties: the X-ray source is remote from these environments, the duration of flash X-ray exposures will stop any anticipated rate of motion, and the film can be insulated from the heat sources with no serious loss in performance. Vibration is also of little concern to this X-ray technique.

Radiographic access to component boundaries of interest for an anticipated pump design appears to be good. Sketches of a prototype pump have been reviewed and as a result of the experience gained with the J-2 pump, we believe the flash X-ray technique is applicable. For example, because the turbine section need not be penetrated to provide displacement data (the shadow of an edge is adequate), it appears that the hollows of the volutes will provide radiographic access. Furthermore, the pump housing appears radiographically thin. Thus, the application to the anticipated pump should yield results similar to those obtained to date using the J-2 pump.

It appears at this time that the flash radiography approach will require no alteration of the pump design. Based on the present results, it seems that tagging, or keying with radiographically dense buttons or the like, is unnecessary. It also seems likely that stationary reference points will be found for any given radiographic orientation. Of course, the results presented need to be translated to the prototype pump for reverification.

Optical Light-Pipe Reflectance Device

During the first and second quarters, a variety of optical devices was evaluated. All of the methods considered required modification of a pump to the extent necessary to provide a window of some sort to admit light into and out of the pump. The most attractive method involved a commercially available unit which senses displacement by measuring reflected light intensity from the vibrating surface. Light is admitted into the surface through a flexible fiber-optic bundle, which serves as the window. Although this technique requires greater pump modification than the ultrasonic, the fast neutron and the flash X-ray techniques, it is simpler and more flexible in its application than the currently used inductance transducers. The light-pipe reflectance technique was, therefore, advanced to Phase II partly as a backup effort to the more exotic techniques also being developed in Phase II.

A commercial light-pipe-reflectance unit ("Fotonic") was purchased and a series of experimental evaluations was conducted to provide a preliminary evaluation of the technique. Subsequently, measurements were made on the J-2 pump. The general effects of high pressure and cryogenic temperature on the fiber-optic probe were also investigated.

Preliminary Evaluations

Evaluations of the performance of the Fotonic sensor under ordinary laboratory conditions confirmed the manufacturer's claims. A high-speed grinding attachment was mounted on the crossfeed of a small lathe. A small rotor was chucked in the grinder collet. Each fiber-optic-sensor probe was mounted, in turn, into the stationary lathe chuck. The average separation between the probe end and the rotor was adjusted by using the tool-feed micrometer drive. A solid state voltage control was used to select rotor speeds up to 4500 rpm. Six small flats located around the rotor periphery served to yield distinct displacement pulses at rates up to 27,000 pulses per minute. Surface roughness contributed less distinct and less uniform pulses at rates roughly 10 times higher (or the equivalent of 200,000 pulses per

minute). The manufacturer's data indicate a flat response for the instrument out to 6 x 10^6 pulses per minute with an attenuation of 5 percent at 10^7 pulses per minute. The experiments showed that the instrument was quite stable and it should be capable of a precision of several percent of the linear range, as claimed.

A second experiment was performed in which the signal output from the sensor was fed into a tunable frequency detector. As anticipated, a band of frequencies was generated by surface imperfections whose center frequency was linearly proportional to the rotor surface velocity. The band width at half maximum was about 10 percent of the center frequency. It is estimated that one could determine dynamic changes in surface speed to within several percent using an FM detection scheme. He-Ne laser illumination was used in some of the experiments; however, there was no improvement in operation. The sensor gain could be turned down considerably since the laser provided more irradiance of the surface, but this technique is not sensitive to signal amplitude. . .it is sensitive to frequency only. The laser might be of more value in creating a more distinctive frequency spectrum in cases where the surface is much smoother than was the test rotor used here.

Some consideration was also given to the problem of sealing the sensor end where it will be subjected to hostile environments. The manufacturer of the Fotonic sensor has used this type of sensor at liquid-nitrogen temperatures. They have also operated others at pressures of 10.3 MN/m^2. The fibers in the standard probes are of the clad type, and this type is necessary to keep down the optical cross talk. A quick experiment with a rigid fiber-optical pipe containing unclad fibers showed that a second section of the fiber pipe could be used as a "window". However, the experiment also showed that the cross talk from the 5-cm length of unclad fibers lowered the sensitivity by an order of magnitude. The use of clad fibers or of a much shorter length of unclad fibers could result in nearly full regaining of sensitivity. The interest in this involves the possibility of using a rigid section of fiber bundles as a high pressure window and the normal flexible section as a lead out. This has good promise for solving the problem

at cryogenic temperatures. The elevated temperatures in the turbine section are a more difficult matter. We were unable to locate clad fiber components having promise of an usefulness above 605 C, and there is no guarantee of extended life above 450 C. Consequently, we hold out very little hope of measuring using optical means in the vicinity of the 930 C regions in the turbine. On the other hand, we believe that there is reasonable promise that small transparent gaps can be measured with high precision in the cryogenic pump system using the fiber optic/reflectance approach. The major impediment appears to be the possibility of cavitation in the measurement gap which would render the signal meaningless insofar as displacement is concerned. (The cavitation itself might be revealed by a strong output signal whose central frequency corresponds to one-half the relative lateral velocity between the probe and the surface being measured.) There are optical methods for carrying signals to and from the shaft of the pump. Therefore, sensors might be mounted in the rotating member if desired without the necessity for any electrical or mechanical connection to the shaft.

Runout Measurement in J-2 Pump

A modification of the J-2 turbopump was made to incorporate the light-reflectance probe. The probe was inserted into the exit stream region of the pump through an elastomer-sealed pressure fitting. The fitting was located so that the probe looked at the lower flange of the centrifugal impeller. Figure 30 shows the probe mounted in the pump.

A cyclically varying signal was obtained with kerosene in the pump when the shaft was turned by hand. When the shaft was rotated at 1070 rpm with the drive motor, the cyclic signal was completely obscured by a random signal. This indication of bubble entrainment was confirmed by the observation of bubbles through the transparent lid and hoses on the pump. Further confirmation came when the kerosene was drained from the pump so that the probe operated in air. A repetitive, cyclic signal was obtained with almost no random noise.

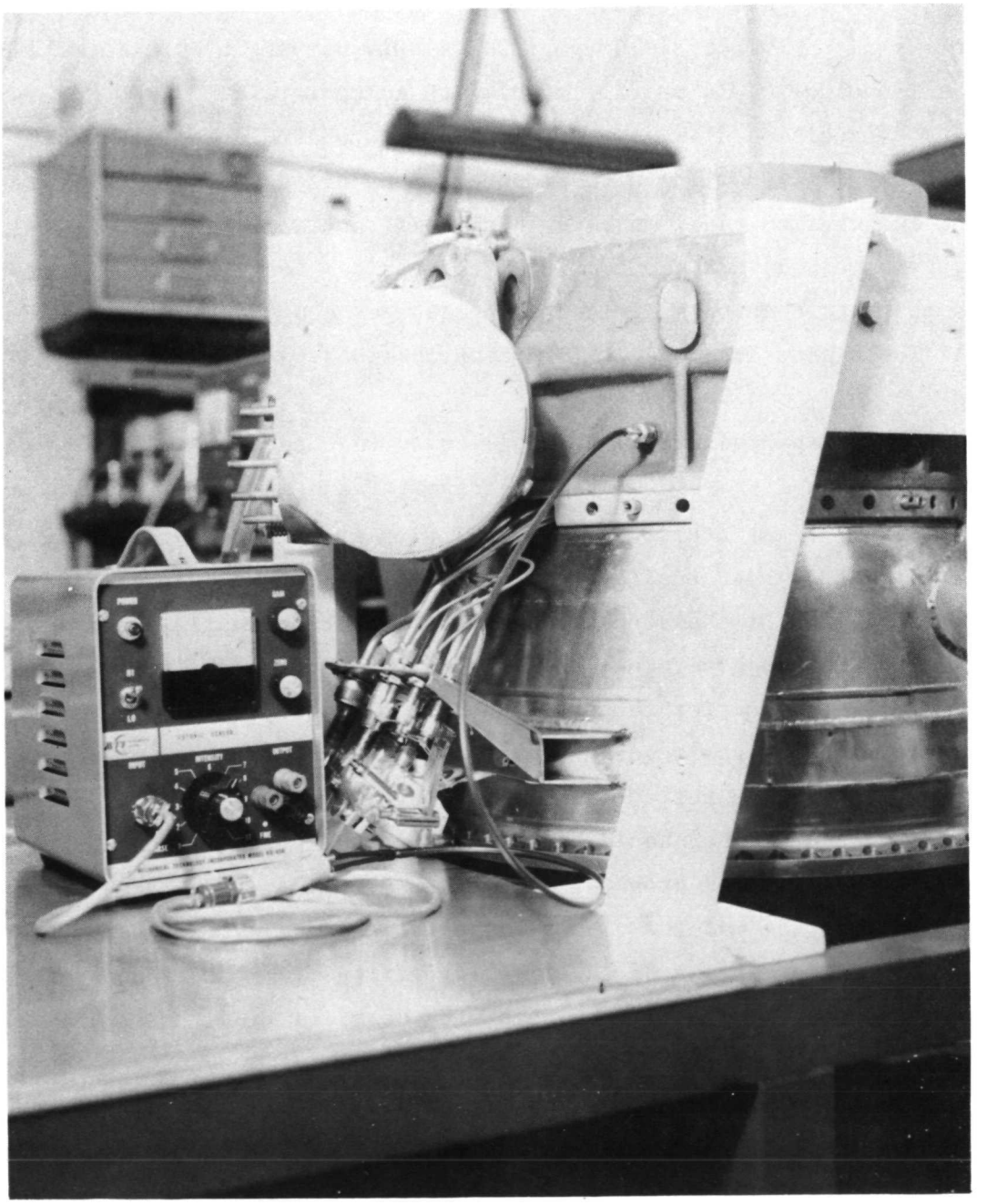

FIGURE 30. LIGHT-PIPE-REFLECTANCE PROBE MOUNTED IN TURBOPUMP AND INSTRUMENTATION

The upper trace in Figure 31 was obtained with the kerosene drained and with the shaft driven at 1070 rpm. The slowly varying cyclic signal indicates a runout of 0.078 mm (3.1 mils) with an uncertainty of $\pm$0.005 mm (0.2 mil). A precision dial gage with the shaft rotated stepwise by hand gave a value of 0.074 mm (2.9 mil) with an uncertainty of $\pm$0.008 mm (0.3 mil). the maximum and minimum radii matched in circumferential location between the two measurement methods further confirmed the optical measurement. These results demonstrate that this optical technique has the potential for high precision. The higher frequency information obtained in the scope trace was unexpected.

It was suspected that variations in surface reflectance around the periphery of the impeller resulted in the repetitive high-frequency components of the signal. This was confirmed by withdrawing the probe sufficiently far from the surface that the sensitivity to the gap was virtually nullified. The lower trace in Figure 31 shows that under this condition, while the effect of runout on the signal is gone, the probe indicates that the reflectance does indeed vary in a very complex manner around the periphery of the impeller. The correspondence of the high-frequency variation between the upper and lower traces shows that surface reflectance variation can be a problem but that high-precision measurements should be possible in the presence of such variance by suitably designed duplex probe arrangements.

An effort was made to reduce these reflectance variations by careful vapor-blasting of the surface of the impeller periphery. After replacing the impeller in the pump and filling the pump with degassed vacuum oil, the replicate traces shown in Figure 32 were obtained. The absence of extensive high frequency hash demonstrates the efficiency of careful surface preparation for reducing reflectance variations. Therefore, it should be possible in some applications of the probe to obtain high precision without resorting to reflectance compensation techniques.

The two single traces shown in Figure 32 were obtained about 100 revolutions apart. The exact duplication of signal between these and the many other traces recorded with the degassed oil in the pump show that the optical probe can be used in flowing liquid if bubble entrainment and cavitation is absent.

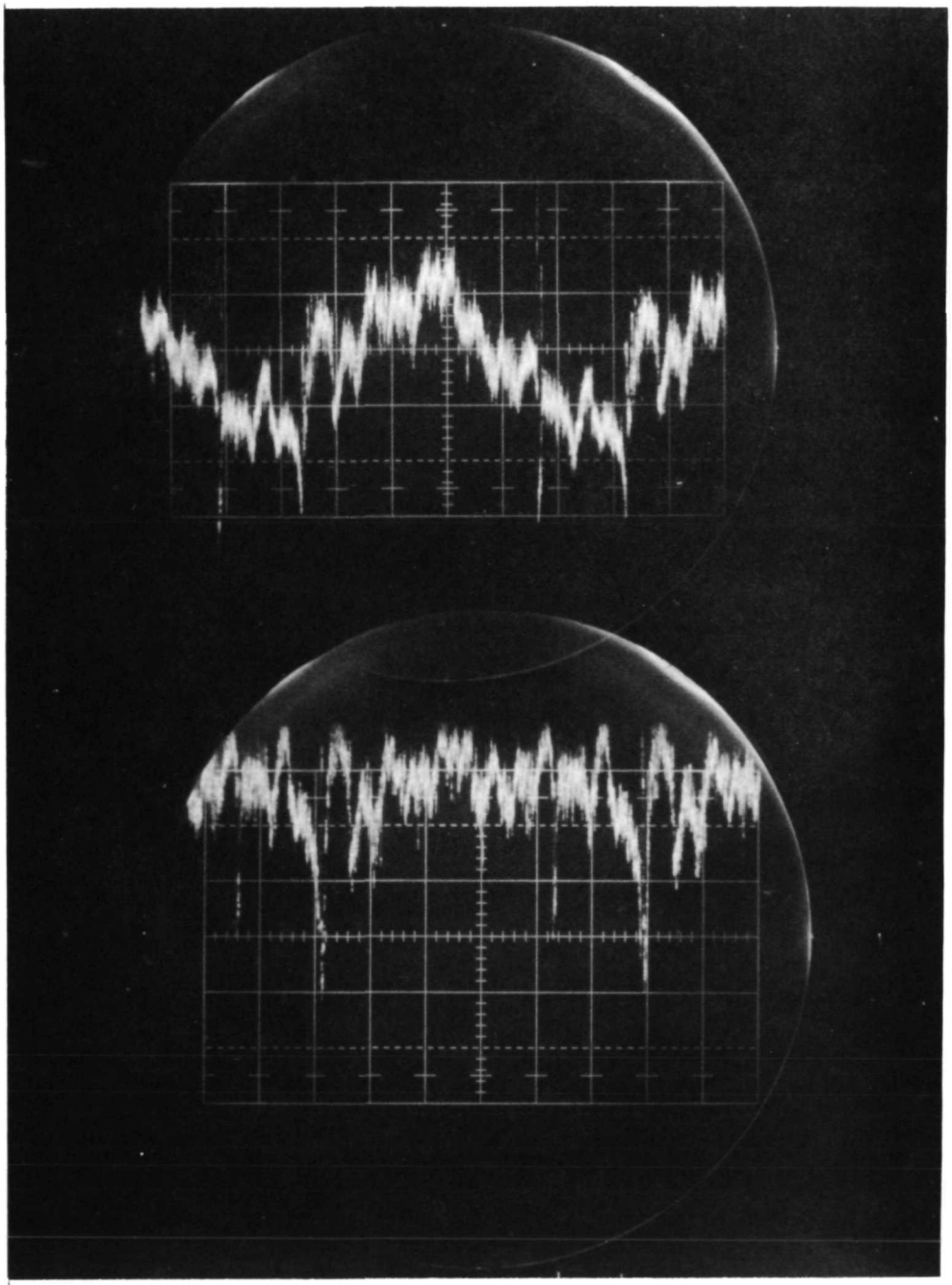

FIGURE 31. OSCILLOSCOPE TRACES OF OUTPUT FROM LIGHT-PIPE-REFLECTANCE UNIT

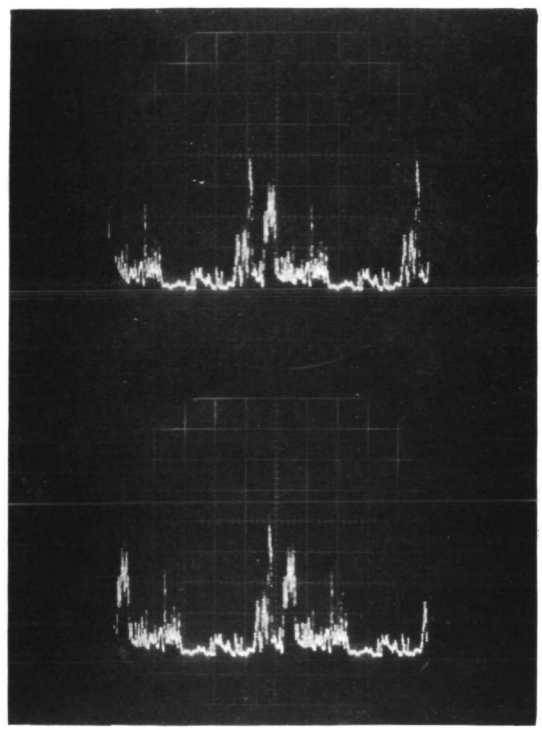

FIGURE 32. REPLICATE OSCILLOSCOPE TRACES OF OUTPUT FROM LIGHT-REFLECTANCE UNIT

Cryogenic and High-Pressure Endurance

Endurance testing of a probe tip under helium pressure and at liquid-nitrogen temperatures has been conducted using the system shown in Figure 33. Connected to a helium tank is a pressure gage, a needle valve, high-pressure tubing to another needle valve, a high-pressure "T", and finally the pressurization chamber for the probe.

The pressurization tubing is arranged so that the test chamber can be lowered into a medium-sized cryogenic dewar. The photograph shown in Figure 33 was taken shortly after completion of a run with liquid nitrogen cooling. The dewar has been removed but the frost on the test chamber indicates that it has not yet warmed back to room temperature.

At the beginning of a pressure test, the probe is adjusted so that when the high-pressure Conax fitting is tightened, the probe is spaced from the bottom of the pressure chamber so as to be operating in the middle of its high sensitivity range. Operation of the reflectance probe system during pressure evaluation has shown that there is no noticeable effect on the optical performance of either cryogenic temperatures or pressurization to about 2200 psig.

The probe showed no signs of breakdown when first subjected to helium pressures of 15 MN/m^2 and then to liquid nitrogen immersion, each applied separately. When cooling and pressurization were combined, the probe leaked slightly.

Examination after disassembly revealed that some dozens of the 600 glass fibers of the bundle had been forced several fiber diameters back into the tip. Stereo enlargements of the probe tip under two lighting conditions are shown in Figure 34. The tip area stretching from the center to the edge at the 7 o'clock position suffered the most extensive extrusion. This area had been roughened by slight contact with the rotating impeller during optical evaluations made earlier in the program and may, therefore, have been weakened.

The probe tip was repaired by forcing Armstong A-31 epoxy adhesive (an adhesive developed for cryogenic applications) into the probe surface using ~7 MN/m^2 of helium pressure. The probe was removed from the pressure

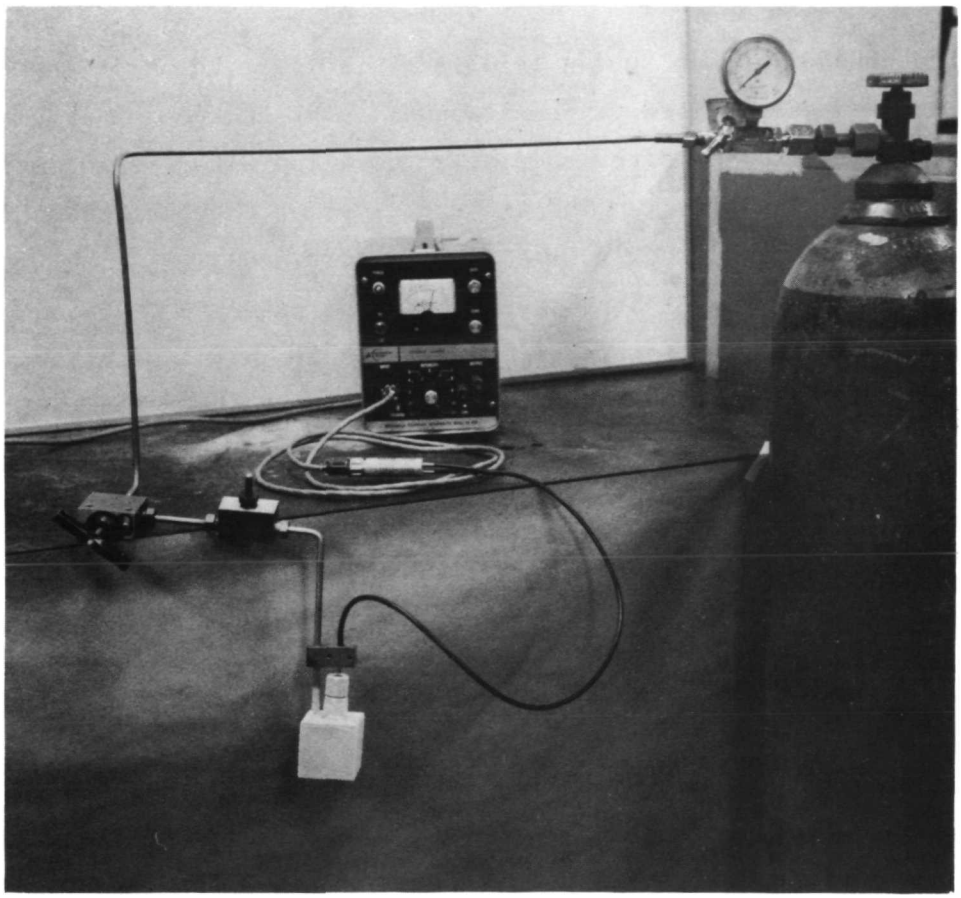

FIGURE 33. SYSTEM FOR TESTING EFFECT OF PRESSURE ON REFLECTANCE PROBE

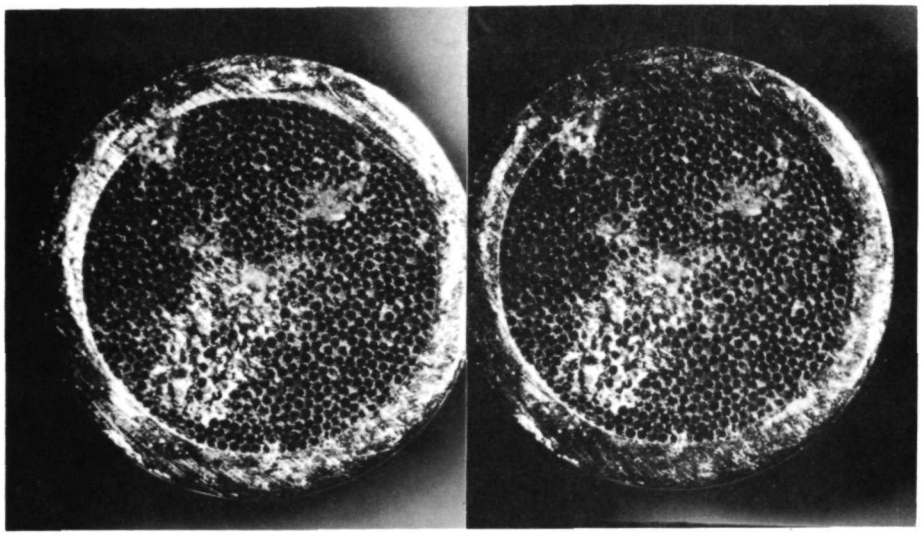

a. Reflected Light

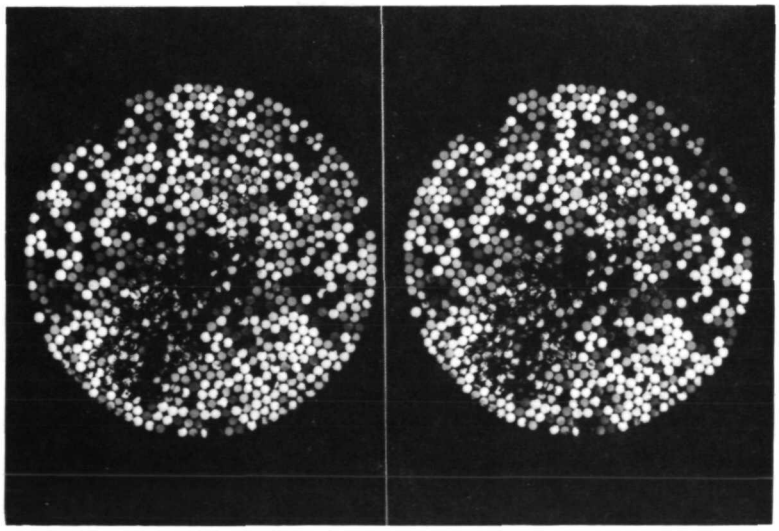

b. Transmitted Light

FIGURE 34. STEREOPHOTOGRAPHIC PAIRS OF OPTICAL SENSOR PROBE TIP FOLLOWING HIGH PRESSURE CYROGENIC EXPOSURE

chamber, wiped free of excess adhesive, and baked at 74 C overnight in order to thoroughly cure the adhesive. The tip was then ground and lapped to remove the previously damaged surface and return it to a planar condition. The pressurization was repeated at room temperature and then at liquid nitrogen temperature. There was no sign of leakage this time when the pressure reached the maximum of $\sim$ 15 MN/m^2 even at 77 K. The probe tip was examined subsequently and showed no sign of change. Whether or not the probe could withstand 48 MN/m^2 was to be determined in Phase III.

The optical signal was carefully monitored as the pressure was raised in steps. The data indicate a linear change in gap as a direct function of pressure. The gap opened up by 7.05 microns at room temperature with a pressure increase of $\sim$ 15 MN/m^2, at 77 K the change in gap was 2.77 microns. Since these changes were reversible, they indicate a mechanical flexing within the system as a function of pressure. If the flexing is assumed to take place in a length equivalent to the internal length of probe, then the equivalent modulus of rigidity is $\sim$ 90 GN/m^2 and $\sim$ 220 GN/m^2 at room temperature and 77 K, respectively. These are values that would be expected for glass at these temperatures. The observed gap enlargement may, therefore, result from compression of the glass fiber in the probe. Since this deflection is reversible and is predictable, it can be taken into account when measuring in a high-pressure pump.

Conclusions and Recommendations

The Phase II evaluation of the optical light/reflectance technique led to the following conclusions (based on the literature and on the evaluations made during the current program).

- Vibration amplitudes of 0.08 to 2.5 mm can be measured with a sensitivity of ±1 percent of full range.
- Vibrational frequencies up to 100 kHz can be measured readily.
- Uniform surface reflectance is desirable in high precision measurements but compensation methods can be employed to circumvent such problems.

- Currently available probes are capable of at least $\sim$ 15 MN/m^2 at 77 K.
- Custom made probes should be capable of enduring 480 C at pressures of about 1.38 MN/m^2 (200 psig).
- Conax pressure fittings with Teflon glands are suitable for $>$ 15 MN/m^2 at temperatures down to 77 K.
- Wall penetration of at least 2.5 mm diameter is required for a probe.
- The optical technique becomes inoperable in the presence of gas entrainment or cavitation.

PHASE III. EXPERIMENTAL VERIFICATION

Experimental verification was conducted under conditions anticipated for shuttle turbopumps: 35,000 rpm, 48.2 MN/m^2*, cryogenic temperatures and the shuttle vibration spectrum. The optical technique was the only one exposed to high-pressure and cryogenic conditions, since the flash X-radiographs are taken without contacting the pump, and the ultrasonic sensors attach to the outside of the pump case. The ultrasonic transducers and the optical probe were exposed to a vibration spectrum anticipated for Shuttle applications. The ultrasonic device was also applied to the shaft in the J-2 pump to demonstrate applicability to more than the impeller. The fiber optic probe was exposed to a high-velocity fluid stream representative of that expected if it were located in the output volute of a shuttle pump. Appendix B gives the test requirements satisfied by the Phase III effort.

Experimental Verification of Ultrasonic Doppler Method

Experiments were conducted to verify the effectiveness of the proposed ultrasonic Doppler method. Transducers having various operating characteristics were fabricated and evaluated initially using a simple laboratory device consisting of an aluminum block and an eccentric as shown in Figure 35. Transducers were clamped to the aluminum plate. The eccentrics were rotated at the rate of approximately 27 rev/sec. The circuitry of Figure 14, minus the side branch and the integrator was supplied by the Hammerlund 100A (5 MHz amplifier, heterodyne oscillator, mixer, and filter), frequency-to-voltage convertor (GR1142-A), and tunable filter (GR1232-A).

Measurements were made using eccentricities ranging from 0.127 mm to 0.635 mm**. Figure 36 shows two oscilloscope traces obtained from two different eccentricities. The eccentricity used to produce Figure 4a is 0.318 mm and that for Figure 36b is 0.635 mm.

Two miniature probes consisting of one-half section of a Branson 5 MHz, 12.7 mm diameter, dual-element probe used as a transmitter, and a

---

* 7000 psi.

** 0.005 in. to 0.025 in.

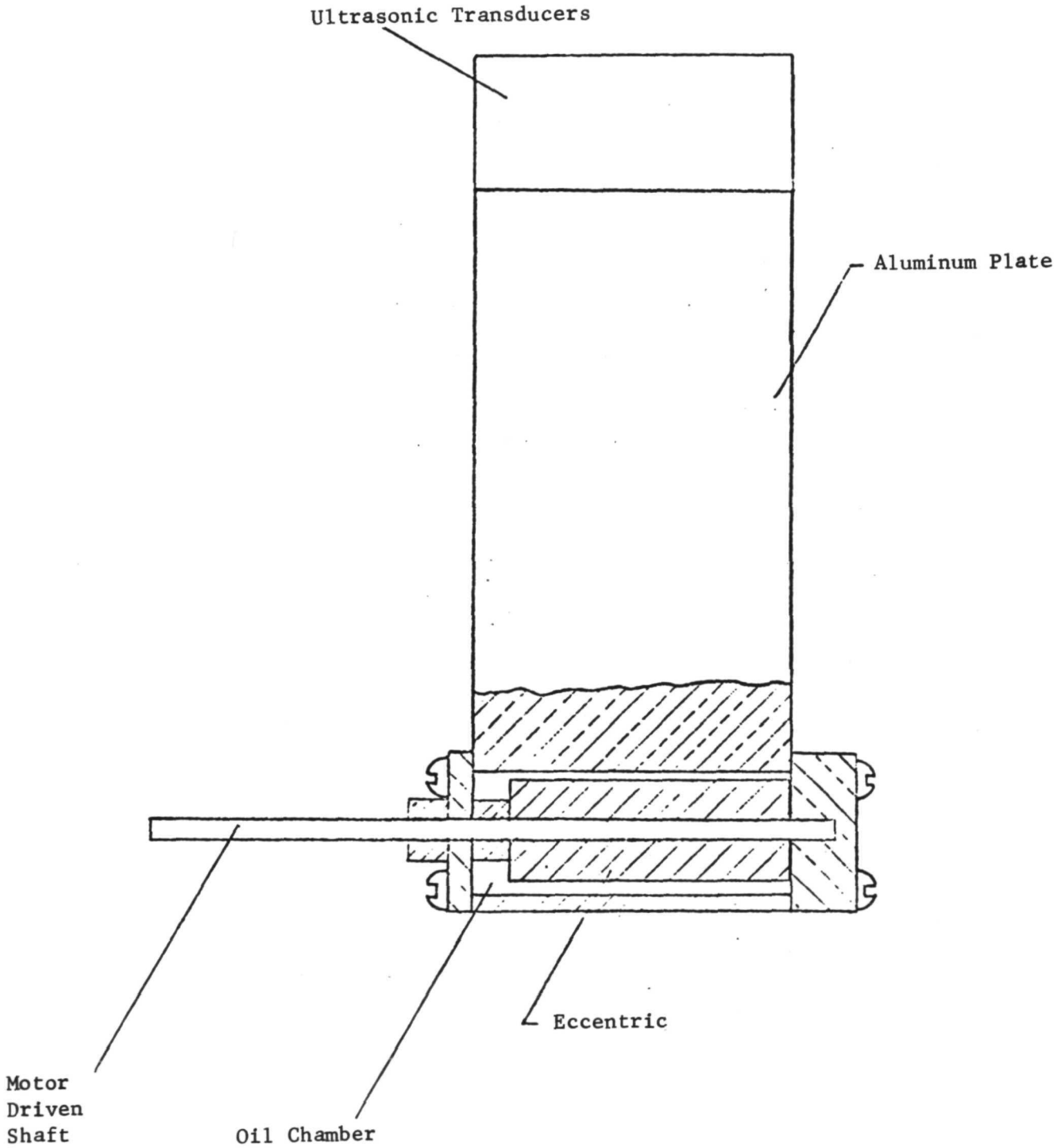

FIGURE 35. LABORATORY APPARATUS FOR EVALUATING ULTRASONIC DOPPLER METHOD OF MEASURING VIBRATORY DISPLACEMENTS OF ROTATING PARTS

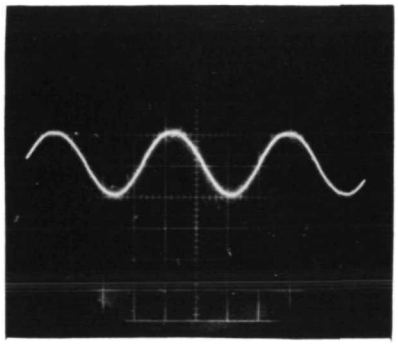

a. With an Eccentricity of 0.318 mm

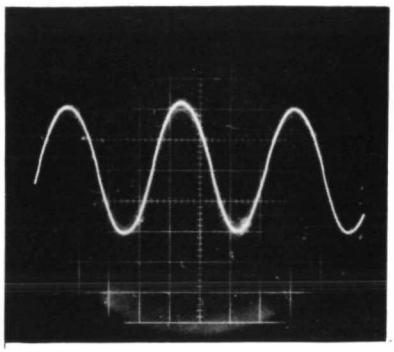

b. With an Eccentricity of 0.635 mm

FIGURE 36. ULTRASONIC DOPPLER SIGNALS RECEIVED FROM THE ECCENTRICS OF FIGURE 35 ROTATING AT 27 REV/SEC

Nortec 5 MHz, 1/4-inch diameter probe used as a receiver were used to measure the displacements of reflecting surfaces attached to the impellers of the J-2 turbopump. (The two elements of the Branson dual-element probe are not electrically isolated so that a separate probe was necessary to prevent excessive cross-talk.) The transducers were oil-coupled to the rough cast surface of the turbopump housing. The ultrasonic beam was transmitted through the wall and through a considerable distance in the oil used inside the turbopump. In spite of the rough surface of the pump and the low sensitivity of the miniature probes, the signal levels were more than adequate for the measurement. Figure 37 is an oscilloscope trace obtained with the miniature transducers.

The only problem encountered in the experiments involving the miniature transducers was associated with using an oil couplant on a vertical, rough surface. The oil drained from the surfaces fairly rapidly. This is not considered to be a significant problem in that it can be corrected easily by any of several means: (1) smoothing the rough surface, (2) using grease instead of oil, or (3) bonding the transducers to the surface.

Transducer

During Phase III of the research program, a miniature transducer was designed and constructed which incorporated features found to be necessary. This is a dual-element transducer, the two elements being electrically isolated but housed in a common epoxy block as shown in Figure 38.

Originally it was planned to use a ceramic (aluminum oxide) face plate; however, potting with Armstrong A31 epoxy provides a more rugged transducer for use at cryogenic temperatures.

Each of the two Vernitron 1/2-inch diameter PZT-4 ceramic disk piezoelectric elements is housed in a separate 15.90 mm OD copper tube. The elements are molded together in a block of Armstrong epoxy.

The new transducer was checked for electrical cross-talk and for electrical continuity after each step of its fabrication. This transducer was used in all experiments conducted during Phase III. It has excellent sensitivity, no electrical or ultrasonic cross-talk, and good ruggedness.

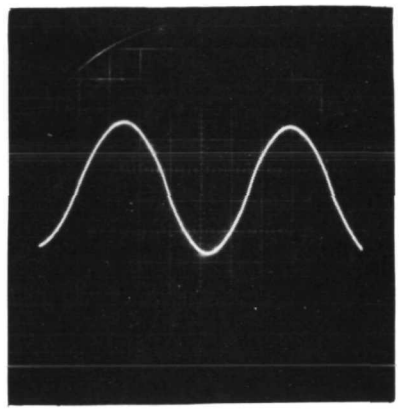

FIGURE 37. ULTRASONIC DOPPLER SIGNAL OBTAINED FROM REFLECTING SURFACES BONDED TO THE IMPELLER OF THE J-2 TURBOPUMP SIMULATING A VIBRATION AT 37 Hz AND A TOTAL DISPLACEMENT OF 3.2 mm

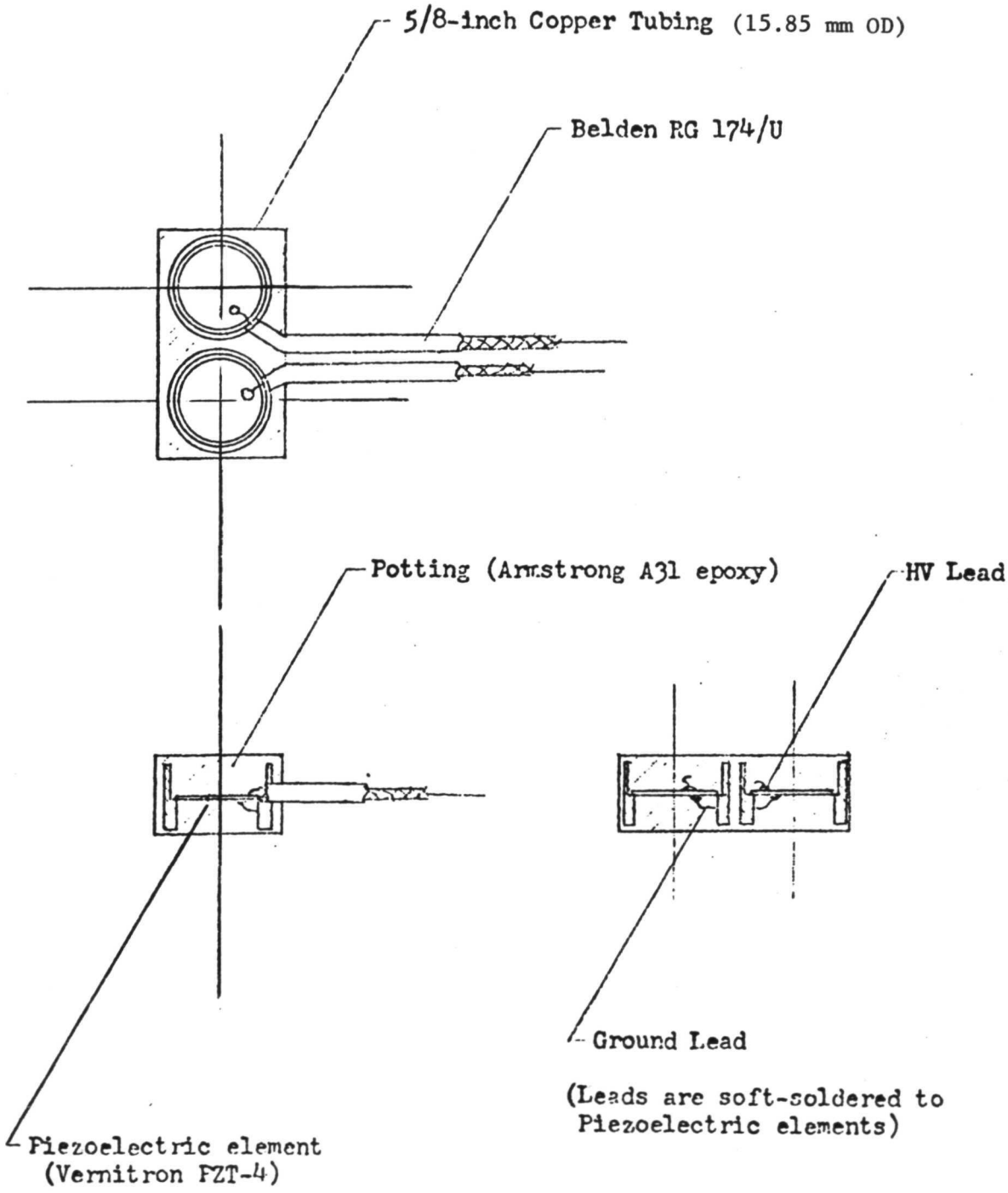

FIGURE 38. SCHEMATIC VIEW OF ULTRASONIC TRANSDUCER DEVELOPED FOR USE IN MEASURING VIBRATIONS IN PUMP SECTION OF TURBO-PUMP BY DOPPLER TECHNIQUE

Vibration Test

NASA specified that the following data were to be used as a guide for the Phase III vibration test.

5 to 30 Hz at 7.61 mm peak to peak

30 to 400 Hz at 15 "g" peak*

400 to 900 Hz at 0.042 mm peak to peak

900 to 3000 Hz at 50 "g" peak.

The transducer was glued to an aluminum test apparatus designed for testing the optical probe simultaneously.

Two shake tables were required to cover the entire frequency range specified by NASA. A mechanical shake table was used to meet the requirements within the range 5 to 30 Hz. A Calidyne (electrodynamic) shake table was used to cover the remaining frequencies.

The amplitude of the mechanical shake table was measured statically. The peak-to-peak displacement was 7.92 mm (5/16 in.). The amplitude of vibration of the Calidyne shake table was monitored using an accelerometer. The vibration amplitudes obtained using the Calidyne were

From 30 to 400 Hz	15 "g" peak
From 400 to 900 Hz	0.0432 mm peak-to-peak
From 900 to 2500 Hz	50 "g" peak or greater
From 2500 to 3000 Hz	approximately 66 "g".

These data indicate that the specifications were either met or exceeded during the vibration tests.

The ultrasonic Doppler device was tested under the above-stated conditions at room temperature. The test was repeated under cryogenic conditions in conjunction with the optical probe test.

---

* "g" ≡ force of gravity at surface of earth.

Vibration Test Results

The output of the Doppler system was monitored during the entire vibration test procedure. The primary concern was whether the vibrations would produce noises that would cause errors in the Doppler signal corresponding to displacement amplitudes. Since the transducer bonded to the Duco cement is similar to a mass on a stiff spring, very slight flexing could be expected at certain frequencies corresponding to resonances. These were observed as follows

(1) During both the room temperature and the cryogenic runs, small Doppler shift was observed between 15 and 20 Hz.

(2) During the room-temperature test, slight Doppler shift was observed between 110 and 190 Hz, between 580 and 590 Hz, and at 2700 Hz.

(3) During the cryogenic test, very slight Doppler was observed from 1200 to 3000 Hz.

No noise was recorded by the ultrasonic Doppler system during the tests.

The transducer was examined following the vibration tests. It showed no apparent damage or change in sensitivity. Therefore, the ultrasonic Doppler system appears to be immune to extraneous noises. There appears to be no difficulty in constructing transducers that can withstand both the vibrational and the cryogenic environments specified.

Following the vibration tests, the transducer was removed and used for all subsequent experiments.

35,000 rpm Test

The 35,000 rpm test was simulated by using a universal motor rated at 18,000 rpm to drive a cylindrical rod with two flats 180 degrees apart machined along its length. A rod with an elliptical cross section would have been the ideal. The flats were accepted as a compromise to make fabrication easier.

The rod was 5.84 mm in diameter. The flats were 0.051 mm deep on the radius of the rod and slightly less than 1.01 mm wide.

The dimensions of the rod were determined by the torque capabilities of the motor. The dimensions of the flats were determined by the range of the instruments used.

Theoretically, in the absence of voids (vortices, bubbles, or cavitation) in the liquid surrounding the shaft, at a speed of 18,000 rpm, no Doppler signal should occur when the curved surfaces move through the ultrasonic beam. However, as the flat moves into the beam (at 5 MHz) the Doppler shift drops rapidly to -3170 Hz until the center of the flat coincides with the axis of the beam. Then it rises rapidly to +3170 Hz and drops back to zero as the round surface moves into the beam. The period between such shifts for a shaft with two flats rotating at 18,000 rpm is 1.67 msec. (The period of the Doppler signal caused by the flats on the shaft corresponds to the period of a smooth shaft vibrating at 4750 Hz, corresponding to 284,000 rpm.) The theoretical curve of a shaft with flats 0.051 mm deep on the radius rotating in water at 18,000 rpm under ideal conditions is as shown in Figure 7.

Oscilloscope traces of the Doppler signal produced with the shaft immersed in water, in a rectangular solvent can, had an appearance similar to that of Figure 39. However, the appearance of the "pips" was intermittent. Occasionally, a sequence of indications would appear at regualr intervals of 3.6 msec. This corresponds to the period of one complete revolution at 16,700 rpm. Sometimes, other indications would appear corresponding to the period of half a revolution at the same speed. At other times the period between indications would correspond to more than one revolution. These results were somewhat puzzling. A second experiment was conducted with the shaft immersed in water in a cylindrical container (see Figure 40). When the shaft was located at the center, the water flow experienced negligible restraint and the shaft produced strong vortex action. Some air bubbles were observed. The depth of the vortex varied sporadically, occasionally permitting enough water to surround the shaft to permit the ultrasonic beam to contact it. On collapse of the vortex, the Doppler would correspond to that expected from the flats. However, this happened too seldom to record any significant data. When the shaft was located off-center to reduce the vortex action, the rod stirred so much air into the water that no significant data could be observed.

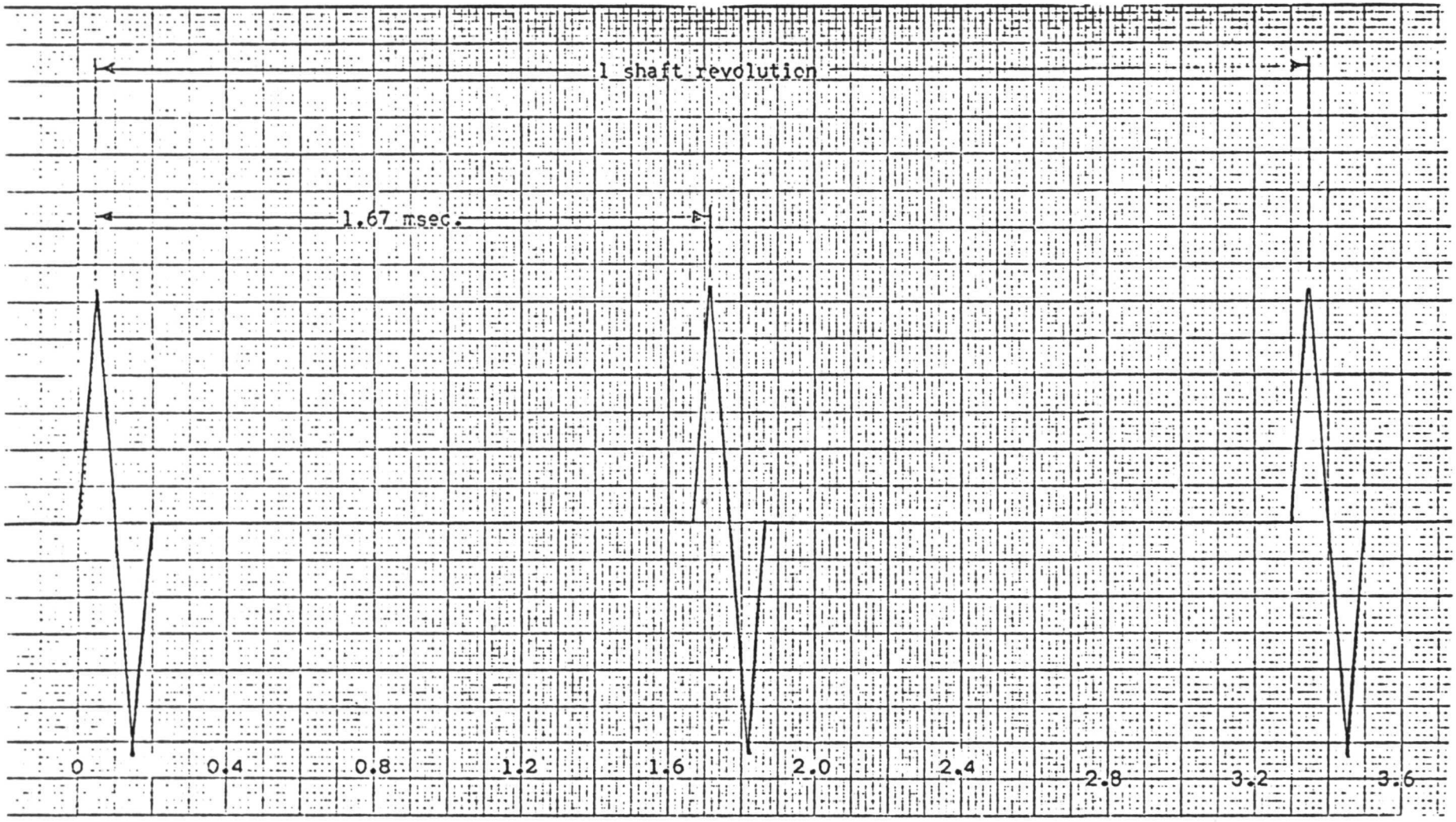

FIGURE 39. THEORETICAL DOPPLER SHIFTS DUE TO 0.051 mm DEEP FLATS ON A 5.84 mm SHAFT ROTATING AT 18,000 RPM IN WATER WHEN THE CARRIER FREQUENCY IS 5 MHz

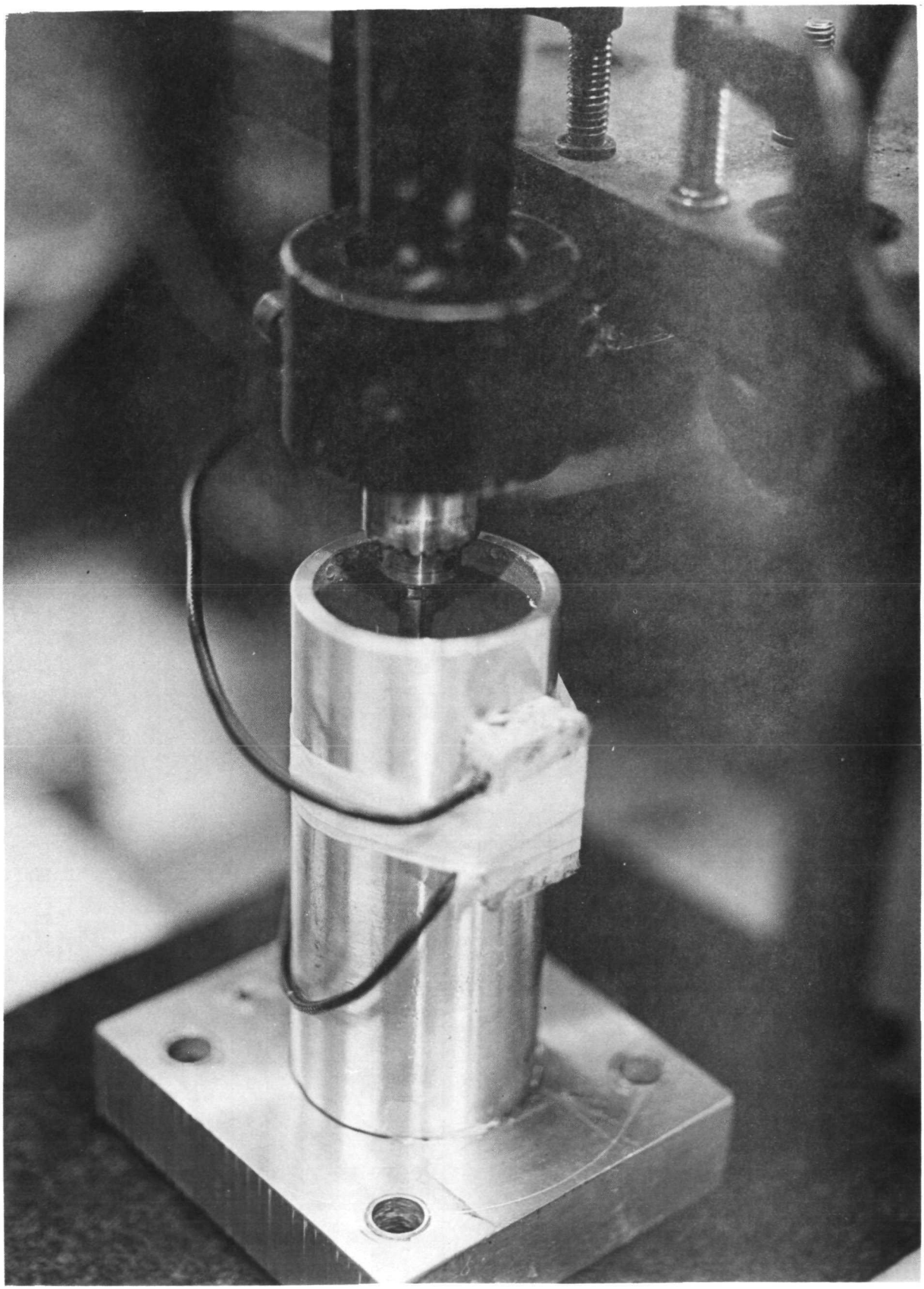

FIGURE 40. EXPERIMENTAL APPARATUS

The rectangular can of solvent apparently reduces the size of the vortices. Formation and collapse of these vortices is apparently the explanation for the intermittent indications recorded when the tests were run in the solvent can.

The speed of rotation of the shaft immersed in water was measured. It varied from approximately 16,000 rpm to approximately 17,000 rpm. The periods measured during the tests in the solvent can corresponded to 16,700 rpm as mentioned previously.

In order to obtain a more satisfactory test of the system to detect vibrations corresponding to rotation at 35,000 rpm, the experimental setup was changed. An electromagnetic driver was coupled to the wall of the solvent can by means of a length of piano wire. The wall of the can was driven at 600 Hz corresponding to 36,000 rpm. The Doppler system responded not only to the 600 Hz vibration of the can wall but it also detected other vibrations which were superimposed. These "other vibrations" were building vibrations to which the can responded as a microphone. These were large enough that they could be detected easily by feel when the oscillator was turned off. Figure 41 is a sample indication showing the Doppler signal of the 600 Hz vibration.

These tests indicate that the Doppler system is capable of measuring the vibration of shafts rotating at 35,000 rpm (and at much higher speeds) in the absence of gas bubbles or cavitation.

Indicating Vibrations of the Shaft of the Pump

Phase III requirements included the measurement of runout of an alternate pump component. The shaft between the bearings was selected for this purpose. Reflectoscope measurements demonstrated that we could attach probes to the pump in the vicinity of the junction between the impeller housing and the turbine housing. From this area, ultrasonic waves could be conducted to the shaft and reflected back out the same way.

Careful preparation was made for this experiment. A theoretical Reflectoscope image was developed by studying the area of the assembly drawing corresponding to the pump section through which ultrasonic access to the

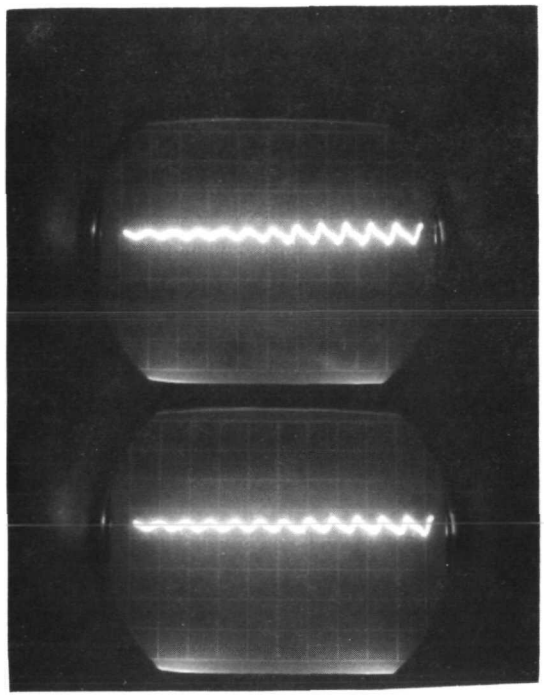

FIGURE 41. DOPPLER SIGNAL ASSOCIATED WITH 600 Hz VIBRATION

shaft was available. The correct position of the ultrasonic probes was determined by scanning the area with a Reflectoscope until an identical image was observed on the CRT screen. An epoxy block molded to the contour of the pump housing was then bonded with epoxy to the housing. The outside of the block was machined flat for convenience in mounting and manipulating the transducers. The transducer was then located in its proper position on the epoxy block, with the aid of the Reflectoscope, and then glued in place.

Three critical speeds between zero and the maximum speed of the test had been observed in the pump. It was hoped that vibrations associated with these speeds would be sufficiently large to measure with the Doppler system without having to add something to the shaft to simulate vibrations.

We were prepared with a standby power oscillator capable of driving the transducers at 1.2 MHz if attenuation at 5.0 MHz proved to be too great to permit a successful measurement. Fortunately, the second generator was not needed. The instrumentation produced a good signal without difficulty. The pump was brought to the maximum speed and then turned off and allowed to coast to a standstill. This procedure was repeated at least 6 times, and each time low-amplitude vibrations were indicated at each of the critical speeds. Photographs of the traces were not possible due to the transient nature of the indications and to the difficulty of coordinating the oscilloscope traces and the camera shutter.

General Remarks

Results of all experiments conducted during this research program have confirmed the theory upon which the ultrasonic Doppler vibration measuring device was based. Therefore, we are confident that the ultrasonic system is capable of measuring the vibrations of any surface if the ultrasonic beam has access to that surface and can be reflected back to the receiver. The system can work in a gas or in a liquid. The conditions for successful application are that the probes be designed for operation in the specified media.

Optical Light-Pipe Reflectance Technique

The "Fotonic" sensor, Model KD-45A, was subjected simultaneously to 48.2 MN/m^2 and liquid nitrogen and a calibration was made before and after exposure. Next, the probe was subjected to a high vibration environment while at cryogenic temperatures. Finally, the probe, in a protective sleeve, was exposed to a high-velocity fluid stream simulating the output volute of a Shuttle pump.

Cryogenic and High-Pressure Compatibility

To protect the probe from damage, a 1 mil protruding collar was first bonded to the sheath of the sensor probe tip using the low-temperature epoxy technique described previously. A photograph of the recessed tip geometry is displayed in Figure 42. The presence of the collar produced some variation in the shape of subsequently made calibration curves. The method of "zeroing" the Fotonic meter by bringing the tip into contact with the surface being sensed could no longer be used. Consequently, the range of light intensities (as expressed on the meter) was decreased by approximately 30 percent, and this precluded the possibility of using the 0 to 100 meter readings as percentage figures. Of somewhat more significance is the related reduction in readability of the meter--the sensitive measuring range of the probe* then required approximately 75 meter divisions instead of 100 as was the case before installation of the protruding collar. The result of the changed performance is to shorten the effective probe range by 1 mil (25 microns). Whether or not this constitutes a significant deficiency depends on the individual application and the case of checking calibration during use. The latter statement is made in view of the fact that a greater (nonlinear) range would be practicable provided the presence of any drift is detectable and appropriate compensation is made.

---

* Our calibrations involved separation of the probe tip from the test surface by about 0.3 mm (12 mil). This constituted the entire "rising" portion of the overall sensitivity curve. The "linear" portion of the curve extends from approximately 25 to approximately 76 microns (1 to 3 mil).

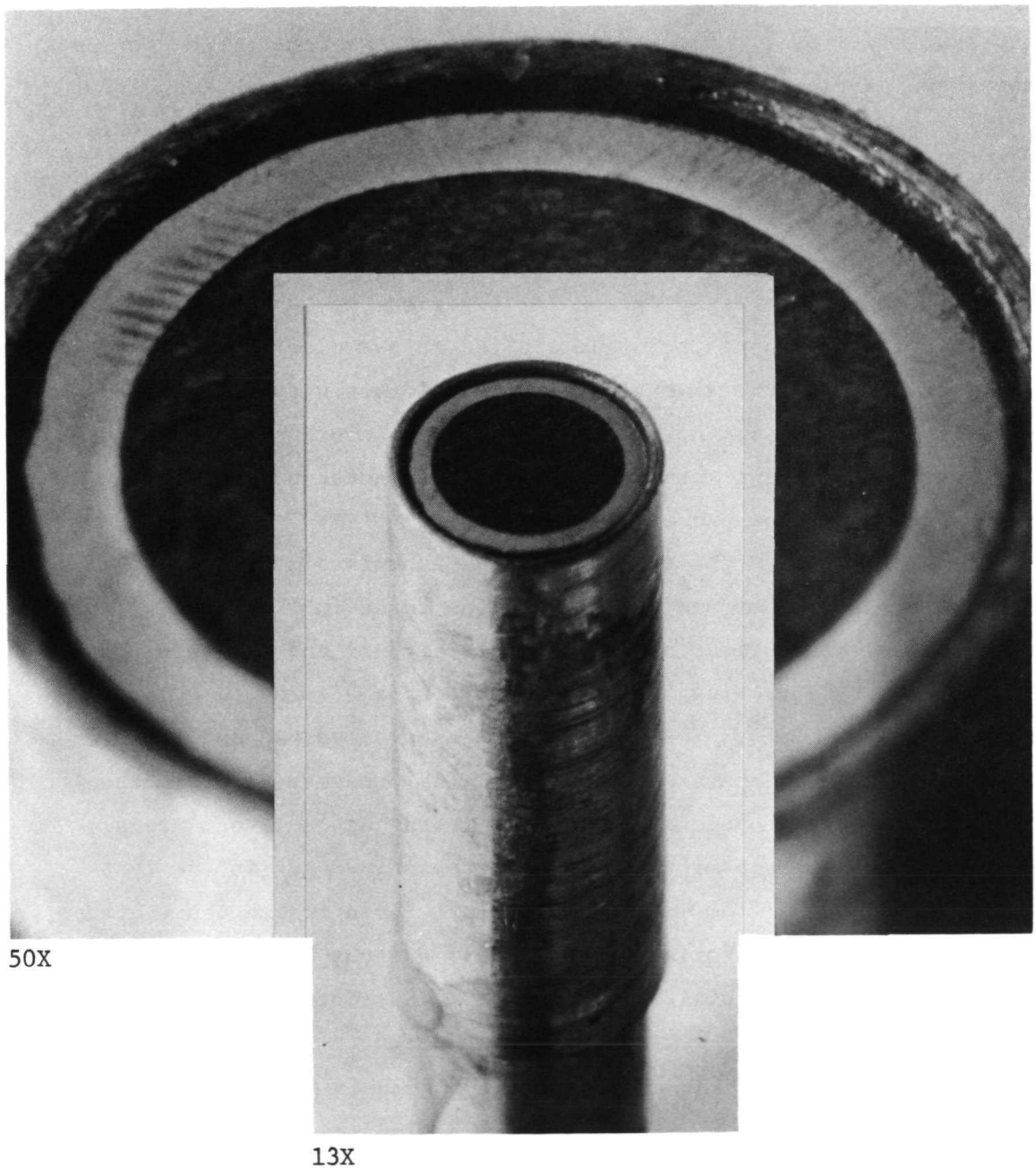

FIGURE 42. FOTONIC-SENSOR-PROBE TIP WITH PROTRUDING COLLAR

The simple test fixture constructed to facilitate sensitivity calibrations during liquid nitrogen immersion is illustrated in Figure 43. The spindle micrometer is used to raise or lower the thick disc. The light-pipe probe, perpendicular to the disc upper surface, senses the amount of disc rise and fall by its output as indicated on the meter. The thin-wall tubing, shown vertically at the right side in the photograph, is used to lower and support the working components below the surface of a liquid nitrogen bath.

At 77 K, the micrometer froze solid--in spite of the fact that all lubricant had been removed. Successful operation was achieved by considerably loosening the thread collet. Except for irregular waviness--probably associated with the surface finishing technique applied to the disc--adequate calibrations were carried out with the immersion fixture. Sensitivity to local surface reflectivity variation was noted--but this is an inherent characteristic of the light-pipe sensing technique and has been noted previously.

The light-pipe probe was subjected to 48 MN/m^2 N_2 using the same fixture that was applied for the 15 MN/m^2 He experiments. A photograph of the high-pressure pump and system is illustrated in Figure 44. This system permitted pressurization of the probe fixture and the upper volume of an accumulator by valving in full pressure from a standard N_2 bottle (approximately 18 MN/m^2). Then, with the N_2 source valved out, a 10,000 psi hydraulic pump was operated to increase the pressure in the accumulator to above 48 MN/m^2--by movement of a piston in the accumulator. This technique assures noncontamination of the pressurized gas in the test fixture. It was found from melting point data for nitrogen that, at the test pressure of 48 MN/m^2 (approximately 467 atm), gaseous N_2 becomes liquid below the critical temperature of 126 K; also, at 77 K (liquid N_2 temperature at 1 atm), a pressure of 76.7 MN/m^2 would be required to cause the liquid N_2 to become solid. These fortuitous transition properties led to a simple solution for subjecting the optical probe to liquid N_2 at 48 MN/m^2. It was only necessary to introduce the gas, cool to 77 K by immersion in a dewar of liquid N_2, then raise the pressure to 48 MN/m^2. The gas volume contained in the accumulator was very large compared with the test block and connecting tubing; thus, an adequate supply was available for condensation.

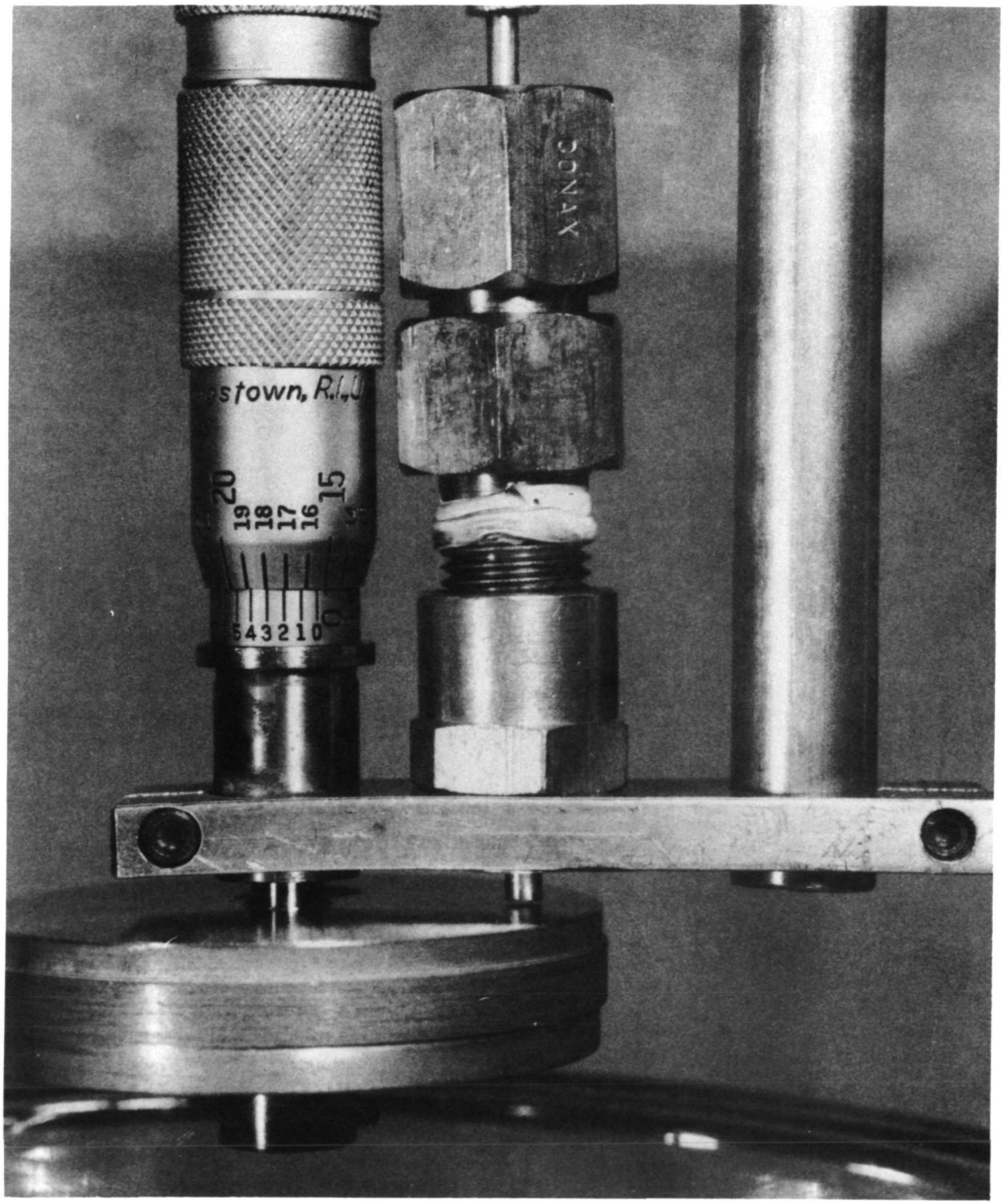

FIGURE 43. FOTONIC SENSOR CALIBRATION FIXTURE FOR CRYOGENIC IMMERSION

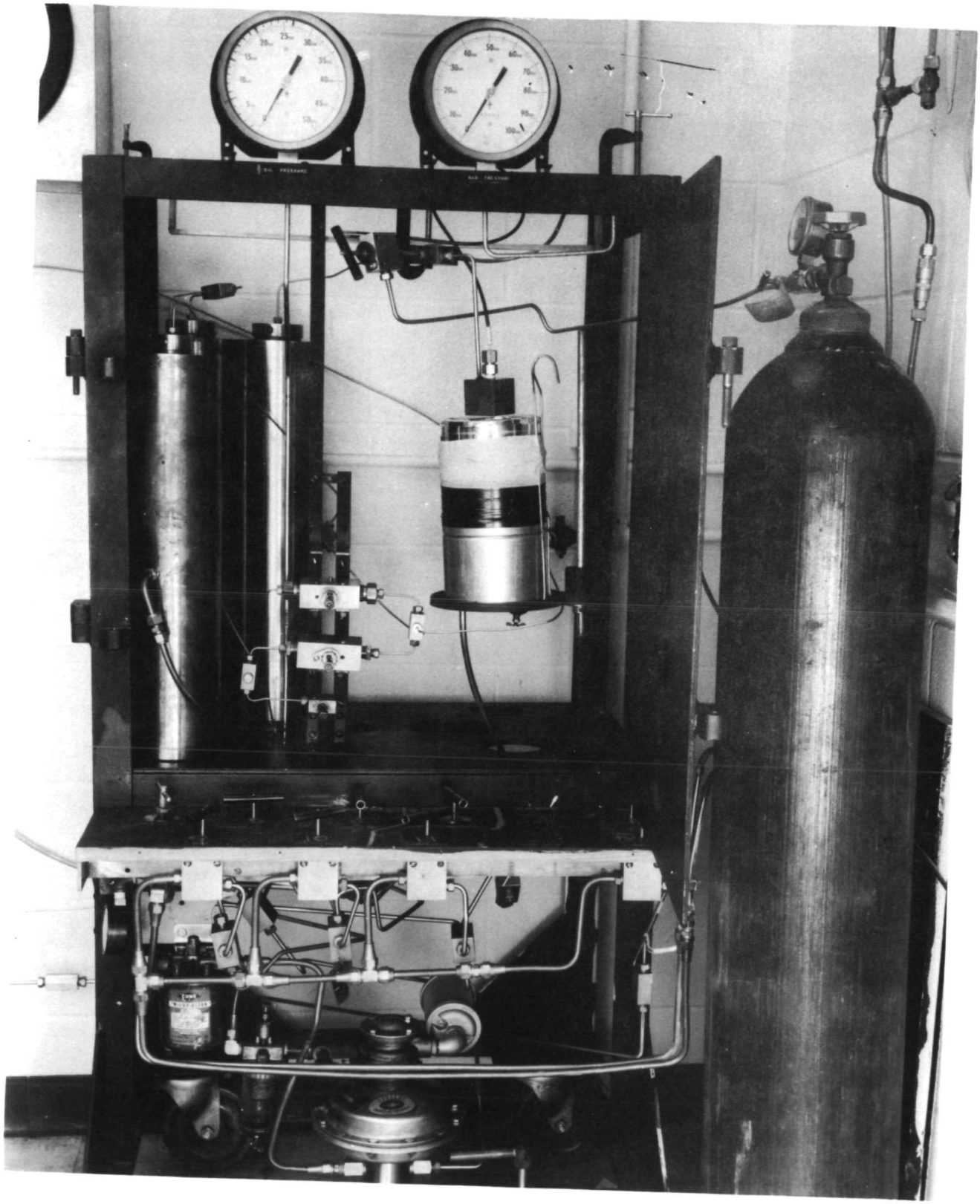

FIGURE 44. 7000 PSI PRESSURIZING SYSTEM

It was intended that the Fotonic sensor read-out meter would monitor response of the probe during the entire test. Unfortunately, the Teflon packing gland could not mechanically secure the probe at pressures above 20 MN/m^2. Axial slippage occurred allowing the sensed gap-width to increase beyond the linear range of probe sensitivity. As a result, the probe response could only be checked after removal from the high-pressure fixture. Neither the sensitivity performance nor the physical integrity appeared to be significantly altered by this exposure.

Calibrations of the sensor would be carried out with the turbopump in a nonrotational condition. The probe tip is advanced until contact is made with the surface under measurement, and the Fotonic meter adjusted to zero or to some other predetermined valve. The probe is subsequently withdrawn in half-mil steps and a meter reading recorded for each. The slope of the resulting data plot is then compared with previously made calibration plots. If agreement is good, no sensitivity factor change is necessary. If the slope shows change, the most likely cause is from a changed reflectivity of the surface under measurement. A second possible reason for a change is damage to the probe tip which would effect a change in light transmission. The least likely reason for a change is degradation of performance of the Fotonic sensor light source or photocell components. The lamp can, of course, be expected to gradually weaken with age and thereby require increased brightness settings during its use. This behavior, however, could be monitored outside the pump. One problem which might arise with applying the above calibration procedure involves the accurate detection of the point-of-touching position between the probe tip and the sensed surface. The mechanical drive for this adjustment would likely be a micrometer head located outside the shell of the turbopump, and this would drive the probe axially through a Teflon-packed gland. Temporary loosening of the packing might be necessary to facilitate the sliding movement. If the design of the gland fitting allows the probe sheath to be electrically isolated, then the point-of-touching can be easily and accurately determined with an ohmmeter. An alternative technique for setting the proper null value for the Fotonic sensor meter is to withdraw the probe tip about 0.6 mm (1/4 in.) or more from the surface being sensed. This results in very low sensor response--almost identical with the point-of-touching value. In this case the meter values would be noted as the probe tip is advanced <u>toward</u> the test surface.

Vibration Experiments

The optical (light-pipe) probe was exposed to the same vibration environment as described for the ultrasonic transducer.

The probe was screwed by means of its 1/4-in. thread (Conax fitting) into one edge of a flat, ~ 19 mm -thick aluminum plate. The probe tip was located close to a flat surface exposed from above. By this technique, the sensor's response could be monitored during the experiments.

The probe survived the vibration/cryogenic exposures without apparent deleterious effects. During room-temperature exposures, no variation in probe output was observed; when liquid nitrogen was added to the standpipe over the probe-measured gap, a change was indicated. This was probably due to thermally produced distortion--when the temperature reached equilibrium the probe output was stabilized (except for spikes produced by liquid nitrogen boiling). After this initial change, the gap measurement remained stable throughout vibration experiments. When room temperature was eventually restored, the gap reading had returned to approximately the original value. No physical damage to the light-pipe bundle was evident following the vibration exposures.

The output change resulting from the cooling would probably also occur during pump prototype by sliding through the Teflon packing to obtain the original gap output, if desired. A small change in apparent gap will also occur due to the changed index of refraction. The resultant small change in apparent sensitivity is, however, very small.

Fluid Jet Experiment

The light reflectance probe was subjected to a jet stream of water having a velocity slightly greater than that anticipated for the turbopump application-- 9.28 m/sec as compared with 8.98 m/sec.

The geometry and dimensions of the fixture used for the jet-flow exposure are indicated on Figure 45. The performance of the probe was not altered by the exposure and no damage to the tip was evident. During

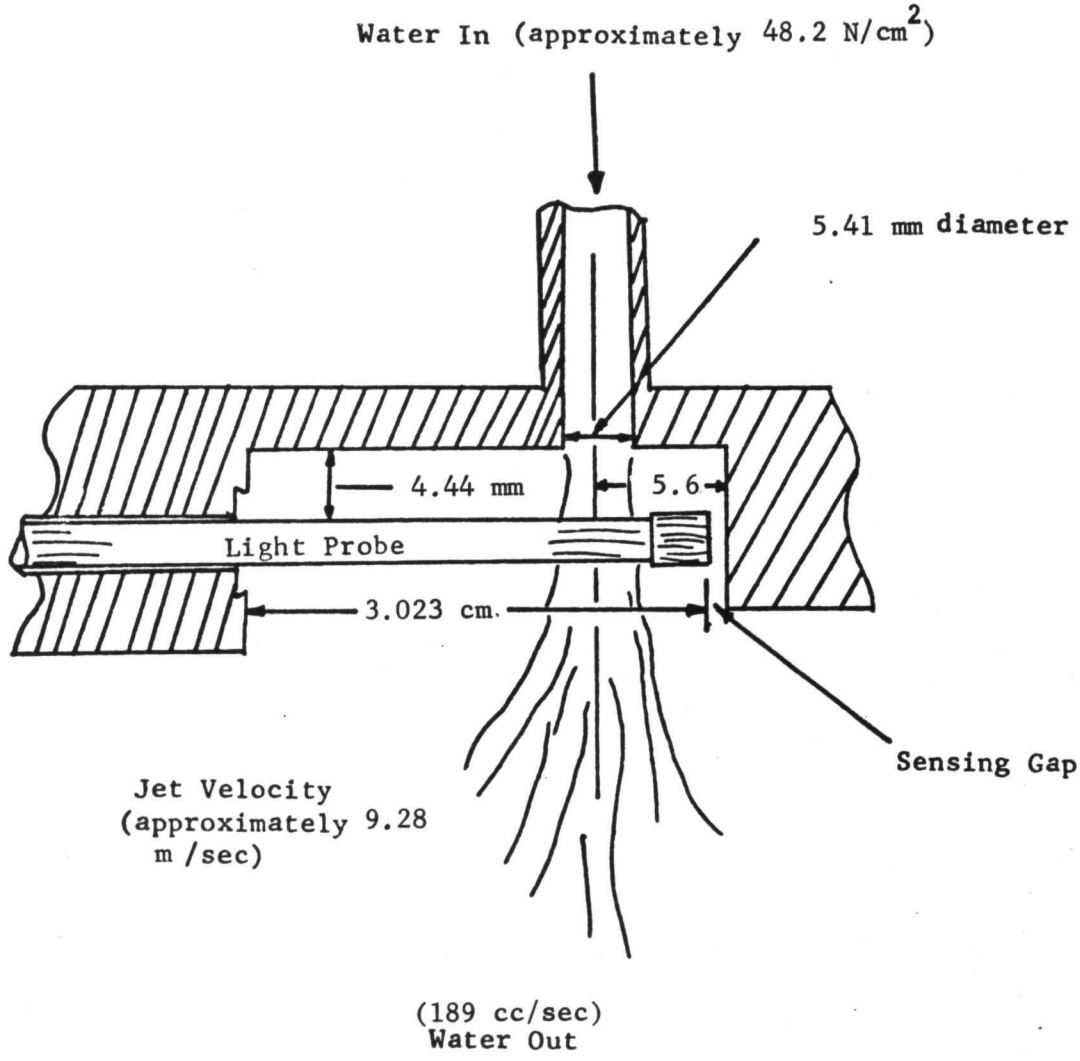

FIGURE 45. SCHEMATIC OF INSTALLATION OF LIGHT-PIPE SENSOR FOR FLUID-VELOCITY TEST

exposure, erratic performance was observed, due probably to cavitation in the liquid medium present in the sensing gap. This situation would not exist in the turbopump environment where pressures exceed the critical pressures of the cryogens.

This test of the light-probe serves to illustrate its durability against bending and vibration in a liquid jet stream. In the prototype design, strength rigidity and natural frequency of the probe sheath would be increased beyond the commercial model presently under test.

Discussion and Recommendations

A summary of the Fotonic's sensitivity performance is contained in Table 5. This lists the "linear slope" of the sensitivity plots from a number of calibration runs. The "linear slope" figures represent the percent of full-scale (PFS) output per micron (one-thousandth in.) of gap change. The linear range varied somewhat but was always within 25 to 90 microns (1 to 3.5 mil). It can be noted that the root-mean-square deviation from the average slope of all runs is ±2.5 percent. Significance of an "average" is based on the supposition that any internal (electronic or amp source) changes were negligible throughout the calibration runs for the various environmental exposures. One source of variability that exists within the sensor itself involves the built-in nonlinearity for range changes and intensity setting changes. Thus, it is recommended that calibrations be performed at the same sensitivity-range settings as are to be used during the application measurements. Obviously, the only meaningful calibration must be made on the final turbopump application. In fact, calibration, a relatively simple procedure, should be repeated frequently during the application (prototype) runs. To make this feasible, the probe will have to be mounted in a sealing gland designed to permit a few hundred microns of movement in a direction perpendicular to the surface being sensed.

TABLE 5. FOTONIC SENSOR, LINEAR-RANGE SENSITIVITY

Description of Data Source	Environment		Linear Slope[(a)], PFS/micron
	Temperature, K	Fluid	
1. Calibration supplied by manufacturer	300	Air	0.665
2. Repolished probe tip versus vapor-blasted brass disc	300	Air	0.827
3. Repolished probe tip versus vapor-blasted brass disc, 1-mil protruding collar installed	300	Air	0.788
4. Repolished probe tip plus collar machined brass disc surface	300	Air	0.764
5. Same as 4 plus immersion in liquid N_2	77	N_2-liquid	0.642 (average of 2)
6. Repeat of 5 but approximately 20 hr later	77	"	0.780
7. As in 4 but following exposure in liquid N_2	300	Air	0.622
8. Repeat of 7, three days later	300	Air	0.914
		Average (all of above)	0.752 ± 0.0984 PFS/mu

(a) Reference Appendix A for examples of "linear slope". PFS = percent of full scale.

The probe chosen for application to these verification experiments contained 300 light-transmitting fibers and 300 light-receiving fibers, all exposed at the polished probe tip. The two kinds of fibers are randomly interspersed to provide the maximum sensitivity for a very short range. The range from 25 to 76 micron being very close to a linear response. Other designs are available--for example, all light transmitters on one side of a cross-sectional diameter and all light receivers on the other. This geometry of distribution provides maximum sensitivity over the linear range from 0.5 to $\sim$ 1.3 mm for an otherwise equivalent probe design. Many other fiber distributions are possible and each produces an optimum working range. Other possible modifications involve fiber size, fiber number, fiber length, and fiber composition; also, bundle number, size, and shape. Since each modification combination can be expected to provide optimum performance under a closely defined set of operating conditions, it follows that a very detailed knowledge of the application conditions should be applied to the probe-design specifications. Thus, in principle, a probe should be designed specifically for each situation.

Flash X-Radiography

The time interval over which the flash X-ray pulse occurs is about 20×10^{-9} seconds. This interval is sufficiently short that the rotation of a high speed part during the interval would not be expected to affect the resolution of the radiograph. For example, a point on the circumference of a half-meter diameter wheel would move less than 25 microns (1 mil) in 20 nanoseconds. Since this movement is tangent to the line of view, no deleterious effects on resolution can be imagined. Nevertheless, in order to be certain that high-speed motion did not affect the flash X-ray technique, an experiment was performed in which a radiograph taken of an object rotating at 18,000 rpm was compared to one taken of the object while stationary.

The object used was a piece of stiff, bent wire inserted into a small chuck driven by a DC motor. Flash X-radiographs were taken with Battelle's 300 kv unit.

Comparison of the radiographs shows no difference in resolution between stationary and rotating cases. The outline of the wire is as sharp in one radiograph as the other. Resolution of the chuck is also the same on either radiograph. No effects of high speed motion were detected in comparing the two radiographs.

DISTRIBUTION LIST

	Copies
NASA Headquarters Washington, D.C. 20546 Contracting Officer	1
NASA Lewis Research Center 21000 Brookpark Road Cleveland, Ohio 44135 Office of Technical Information	1
NASA Manned Spacecraft Houston, Texas 77001 Office of Technical Information	1
NASA Marshall Space Flight Center Huntsville, Alabama 35812	
Office of Technical Information, A&PS-MS-IP	2
Technical Library	1
B. Birdwell, S&E-ASTN-RRI	1
H. Attaya, S&E-R-R	1
F. D. Pitsenberger, S&E-ASTN-PPM	5
A&PS-TU	1
Jet Propulsion Laboratory 4800 Oak Grove Drive Pasadena, California 91103 Louis Toth	2
Chief, Liquid Propulsion Technology RPL Office of Advanced Research and Technology NASA Headquarters Washington, D.C. 20546	3
Director, Technology Utilization Division Office of Technology Utilization NASA Headquarters Washington, D.C. 20546	1
NASA Scientific and Technical Information Facility P. O. Box 33 College Park, Maryland 20740	20
Director, Launch Vehicles and Propulsion, SV Office of Space Science and Applications NASA Headquarters Washington, D.C. 20546	1

	Copies
National Aeronautics and Space Administration Lewis Research Center 21000 Brookpark Road Cleveland, Ohio 41135 Mr. Irvin Johnsen	1
Captain Robert Probst Engineering Development Branch Air Force Rocket Propulsion Laboratory Edwards, California 93523	1
National Aeroanutics and Space Administration Washington, D.C. 20546 Dr. Eldon Hall, Code MTG	1
Mr. Stanley E. Write Defense Supply Agency DCASR-Cleveland Office of Engineering-DCRO-Y 1240 E. 9th Street Cleveland, Ohio 44199	1
Director, Advanced Manned Missions, MT Office of Manned Space Flight NASA Headquarters Washington, D.C. 20546	1
NASA Pasadena Office 4800 Oak Grove Drive Pasadena, California 91103 Patents and Contracts Management	1
Western Support Office 150 Pico Boulevard Santa Monica, California 90406 Office of Technical Information	1
Jet Propulsion Laboratory 4800 Oak Grove Drive Pasadena, California 91103 D. D. Lawson, Technical Monitor	1
Ames Research Center Moffett Field, California 94035 Hans M. Mark	1
Goddard Space Flight Center Greenbelt, Maryland 20771 Merland L. Moscson - Code 620	1

	Copies
Jet Propulsion Laboratory California Institute of Technology 4800 Oak Grove Drive Pasadena, California 91103 Henry Burlage, Jr. Propulsion Division 38	2
Langley Research Center Langley Station Hampton, Virginia 23365 Ed Cortwright, Director	1
Lewis Research Center 21000 Brookpark Road Cleveland, Ohio 44135 Director	1
Marshall Space Flight Center Huntsville, Alabama 35812 Hans G. Paul S&E-ASTN-P, Bldg. 4666	1
Manned Spacecraft Center Houston, Texas 77001 J. G. Thibodaux, Jr. Chief, Prop. & Power Division	1
John F. Kennedy Space Center, NASA Cocoa Beach, Florida 32931 Dr. Kurt H. Debus	1
Western Operating Office 150 Pico Boulevard Santa Monica, California 90406 Robert W. Kamm, Director	2
Air Force Missile Test Center Patrick Air Force Base, Florida L. J. Ullian	1
Space and Missile Systems Organization Air Force Unit Post Office Los Angeles, California 90045 Colonel Clark, Technical Data Center	1
Arnold Engineering Development Center Arnold Air Force Station Tullahoma, Tennessee 37388 Dr. H. K. Doetsch	1

	Copies
Headquarters, U. S. Air Force Washington, D. C. 20546 Colonel C. K. Stambaugh, AFRST	1
Picatinny Arsenal Dover, New Jersey 07801 T. Forsten, Chief Liquid Propulsion Laboratory	1
Air Force Rocket Propulsion Laboratory Research and Technology Division Air Force Systems Command Edwards, California 93523 RPRPD/Mr. H. Main	1
U. S. Army Missile Command Redstone Arsenal Alabama 35809 Dr. Walter Wharton	1
U. S. Naval Ordnance Test Station China Lake, California 93557 Code 4562, Chief, Missile Propulsion Div.	1
Aeroanutical Systems Division Air Force Systems Command Wright-Patterson Air Force Base Dayton, Ohio 45433 D. L. Schmidt, Code ASRCNC-2	1
Air Force Missile Development Center Holloman Air Force Base New Mexico 88330 Major R. E. Bracken	1
Chemical Propulsion Information Agency Applied Physics Laboratory 8621 Georgia Avenue Silver Spring, Maryland 20910 Tom Reedy	1
Aerojet-General Corporation P. O. Box 296 Azusa, California 91703 W. L. Rogers	1
Aerojet-General Corporation P. O. Box 1947 Technical Library, Bldg. 2015, Dept. 2410 Sacramento, California 95809 R. Stiff	1
Space Division Aerojet-General Corporation 9200 East Flair Drive El Monte, California S. Machlawski	1

	Copies
Aerospace Corporation 2400 East El Segundo Boulevard P.O. Box 95085 Los Angeles, California 90045 John G. Wilder, MS-2293	1
Atlantic Research Company Edsall Road and Shirley Highway Alexandria, Virginia 22314 Dr. Ray Friedman	1
Avco Systems Division Wilmington, Massachusetts Howard B. Winkler	1
Beech Aircraft Corporation Boulder Division Box 631 Boulder, Colorado J. H. Rogers	1
Bell Acrosystems Company P. O. Box 1 Buffalo, New York 14240 W. M. Smith	1
Bellcomm 955 L'Enfant Plaza, S. W. Washington, D. C. H. S. London	1
Bendix Systems Division Bendix Corporation 3300 Plymouth Road Ann Arbor, Michigan 48105 John M. Brueger	1
Boeing Company P. O. Box 3707 Seattle, Washington 98124 J. D. Alexander W. W. Kann	1
Boeing Company 1625 K Street, N. W. Washington, D.C. 20006 Library	1

	Copies
Missile Division Chrysler Corporation P. O. Box 2628 Detroit, Michigan 48231 John Gates	1
Wright Aeronautical Division Curtis-Wright Corporation Woodridge, New Jersey 07075 G. Kelley	1
Research Center Fairchild Hiller Corporation Germantown, Maryland Ralph Hall	1
Republic Aviation Corporation Fairchild Hiller Corporation Farmingdale, Long Island, New York Library	1
General Dynamics, Convair Division Library & Information Services (128-00) P. O. Box 1128 San Diego, California 92112 Frank Dore	1
Missile and Space Sytems Center General Electric Company Valley Forge Space Technology Center P. O. Box 8555 Philadelphia, Pennsylvania F. Mezger F. E. Schultz	1
Grumman Aircraft Engineering Corporation Bethpage, Long Island, New York 11714 Joseph Gavin	1
Honeywell, Inc. Aerospace Division 2600 Ridgway Road Minneapolis, Minnesota Gordon Harms	1
Hughes Aircraft Company Aerospace Group Centinela and Teale Streets Culver, City, California 90230 F. H. Meter V. P. and Div. Mgr. Research and Development Div.	1

	Copies
Walter Kidde and Company, Inc. Aerospace Operations 567 Main Street Belleville, New Jersey R. J. Hanville Dir. of Research Engr.	1
Ling-Temco-Vought Corporation P. O. Box 5907 Dallas, Texas 75222 Warren G. Trent	1
Arthur D. Little, Inc. 20 Acorn Park Cambridge, Massachusetts 02140 Library	1
Lockheed Missiles and Space Company Technical Information Center P.O. Box 504 Sunnyvale, California 94088 J. Guill	1
Lockheed Propulsion Company P. O. Box 111 Redlands, California 92374 Library	1
The Marquardt Corporation 16555 Saticoy Street Van Nuys, California 91409 Library	1
Baltimore Division Martin Marietta Corporation Baltimore, Maryland 21203 John Calathes (3214)	1
Denver Division Martin Marietta Corporation P. O. Box 179 Denver, Colorado 80201 Dr. Morgenthaler A. J. Kullas	1
Astropower Laboratory McDonnell Douglas Astronautics Company 2121 Campus Drive Newport Beach, California 92663 Dr. George Moe Director, Research	1

	Copies
Astrosystems International, Inc. 1275 Bloomfield Avenue Fairfield, New Jersey 07007 A. Mendenhall	1
Missile and Space Systems Division McDonnell Douglas Astronautics Company 3000 Ocean Park Boulevard Santa Monica, California 90406 Mr. R. W. Hallet, Chief Engineer Adv. Space Tech.	1
Space & Information Systems Division North American Rockwell 12214 Lakewood Boulevard Downey, California 90241 Library	1
Rocketdyne (Library 586-306) 6633 Canoga Avenue Canoga Park, California 91304 Dr. R. J. Thompson S. F. Iacobellis	1
Northrop Space Laboratories 3401 West Broadway Hawthorne, California 90250 Dr. William Howard	1
Aeronutronic Division Philco Corporation Ford Road Newport Beach, California 92663 D. A. Garrison	1
Astro-Electronics Division Radio Corporation of America Princeton, New Jersey 08540 Y. Brill	1
Rocket Research Corporation 520 South Portland Street Seattle, Washington 98108 Foy McCullough, Jr.	1
Sunstrand Aviation 2421 11 th Street Rockford, Illinois 61101 R. W. Reynolds	1

	Copies
Stanford Research Institute 333 Ravenswood Avenue Menlo Park, California 94025 Dr. Gerald Marksmen	1
TRW Systems Group TRW Incorporated One Space Park Redondo Beach, California 90278 G. W. Elverurn	1
Thiokol Chemical Corporation Aerospace Services Elkton Division Bristol, Pennsylvania Library	1
Research Laboratories United Aircraft Corporation 400 Main Street East Hartford, Connecticut 06108 Erle Martin	1
Hamilton Standard Division United Aircraft Corporation Windsor Locks, Connecticut 06096 R. Hatch	1
United Technology Center 587 Methilda Avenue P. O. Box 358 Sunnyvale, California 94088 Dr. David Altman	1
Republic Aviation Corporation Farmingdale, Long Island, New York Dr. William O'Donnell	1
Space General Corporation 9200 East Flair Avenue El Monte, California 91734 C. E. Roth	1
Thiokol Chemical Corporation Huntsville Division Huntsville, Alabama John Goodloe	1
Parker Aircraft 5827 W. Century Boulevard Los Angeles, California 90009 Library	1
Solar Division of International Harvester Company 2200 Pacific Avenue San Diego, California Library	1

APPENDIX A

SCOPE OF WORK

APPENDIX A

SCOPE OF WORK

MEASURING DEVICE TO INDICATE DEFLECTION OF INTERNAL ROTATING PARTS WITHOUT DIRECT MECHANICAL CONTACT

Introduction

The determination of actual deflection and dynamic loads imposed on internal rotating parts of turbopumps during operation in cryogenic propellants is a complicated and expensive procedure with current measuring practices. A device capable of measuring deflections without a mechanical interconnect through the stationary part to the rotating part will greatly simplify the determination of loads and clearances as well as provide a means of determining a probable failure prior to actual failure.

Purpose

The purpose of this program is to provide the required technology to establish the design criteria, material, and concepts necessary to develop an accurate and practical measuring device capable of measuring deflection of internal rotating parts without direct mechanical contact.

Task

This task shall be accomplished in three separate, but interrelated phases as set forth below.

Phase I.

Conduct a comprehensive literature search and evaluate presently available techniques of remote signal devices to determine the most feasible approaches to adapting to measurement of internal rotating, cryogenic turbopump components. Three different approaches are considered to be the optimum number to be studied. Approval of the approaches selected must be received from the Contracting Officer's Representative (COR) before the start of Phase II.

Phase II.

Perform analytical analysis for the three approaches approved in Phase I. Perform analytical studies to determine the best approach for simulating environmental testing of the three measuring devices and prepare detail design drawings of the test equipment. The test plans, test procedures, and design drawings of the measuring devices and test equipment are to be submitted to the COR for approval prior to procurement of hardware. Manufacture or procure one measuring device of each configuration.

Phase III.

Perform testing of each configuration to experimentally determine the one which is most accurate and practical for future use in production of turbopumps. Test data will be obtained under simulated environment of 35,000 rpm and 7,000 psi*. The tests will be conducted in both liquid hydrogen and liquid oxygen environment under vibrational conditions of the shuttle engine.

The test results will be recorded, analyzed, and furnished to the COR at the completion of testing of each device. These results shall also be included in the final report.

All units or remaining parts, properly identified, after completion of all testing, shall be shipped to this Center or as otherwise directed by the COR. All hardware shall be shipped on DD Form 250.

---

* 7000 psi $\equiv$ 48.2 MN/m^2.

APPENDIX B

PHASE III TEST PLAN

APPENDIX B

PHASE III TEST PLAN

The following represents the recommended sequence for Phase III (Experimental Verification). The sequence covers the ultrasonic Doppler device and the light-pipe reflectance. The sequence was modified according to the letter, dated April 13, 1972, from Charles C. Linn, Contracting Officer. In addition, flash X-radiographs were taken of a high speed rotating device intended to approximate the 35,000 rpm requirement.

ULTRASONIC DOPPLER DEVICE

We recommend that experiments be conducted to verify measurement capability for vibrational frequencies of 35,000 cpm, to subject ultrasonic transducers to vibrations representative of actual turbopump vibrations, and to measure vibrations of an alternate component in the existing J-2 LOX turbopump. In regard to high pressure or cryogen compatibility, we believe that these are not relevant since the transducers will be mounted on the outside of the case. In regard to acoustic properties of cryogens, we believe that the published data accurately characterizes LOX and LH_2, so no further verification is necessary. The following lists the test sequence.

A. Measurement of 35,000 cpm vibrational frequency
   (1) Adapt existing apparatus to produce a 35,000 cpm vibration. This will either be done by driving a shaft with a single eccentric at 35,000 rpm or a shaft with a multiple eccentric at a correspondingly lower speed, whichever proves more efficient.
   (2) Measure vibration amplitude and compare with slow-speed or static-calibration measurements.

B. Vibration tests
   (1) Construct a new, rugged set of transducers according to the basic design of Figure 4.

(2) Determine lead noise and efficiency of vibration coupling during operation while vibrating according to pump vibration specifications to be provided by NASA-MSFC.

C. Alternate component-vibration measurements

(1) Select alternate vibrating J-2 pump component (shaft, inducer, seal).

(2) Attach transducers to J-2 pump.

(3) Measure vibration amplitudes while rotating pump.

(4) Compare with static-calibration measurements.

LIGHT PIPE REFLECTANCE

Our Phase III recommendations involve subjecting the fiber optic bundle to conditions representative of turbopump operation, and evaluating the degree of effectiveness afforded by a rigid jacket to protect the probe from high-velocity fluid flow. In regard to measurement of vibration frequencies up to 35,000 cpm, we believe the Phase I effort verified this capability of the device. With respect to shock, our Phase II work has demonstrated the probe's ability to withstand considerable abuse.

The following experimental sequence is recommended.

A. Compatibility with high pressures and cryogens.

(1) Expose fiber-optic probe simultaneously to 48 MN/m^2 and 77 K liquid nitrogen.

(2) Measure calibration stability during exposure.

B. Exposure to high-velocity fluid flow.

(1) Fabricate a protective jacket.

(2) Install probe in high-velocity fluid stream.

(3) Verify optical properties following exposure.

NATIONAL AERONAUTICS AND SPACE ADMINISTRATION
GEORGE C. MARSHALL SPACE FLIGHT CENTER
MARSHALL SPACE FLIGHT CENTER, ALABAMA 35812

REPLY TO
ATTN OF: A&TS-PR-MB

April 13, 1972

Battelle Memorial Institute
505 King Avenue
Columbus, OH 43201

Subject: Contract NAS8-26903

Your recommended Phase III Test Plan, submitted with the fourth quarterly report for subject contract has been reviewed. The following exceptions are noted and require corrective action:

a. Items A.(2) and C.(2)(page A-2) do not indicate what design of measuring equipment will be used to test at 35,000 RPM and on the J-2 LOX pump. Battelle is to use the transducer design of Fig. 4 as noted in item B.(1) for all ultrasonic testing in phase III.

b. In item A.(1)(page A-3) 77F should be 77K.

c. Item C is to be added to the light pipe reflectance testing (page A-3) as follows:

C. Exposure to vibrational environment

(1) Expose the fibre-optic probe simulataneously to 77K liquid nitrogen and pump vibration specifications to be provided by NASA-MSFC.

(2) Verify optical properties following exposure.

When above changes are incorporated, you may proceed to construct the ultrasonic transducers and proceed with Phase III work of the ultrasonic and optical light pipe approaches.

The vibrational environment of the shuttle engine turbopump was not specifically stated in the scope of work and was to be furnished by this Center when available. The following data is to be used as a guide for the phase III testing:

5 to 30 Hz @ 0.3 inch peak to peak
30 to 400 Hz @ 15g peak
400 to 900 Hz @ 0.0017 inch peak to peak
900 to 3000 Hz 50g peak

You state on page A-1 that, "unless further phase II effort identifies problems of which we are now unaware, we will recommend that no phase III testing is necessary for the flash X-ray work." To date all of your experimental work has been with the object being photographed in a stationary condition. It may be necessary to do phase III testing to prove or disprove this method with the rotating part turning at 35,000 RPM and subjected to the environmental vibrations of the shuttle engine; however, this decision will be made after the completion of phase II studies.

It is requested that you furnish a revised Phase III Test Plan at your earliest convenience.

Charles C. Linn
Contracting Officer

cc:
DCASO/Columbus